The Effect of a Trace Element Supplement on the Biomethane Potential of Food Waste Anaerobic Digestion

Kelly Mackenzie Graff

Thesis submitted to the faculty of the Virginia Polytechnic Institute and State University
in partial fulfillment of the requirements for the degree of

Master of Science
In
Biological Systems Engineering

Jactone A. Ogejo - Chair
Biswarup Mukhopadhyay
Ryan S. Senger

May 10, 2022
Blacksburg, VA

Keywords: food waste, anaerobic digestion, trace elements, biomethane potential, greenhouse gas reduction, renewable energy

The Effect of a Trace Element Supplement on the Biomethane Potential of Food Waste Anaerobic Digestion

Kelly Mackenzie Graff

ABSTRACT

Food waste is a desirable feedstock for anaerobic digestion because it is high in moisture and is an easily degradable material. However, mono-digestion of food waste often fails due to the accumulation of volatile fatty acids. Supplementing trace elements is one strategy to combat this issue. This study examined the effect of supplementing trace elements (iron, nickel, selenium, molybdenum, magnesium, zinc, calcium, copper, manganese, cobalt) on the methane yield and organic waste destruction of anaerobically digested food waste. Methane yield of food waste with and without the inorganic salt trace element was determined by the gas density-based biomethane potential method at mesophilic (37°C) conditions over 30 days. The three treatments were inoculum only, food waste and inoculum, and food waste and inoculum with an added trace element solution. There was no significant difference between treatments in terms of waste stabilization (percent volatile solids, total solids, and total chemical oxygen demand reduction) between treatments. The average cumulative biogas produced was 41% higher, and the average total cumulative methane produced was 23% higher in the treatment with the trace element supplement. Mean methane yield was not different ($p > 0.05$) between treatments over the 30 days, and there was no difference ($p > 0.05$) in biomethane potential between treatments.

In addition, greenhouse gas reduction potential was estimated from food waste streams in Montgomery, VA using anaerobic digestion. The purpose of this work was to (1) estimate the total mass of food waste produced in Montgomery, VA in a year, (2) use the results from the biomethane potential analyses to inform the sizing of a theoretical community digester in Montgomery, VA, and (3) estimate the greenhouse gas reduction potential of anaerobically digesting the food waste instead of sending it to landfill. Greenhouse gas reduction was calculated using the Climate Action Reserve Organic Waste Digestion Project Protocol guidelines. The greenhouse gas reduction potential was estimated as 6,532 tonnes of carbon dioxide equivalent per year (tCO_2e/year), with approximately 693 m^3 CH_4 produced per day. In one year, the digester would generate an estimated 7370 kWh of energy which has the potential to power 149 homes for a year in Montgomery, VA. In addition, 4130 tonnes/year of composted digestate would be available as fertilizer for surrounding farms.

The Effect of a Trace Element Supplement on the Biomethane Potential of Food Waste Anaerobic Digestion

Kelly Mackenzie Graff

GENERAL AUDIENCE ABSTRACT

Currently, about one-third of the entire U.S. food supply is lost or wasted. A large portion of that food waste is sent to landfills, where it produces methane, a greenhouse gas. Instead, food waste can be broken down to produce biogas during anaerobic digestion. Anaerobic digestion is a process in which microorganisms break down organic materials in the absence of oxygen to produce biogas and digestate, a material used as a soil amendment or fertilizer. However, anaerobically digesting food waste often leads to process instability and failure due to a buildup of undesirable intermediates. Microorganisms in anaerobic digestion require certain trace elements (i.e., iron, copper) that food waste often lacks; therefore, supplementing key trace elements may improve the anaerobic digestion of food waste. This research aimed to assess the effect of supplementing key trace elements (iron, copper, zinc, calcium, magnesium, nickel, manganese, selenium, molybdenum, cobalt) on organic matter degradation and methane yield. Methane yield of food waste with and without the inorganic salt trace element was determined by the gas density-based biomethane potential method at mesophilic (37°C) conditions over 30 days. The average cumulative biogas produced was 41% higher, and the average total cumulative methane produced was 23% higher in the bottles containing a trace element supplement. No significant difference was seen in the two groups when

comparing organic matter degradation. These results demonstrate that supplementing trace elements can improve biogas and methane production.

Greenhouse gas reductions from anaerobically digesting food waste instead of sending it to landfills were determined for Montgomery, VA. The results from the biomethane potential test informed the design of a theoretical community digester. Greenhouse gas reduction was calculated using the Climate Action Reserve Organic Waste Digestion Project Protocol equations. The greenhouse gas reduction was determined as 6,532 tonnes of carbon dioxide equivalent per year (tCO_2e/year). The digester would produce approximately 693 m^3 CH_4/day, which has the potential to power 149 homes for a year in Montgomery, VA. In addition, 4130 tonnes/year of compost would be produced and available as a fertilizer for surrounding farms.

Table of Contents

List of Figures

List of Tables

1. Literature Review

1.1 Introduction

The USDA estimated that 40 million tons of food are disposed of every year, accounting for 30-40% of the entire U.S. food supply (USDA, 2010). According to the EPA, most wasted food ends up in landfills (55.9%) (US EPA, 2017). Methane, a greenhouse gas (GHG) with a 28 times more significant impact than carbon dioxide in a 100-year period, is produced when food is sent to landfills. In the absence of biogas capture systems, methane is emitted directly into the atmosphere. To some extent, food waste (FW) is inevitable (i.e., potato peels, banana peels), so minimizing and adequately managing it is needed to mitigate the environmental impacts.

Current FW management systems include incineration, composting, and anaerobic digestion (AD). Incineration of FW converts the waste into ash, flue gas, and heat and is often used to produce thermal energy and reduce the volume of the original waste (Gao et al., 2017). Incineration does not completely replace landfilling, as the remaining waste must be disposed of after incineration. Additionally, incineration is energy-intensive and has the potential to contribute to air pollution (C. Zhang et al., 2014). Aerobic composting is the process in which microorganisms break down organic matter in the presence of oxygen and produce carbon dioxide, ammonia, water, heat, and hummus, the organic product. Drawbacks to composting are site preparation and equipment, a long treatment period, and some environmental issues related to odors and dust (Sikora, 1998). The remaining portion of this review will focus on the use of AD for treating FW.

AD is a naturally occurring process in which organic matter is broken down and converted into biogas by microorganisms in the absence of oxygen. Raw biogas produced from AD can be used directly for electricity or heating or upgraded into renewable natural gas (RNG).

Upgrading is the process in which biogas is converted into RNG by removing excess carbon dioxide. RNG is a pipeline-quality gas composed mainly of methane (96-98% methane) that can be used in several applications such as vehicle fuel, compressed natural gas (CNG), and liquid natural gas (LNG) (US EPA, 2018). Additionally, digestate, a byproduct of the AD process, is a nutrient-rich material that can be used as a soil amendment or fertilizer. Upcycling FW into RNG mitigates the environmental impacts of methane produced from landfills and creates economically viable products (Parker et al., 2017).

1.2 AD Process Parameters and Design Considerations

AD is a complex process whose performance depends on numerous process parameters and anaerobic digester design considerations. The most influential factors affecting FW process performance AD are elaborated on below.

Temperature

AD system temperature affects biogas production, external energy requirements, and overall process stability. Psychrophilic digestion occurs at <20 °C, mesophilic digestion occurs between 20 – 40 °C, and thermophilic digestion occurs between 43- 71 °C (Burke, 2001). The optimum temperature for mesophilic and thermophilic digestions are 35 °C and 55 °C, respectively (Meegoda et al., 2018). Psychrophilic temperatures are not relevant as AD reactions stop below 10 °C. Generally, mesophilic digestion produces less biogas than thermophilic digestion due to a lower operating temperature. Thermophilic digestion causes increased reaction rates, leading to higher loading rates and biogas production (Meegoda et al., 2018). However, mesophilic digesters are often preferred over thermophilic digesters because of their lower energy requirement and higher process stability (Rahman et al., 2018).

Retention Time

Retention time is the average time raw material remains in a digester. There are two types of retention time: solids retention time (SRT) and hydraulic retention time (HRT). SRT is the time the solid fraction of the feedstock spends in the digester, and it is the most critical factor controlling the conversion of solids to gas (Burke, 2001). It is defined as the quantity of solids maintained in the digester divided by the quantity of solids coming out of the reactor per day (effluent):

$$SRT = \frac{V * C_d}{Q_w * C_w} \quad \textbf{(1)}$$

Where,

V is the digester volume; C_d is the solids concentration in the digester; Q_w is the volume of effluent each day, and C_w is the solids concentration of the effluent. A low SRT indicates that there is not sufficient time for bacterial growth to replace the bacteria lost through the effluent. If the rate of bacterial loss is greater than the rate of bacterial growth, then "wash-out" occurs (Burke, 2001). In a completely mixed or plug flow digester, the HRT = SRT.

Anaerobic digesters are made to retain a specific volume of waste over a fixed period of days. The HRT is the amount of days the material remains within the digester and is calculated by dividing the volume of the digester by the influent flow rate.

$$HRT = \frac{V_r}{Q} \quad \textbf{(2)}$$

Where,

V_r is the reactor volume (m^3), and Q is the influent flow rate (m^3/day). HRT represents the amount of time available for bacterial growth and, therefore, the time for converting organic material to biogas. A shorter HRT corresponds to a higher loading rate. A higher loading, and consequently a shorter HRT, is associated with process inhibition (accumulation of volatile fatty

acids and decline in methane yield) (Salminen & Rintala, 2002). Generally, mesophilic AD can be accomplished within 15-20 days with optimal operation at a low loading rate and a high HRT (Meegoda et al., 2018).

Loading Rate

The loading rate of a digester is the amount of organic material fed to a digester daily (also referred to as organic loading rate – OLR). OLR is a measure of the biological conversion capacity of an AD system (Velmurugan et al., 2014). It is commonly expressed as the mass of raw material (volatile solids) fed to the digester per unit volume per day. A higher loading rate is associated with process inhibition or failure, so a lower loading rate is recommended for FW AD. The optimum loading rate is dependent on the type of feedstock, retention time, and temperature. The optimum loading rate for mesophilic digestion of FW was determined as 0.30 g volatile solids/L*day (Blasius et al., 2020). In contrast, the optimum loading rate for mesophilic digestion of pig manure was 1.89 g volatile solids/L*day (Duan et al., 2019). Loading rate can be calculated using the following equation (Arsova et al., 2010).

$$Loading\ rate\ \left(\frac{mgCOD}{m^3 * day}\right) = \frac{Organic\ matter\ \left(\frac{mgCOD}{m^3}\right) * Flow\ rate\ \left(\frac{m^3}{day}\right)}{Operating\ volume\ (m^3)} \quad \textbf{(3)}$$

Inoculum Type

Most organic matter, including FW, cannot be digested by itself. Therefore, a source of diverse microorganisms is necessary to start the digestive process. Inoculums contain essential microbial communities that are required for successful AD. Digestates produced from active AD projects are often sources for inoculums. Elbeshbishy et al. (2012) investigated the influence of inoculum pre-incubation and inoculum source (digested sludge from municipal wastewater treatment plant (WWTP) and a digester treating the organic fraction of municipal waste) on FW AD. There was no difference in methane yield or biodegradability of primary sludge using the

pre-incubated or non-incubated inoculum. However, the maximum methane production rates of the non-incubated inoculum were higher than the pre-incubated inoculum at all substrate-to-inoculum ratios tested. Additionally, the inoculum from the municipal WWTP was better at treating FW than the inoculum from an anaerobic digester treating FW (Elbeshbishy et al., 2012). This result may be due to the low levels of trace elements in FW compared to sludge from a WWTP. A study investigating the influence of total solids and inoculum (mesophilic sludge) on mesophilic FW AD found the best performance was a reactor with 20% total solid and 30% of inoculum (0.49 L CH_4/g VS) (Forster-Carneiro et al., 2008).

Carbon: Nitrogen (C:N) Ratio

The C: N ratio is the relationship between the amount of carbon and nitrogen present in a sample. Carbon, in the form of carbohydrates, and nitrogen, in the form of proteins and nitrates, are essential substrates for microorganisms in an AD system. Consumption of carbon is 30 times faster than nitrogen consumption. Hence, the C: N ratio should be between 20 and 30 (Velmurugan et al., 2014). A relatively high C: N ratio reflects high nitrogen consumption, lowering the biogas production rate. However, a lower C: N ratio leads to ammonia accumulation, increasing pH, which is toxic to methanogens (Velmurugan et al., 2014). The C: N ratio of FW is considered low (14.7-36.4) compared to other organic substrates (R. Zhang et al., 2007). A study on the effect of the C: N ratio of FW on methane production in a batch mesophilic anaerobic digester found that adjusting the C: N ratio of mixed FW using meat, fruit, and vegetable wastes from 17 to 30 increased methane yield from 0.352 L/g VS to 0.679 L/gVS (Tanimu et al., 2014). Additionally, FW treatment efficiency of 85% was obtained at a C: N ratio of 30 (Tanimu et al., 2014).

Total Solids (TS) and Volatile Solids (VS)

Total solids (TS) are the solid concentration of biomass (i.e., FW), and volatile solids (VS) are the organic fraction of the total solids. Three leading AD technologies have been developed based on the TS content in feedstocks: wet (≤ 10% TS), semi-dry (10-20% TS), and dry (≥ 20% TS) (Yi et al., 2014). The performance of mesophilic AD of FW with TS contents ranging from 5% to 20% showed better performances (VS reduction and methane yield) in reactors with increasing TS content (Yi et al., 2014). Experimental data studying the effect of TS (5-15%) and pH (5-9) on AD of FW found that a solid concentration of 7.5% TS and a pH of 7 produced a maximum biogas yield (Deepanraj et al., 2015). A different study looking at the effect of TS (5%, 10%, 15%, 20%) on biogas production found that 10% TS yielded the highest biogas production (Paramaguru et al., 2017).

FW often contains high moisture (relatively low TS) and high amounts of biodegradable components (VS content), making it an ideal AD substrate. However, since FW has high moisture and high VS content, it is often rapidly degraded, leading to high volatile fatty acid (VFA) production and process inhibition (W. Zhang et al., 2020). Liotta et al. (2014) studied the effect of TS content (4.5% - 19.2%) on methane and VFA production in FW AD. They found a decreasing trend in the initial methane production rate with increasing TS concentration. In dry and semi-dry conditions, a lack of moisture resulted in VFA accumulation, often responsible for process inhibition.

VS are an essential measure for feedstock biodegradability. The biodegradability of a feedstock is indicated by biogas or methane yield and the percentage of solids (either TS or VS) destroyed in AD. Biogas and methane yield is measured by the amount of biogas or methane produced per unit mass of VS contained in the feedstock (R. Zhang et al., 2007).

An alternative method for analyzing digester performance is calculating a mass balance based on chemical oxygen demand (COD) entering and leaving the system (Harnadek et al., 2015). COD measures the amount of oxygen required to oxidize organic material present in an AD system and is an estimate for the amount of organic material in a system.

1.3 Current Challenges with Food Waste Anaerobic Digestion

AD of FW has been proposed as a better alternative to landfilling, incineration, and composting, as this process can treat large quantities of FW, a high moisture material. AD has been widely adopted to treat wastewater, sewage sludge, and animal manure. However, AD of FW still faces challenges. These challenges include VFA and ammonia accumulation, foaming, low buffer capacity, and relatively low trace element concentrations (Xu et al., 2018).

Volatile Fatty Acid Accumulation

FW is highly biodegradable, making it an ideal feedstock material for AD. The rapid conversion of food into VFA can cause a drastic drop in pH, leading to process instability and even process failure if the buffering capacity is not high enough (Banks et al., 2011). Each stage of AD has specialized and complex groups of microorganisms that operate best under different pH conditions. Acidogenic bacteria produce VFA, while methanogens produce biogas. The optimum pH range for biogas production is between 6.5-and 7.5 (C. Liu et al., 2008). However, the growth rate of methanogens is significantly reduced when pH drops below 6.6 (Reungsang et al., 2012). Therefore, if the buffering capacity of the feedstock and inoculum is not high enough, pH controls such as sodium carbonate are essential to correct for pH decreases associated with VFA accumulation (Velmurugan et al., 2014).

Multiple studies have looked at how AD parameters such as pH (J. Jiang et al., 2013; Lukitawesa et al., 2020; K. Wang et al., 2014), temperature (Jiang et al., 2013), OLR (Jiang et

al., 2013), total solids (TS) (Liotta et al., 2014), inoculum to substrate ratio (ISR) (Lukitawesa et al., 2020), and inoculum adaptation (Lukitawesa et al., 2020) affect VFA accumulation during the AD of FW. The optimal pH and temperature for VFA accumulation are 6 and 45 °C, respectively (J. Jiang et al., 2013; K. Wang et al., 2014). In addition, the presence of initial oxygen (headspace unflushed), pH-controlled at 6, and an ISR of 1:3 all contributed to a higher VFA yield (Lukitawesa et al., 2020). The more acidic pH induced by VFA production contrasts with the optimal pH for biogas production of methanogens, as pH below 6.6 has been shown to reduce the growth rate of methanogens.

A high OLR, or the amount of organic material fed to a digester daily, has led to VFA accumulation during the AD of FW. The percentage of two VFAs (acetate and valerate) increased as OLR increased from 5 to 16 g TS /L *d (J. Jiang et al., 2013), while the percentage of two different VFAs (propionate and butyrate) decreased (Jiang et al., 2013). However, TS is not as reliable as volatile solids (VS) in determining OLR, as TS may include materials such as rocks or debris. In regards to TS, VFA accumulation occurred during the first step of an AD process in both semi-dry (12.87% total solids) and dry conditions (4.52% total solids), leading to a lowered specific methane yield (Liotta et al., 2014). VFA concentrations below 4,000 mg/L allowed for a 65% organic removal rate in an AD process treating FW leachate (D.-J. Lee et al., 2015). The AD process parameters describe the conditions that allow for VFA accumulation but understanding the mechanisms and pathways that allow for VFAs to accumulate faster than methane is essential to improving the AD process of FW.

Ammonia Accumulation

Additionally, FW may contain high lipid and protein contents that can lead to high concentrations of ammonia, hydrogen sulfide, and long-chain fatty acids, leading to process

failure (H. Chen et al., 2016). Total ammonium nitrogen (TAN) is the concentration of ammonium salt (NH_4^+) and ammonia both in the aqueous and gas phases (NH_3). The fraction of NH_3 and NH_4^+ in a digester depends on pH and temperature, which varies between studies. The equilibrium point (pK_a) for NH_3 and NH_4^+ is 9.3, meaning NH_3 and NH_4^+ can act as a buffer in systems where pH is $pK_a \pm 1$.

TAN concentrations between 600 mg/L to 800 mg/L allowed a mesophilic AD system (pH 7.2-7.5) to operate normally. However, concentrations of total ammonium nitrogen higher than 800 mg/L (at pH 7.2-7.5 in mesophilic conditions) inhibited methanogens and reduced biogas production (Procházka et al., 2012; Yenigün & Demirel, 2013). At a neutral pH, the fraction of NH_4^+ is nearly 100%. Different studies have found differing concentrations of TAN to be inhibiting at different pH and temperature conditions, which include 4000 mg/L (Sung & Liu, 2003), between 4000 and 6000 mg/L (Angelidaki & Ahring, 1993), between 1700 mg/L and 14,000 mg/L (Y. Chen et al., 2008), and higher than 6000 mg/L (Sawayama et al., 2004). The vast differences between inhibiting concentrations of TAN greatly depend on the AD system's operating conditions (temperature, pH), type of feedstock, and inoculum source used in each study. Therefore, monitoring nitrogen concentrations in an AD system is crucial to preventing ammonia accumulation.

Foaming

Foaming, which can be produced by microorganisms or high solids content and high gas production, is also a challenge associated with AD. Foaming, a typical challenge associated with AD reduces the working volume of a digester and can decrease digester efficiency (biogas production, organic matter destruction efficiency). However, FW often contains a high protein

content, a known surfactant that can stabilize foaming in anaerobic digesters (Yang et al., 2021). Therefore, foaming is not a central issue in an AD system processing FW.

Trace Element Content in FW

As previously discussed, AD of FW often leads to process instability via VFA accumulation. VFAs, especially propionate, inhibit AD of FW, and a deficiency of essential trace elements in FW is the fundamental reason (W. Zhang et al., 2019). Trace elements are components of cofactors and enzymes required in small amounts for microorganisms to function correctly. Trace elements relevant to the AD process are iron (Fe), cobalt (Co), nickel (Ni), zinc (Zn), copper (Cu), manganese (Mn), magnesium (Mg), molybdenum (Mo), selenium (Se), and calcium (Ca). There is a current lack of knowledge regarding the complex synergistic relationships between trace element-dependent enzymes used during the four stages of AD. Additionally, mixed FW varies greatly, making comparisons between FW AD studies complex regarding trace element supplementation. Table 1 summarizes data related to trace element content in different mixed FW streams.

Table 1. Average trace elements concentrations in mixed food waste streams reported in the literature

Trace element	Average concentration (mg/kg TS)	Food waste type and location	Sources
Cobalt (Co)	1.14 (±0.99)	Synthetic FW: 79% fruits and vegetables, 5% pasta and rice, 6% bread and bakery, 8% meat and fish, 2% dairy product (Delft, The Netherlands and Tampa, USA)	Ariunbaatar et al., 2016
		Kitchen waste (Treviso, Italy)	Facchin, Cavinato, Fatone, et al., 2013b
		Source separated FW (Treviso, Italy)	Facchin, Cavinato, Pavan, et al., 2013
		Restaurant waste: 56% banana and potato peels, 25% citrus fruits, 8.2% non-citrus fruits, 7.6% fibers and minerals (eggshells, celery, herbs, etc.), 3.2% other types of herbs (cilantro, chard, citron, etc.) (Cali, Columbia)	Parra-Orobio et al., 2018
		Source separated domestic FW (Ludlow, UK)	Yirong et al., 2014
		China Agricultural University restaurant FW (Beijing, China)	W. Zhang et al., 2015a
Copper (Cu)	11.15 (±9.77)	Synthetic FW: 79% fruits and vegetables, 5% pasta and rice, 6% bread and bakery, 8% meat and fish, 2% dairy product (Delft, The Netherlands and Tampa, USA)	Ariunbaatar et al., 2016
		Source separated domestic FW (Ludlow, UK)	Y. Zhang et al., 2012
Iron (Fe)	244 (±202)	Synthetic FW: 79% fruits and vegetables, 5% pasta and rice, 6% bread and bakery, 8% meat and fish, 2% dairy product (Delft, The Netherlands and Tampa, USA)	Ariunbaatar et al., 2016
		Restaurant waste: 56% banana and potato peels, 25% citrus fruits,	Parra-Orobio et al.,

		8.2% non-citrus fruits, 7.6% fibers and minerals (eggshells, celery, herbs, etc.), 3.2% other types of herbs (cilantro, chard, citron, etc.) (Cali, Columbia) China Agricultural University restaurant FW (Beijing, China)	2018 W. Zhang et al., 2015a
Manganese (Mn)	54.82 (±35.91)	Synthetic FW: 79% fruits and vegetables, 5% pasta and rice, 6% bread and bakery, 8% meat and fish, 2% dairy product (Delft, The Netherlands and Tampa, USA) Source separated domestic FW (Ludlow, UK)	Ariunbaatar et al., 2016 Yirong et al., 2014
Molybdenum (Mo)	3.66 (±4.72)	Synthetic FW: 79% fruits and vegetables, 5% pasta and rice, 6% bread and bakery, 8% meat and fish, 2% dairy product (Delft, The Netherlands and Tampa, USA) Kitchen waste (Treviso, Italy) Source separated FW (Treviso, Italy) Restaurant waste: 56% banana and potato peels, 25% citrus fruits, 8.2% non-citrus fruits, 7.6% fibers and minerals (eggshells, celery, herbs, etc.), 3.2% other types of herbs (cilantro, chard, citron, etc.) (Cali, Columbia) Source separated domestic FW (Ludlow, UK)	Ariunbaatar et al., 2016 Facchin, Cavinato, Fatone, et al., 2013b Facchin, Cavinato, Pavan, et al., 2013 Parra-Orobio et al., 2018 Yirong et al., 2014
Nickel (Ni)	7.09 (±2.09)	Synthetic FW: 79% fruits and vegetables, 5% pasta and rice, 6% bread and bakery, 8% meat and fish, 2% dairy product (Delft, The Netherlands and Tampa, USA)	Ariunbaatar et al., 2016 Facchin, Cavinato,

		Kitchen waste (Treviso, Italy) Source separated FW (Treviso, Italy) Restaurant waste: 56% banana and potato peels, 25% citrus fruits, 8.2% non-citrus fruits, 7.6% fibers and minerals (eggshells, celery, herbs, etc.), 3.2% other types of herbs (cilantro, chard, citron, etc.) (Cali, Columbia) China Agricultural University restaurant FW (Beijing, China) Source separated domestic FW (Ludlow, UK)	Fatone, et al., 2013b Facchin, Cavinato, Pavan, et al., 2013 Parra-Orobio et al., 2018 W. Zhang et al., 2015a Y. Zhang et al., 2012
Selenium (Se)	0.57 (±0.55)	Synthetic FW: 79% fruits and vegetables, 5% pasta and rice, 6% bread and bakery, 8% meat and fish, 2% dairy product (Delft, The Netherlands and Tampa, USA) Kitchen waste (Treviso, Italy) Source separated FW (Treviso, Italy) Source separated domestic FW (Ludlow, UK) Source separated domestic FW (Ludlow, UK)	Ariunbaatar et al., 2016 Facchin, Cavinato, Fatone, et al., 2013b Facchin, Cavinato, Pavan, et al., 2013 Yirong et al., 2014 Y. Zhang et al., 2012
Tungsten (W)	0.62 (±0.33)	Synthetic FW: 79% fruits and vegetables, 5% pasta and rice, 6% bread	Ariunbaatar et al.,

		and bakery, 8% meat and fish, 2% dairy product (Delft, The Netherlands and Tampa, USA) Kitchen waste (Treviso, Italy) Source separated FW (Treviso, Italy)	2016 Facchin, Cavinato, Fatone, et al., 2013b Facchin, Cavinato, Pavan, et al., 2013
Zinc (Zn)	160 (±170)	Synthetic FW: 79% fruits and vegetables, 5% pasta and rice, 6% bread and bakery, 8% meat and fish, 2% dairy product (Delft, The Netherlands and Tampa, USA) Restaurant waste: 56% banana and potato peels, 25% citrus fruits, 8.2% non-citrus fruits, 7.6% fibers and minerals (eggshells, celery, herbs, etc.), 3.2% other types of herbs (cilantro, chard, citron, etc.) (Cali, Columbia) Source separated domestic FW (Ludlow, UK)	Ariunbaatar et al., 2016 Parra-Orobio et al., 2018 Y. Zhang et al., 2012

Inadequate amounts of trace elements in FW have been reported to cause digester instability. For example, L. Zhang et al. (2011) compared piggery wastewater to FW, and the FW had about one-tenth the trace element content. Supplementing a trace element mixture containing Co, Mo, Ni, and Fe added to a semi-continuous long-term anaerobic digester processing FW resulted in a high methane yield of 0.396 $m^3/kgVS_{added}$ and a 75.6% VS destruction with no significant VFA accumulation (L. Zhang et al., 2011). The addition of granular activated carbon and trace elements (Fe, Co, Mo, Ni, Se, Zn, Cu, Mn) improved VFA consumption during the AD of FW (Capson-Tojo et al., 2018). In particular, adding this mix of trace elements improved propionic acid consumption. Adding granular activated carbon and trace elements is a potential solution to stabilizing FW AD (Capson-Tojo et al., 2018). The effect of supplementing iron ($FeCl_3$) and biochar in the AD of FW indicated that supplementing biochar and trace elements in the form of industrial $FeCl_3$ improved maximum methane production rates (from 897 to 1494 mL/day) and average daily methane production rates (from 298 to 369 mL/day) (Capson-Tojo et al., 2019). Confirming these results, a different research group supplemented conductive material (biochar and magnetite) and trace elements (Fe, Co, Ni, Cu, Zn, Mo, W) into FW AD. Their results indicated that supplementation of biochar and trace elements improved total biogas production and methane yields (Akturk & Demirer, 2020). As these studies indicate, there is great potential of supplementing trace elements in FW AD.

The relationship between retention time and supplementing trace elements have also been studied. Both prolonged retention time and trace element supplementation (Fe, B, Zn, Cu, Mn, Mo, Al, Co, Ni, Se) allowed stable digestion with a high VFA content. However, reactors with an HRT of 25, 50, and 100 days with no trace element supplementation failed, while reactors supplemented with trace element maintained stable digestion (Climenhaga & Banks, 2008).

OLR, related to retention time, has also been studied concerning trace element supplementation. Trace element supplementation was a successful strategy to stabilize the AD of vegetable waste, allowing for OLRs up to 4 g VS/L*d to be achieved (Y. Jiang et al., 2012). During the AD of FW, an optimum dosage of Fe (5000 mg/L), Ni (200 mg/L), Zn (320 mg/L), and Mo (2.2 mg/L) reduced VFA inhibition during an organic load of 6.5 g/L. Additionally, supplementing Cu (250 mg/L) and Co (3 mg/L) decreased ammonia concentration and improved process stability during an organic load of 9.5 g/L (Bardi & Aminirad, 2020). The role of trace elements in long-term AD of FW under increasing loads and early and medium VFA inhibition was also investigated. Supplementing digesters with trace elements (Fe, Co, Mo, Ni) improved methanogenic community composition, and early and medium VFA inhibition was reversed through trace element supplementation (W. Zhang et al., 2020). Supplementing trace elements, therefore, has the potential to reverse process instability caused by ammonia and VFA inhibition.

The inoculum used in FW AD has been widely investigated regarding trace element supplementation. Supplementing trace elements in digesters using an inoculum with a high trace element background (i.e., those from the co-digestion of biowaste and waste-activated sludge) had either neutral or slightly negative effects on the digestion performance. In contrast, trace element supplementation in digesters using FW inoculum, containing low concentrations of trace elements, increased methane production (Facchin et al., 2013). In particular, Mo concentrations between 3-12 mg/kg TS_{fed} and a Se concentration of 10 mg/kg TS_{fed} increased methane production by 30-40% while supplementing a trace element mixture (Co, Mo, Ni, Se, W) increased methane production by 45-65% when using an inoculum with low trace element content (Facchin et al., 2013). The content of trace elements (Ca, K, Fe, Zn, Al, Mg, Co, Ni, Mo) present in inoculum from different sources (agro-industrial and municipal wastewater treatment

plants) can alter AD process requirements and, therefore, methane production (Parra-Orobio et al., 2018). High concentrations of Zn and Al in inoculums taken from municipal wastewater treatment plants negatively affected methane production (<70 mL CH_4/g VS), while high concentrations of Ni (35.2 mg/kg) and Mo (15.4 mg/kg) in the inoculum increased methane production (140.7 mL CH_4/g VS) (Parra-Orobio et al., 2018). Supplementing trace elements (Fe, Ni, Co, Se, Mo) when using an inoculum with a high Fe content (1681 mg/L) adversely impacted methanogenic activity by 20-58% (Yazdanpanah et al., 2018). To conclude, trace element supplementation may adversely affect FW AD if the inoculum used for AD of FW has a high background in trace elements.

The prevention of VFA accumulation in FW AD is of utmost importance as reactor stability is often based on VFA concentration. A trace element addition strategy successful for mesophilic digestion was applied to a thermophilic digester with mixed results. While trace element supplementation (Al, B, Co, Cu, Fe, Mn, Ni, Zn, Mo, Se, W) delayed the rate of VFA accumulation, it was unable to sustain stable digestion after 3-4 months associated with an inhibitory ammonia nitrogen concentration of ~2500 mg N/L (Yirong et al., 2014). A destabilized thermophilic AD process with high VFA accumulation recovered in less than two weeks after supplementing trace elements (Ca, Mg, Co, Ni), and biogas production improved by 40% (Menon et al., 2017). Supplementation of trace elements (Co, Fe, Mo, Ni, Se) improved VFA concentrations in a single-stage anaerobic digester mono-digesting FW. However, the benefit of trace element supplementation in a two-stage (hydrolysis followed by methanogenesis) system treating FW was not apparent (Voelklein et al., 2017).

Long-term AD of FW can be potentially improved through supplementing trace elements. Supplementing a trace element mixture (Fe, B, Zn, Cu, Mn, Mo, Al, Co, Ni, Se) in a long-term

semi-continuous single-stage reactor digesting FW was unsuccessful (L. Zhang et al., 2012). However, there was a correlation between process performance and trace element content during continuous digestion. Decreasing Co, Mo, Ni, and Fe concentrations were postulated as reasons for worsened digester performance (L. Zhang et al., 2012). A follow-up study examined if long-term AD of FW in a semi-continuous single-stage reactor could be stabilized through trace element supplementation (Co, Fe, Mo, Ni) in the long term (L. Zhang & Jahng, 2012). Stable FW AD was achieved for 368 days by supplementing trace elements, and a high methane yield (352-450 mL CH_4/g VS_{added}) with minimal VFA accumulation was achieved with an OLR of 2.19-6.64 g VS/L*day and an HRT between 20-30 days. This study found that iron was essential to maintaining stable methanogenesis (L. Zhang & Jahng, 2012). Methane production of a long-term laboratory-scale semi-continuously fed anaerobic digester treating FW was severely inhibited at a VFA concentration of 30,000 mg/L and an OLR of 4.0 g VS/L*d without trace element supplementation (W. Zhang et al., 2015). Supplementing trace elements (Fe, Co, Ni, Se) improved methane yield to approximately 465.4 mL CH_4/g VS_{added} without inhibitory VFA accumulation at an OLR between 1.0- 5.0 gVS/L*d and an HRT of 40 days (W. Zhang et al., 2015).

Additionally, trace element content in FW differs regionally. Synthetically generated FW composed of 79% fruits and vegetables, 5% pasta and rice, 6% bread and bakery, 8% meat and fish, and 2% dairy product was assembled in The Netherlands (Delft) and the USA (Tampa, FL) with differing trace element contents (Ariunbaatar et al., 2016b). The FW prepared in The Netherlands had a lower trace element content than the FW prepared in the USA. Trace elements (Fe, Co, Ni, Zn, Mn, Cu, Se, and Mo) were supplemented individually and in mixtures with different results based on the two FW sources. The most effective trace elements for the FW

prepared in The Netherlands were Fe, Se, Ni, and Co, while the most effective trace element for the FW prepared in the USA was Se. Regardless of the FW source, Se resulted in a 30-35% increase in biomethane production at 25-50 µg/L (Ariunbaatar et al., 2016b). Therefore, trace element origin should be considered, as food trace element content differs regionally.

The microbial communities formed from FW AD have also been studied regarding how they relate to supplementing trace elements. Laboratory-scale digesters digesting FW were used to investigate the effect of Co, Ni/Mo/B, and Se/W on biogas production and the microbial community (Feng et al., 2010a). The highest methane production was related to high Se/W concentrations (0.80 mg/L / 1.80 mg/L) in combination with a low concentration of Co (0.060 mg/L). There was a limited influence of supplementing trace elements on bacterial community composition. At the same time, the maintenance of methanogenic activity was independent of community composition, suggesting high functional redundancy in methanogens involved in AD (Feng et al., 2010a). A deficiency in essential trace elements in FW greatly limited the growth and metabolism of hydrogenotrophic methanogens and *Methanosarcina*, ultimately leading to propionate inhibition. Supplementing a digester with trace elements (Fe, Co, Mo, Ni) enhanced process stability, maintained the dominant growth of *Methanosarcina*, and sustained stable concentrations of hydrogenotrophic methanogens (~10%) (W. Zhang et al., 2019).

While trace element content in FW AD has been investigated, gaps in the knowledge remain. FW is not a homogenous material. Trace element content in a food type may differ depending on the region it is collected (Ariunbaatar et al., 2016a). Table 1 indicates the need for more studies to explicitly list the food types used in their FW AD studies. Since FW is not homogenous, further classifying food types would increase understanding of how to supplement trace elements in FW AD more effectively.

Additionally, the inoculum used in FW AD is another critical consideration regarding trace element supplementation studies, as high trace element content in an inoculum may remove the need for some or all trace element supplementation (Facchin et al., 2013; Parra-Orobio et al., 2018; Yazdanpanah et al., 2018). Overall, there is still a lack of knowledge regarding the complex synergistic relationships between trace element-dependent enzymes used during the four stages of AD. Therefore, it is crucial to understand the metabolic pathways involving trace element-dependent enzymes.

1.4 Anaerobic Digestion Process

The AD process can be broken down into four stages: hydrolysis, acidogenesis, acetogenesis, and methanogenesis (Figure 1). The AD process depends on distinct and complex interactions between microorganisms carrying these four stages. The AD processes are described in the following sections.

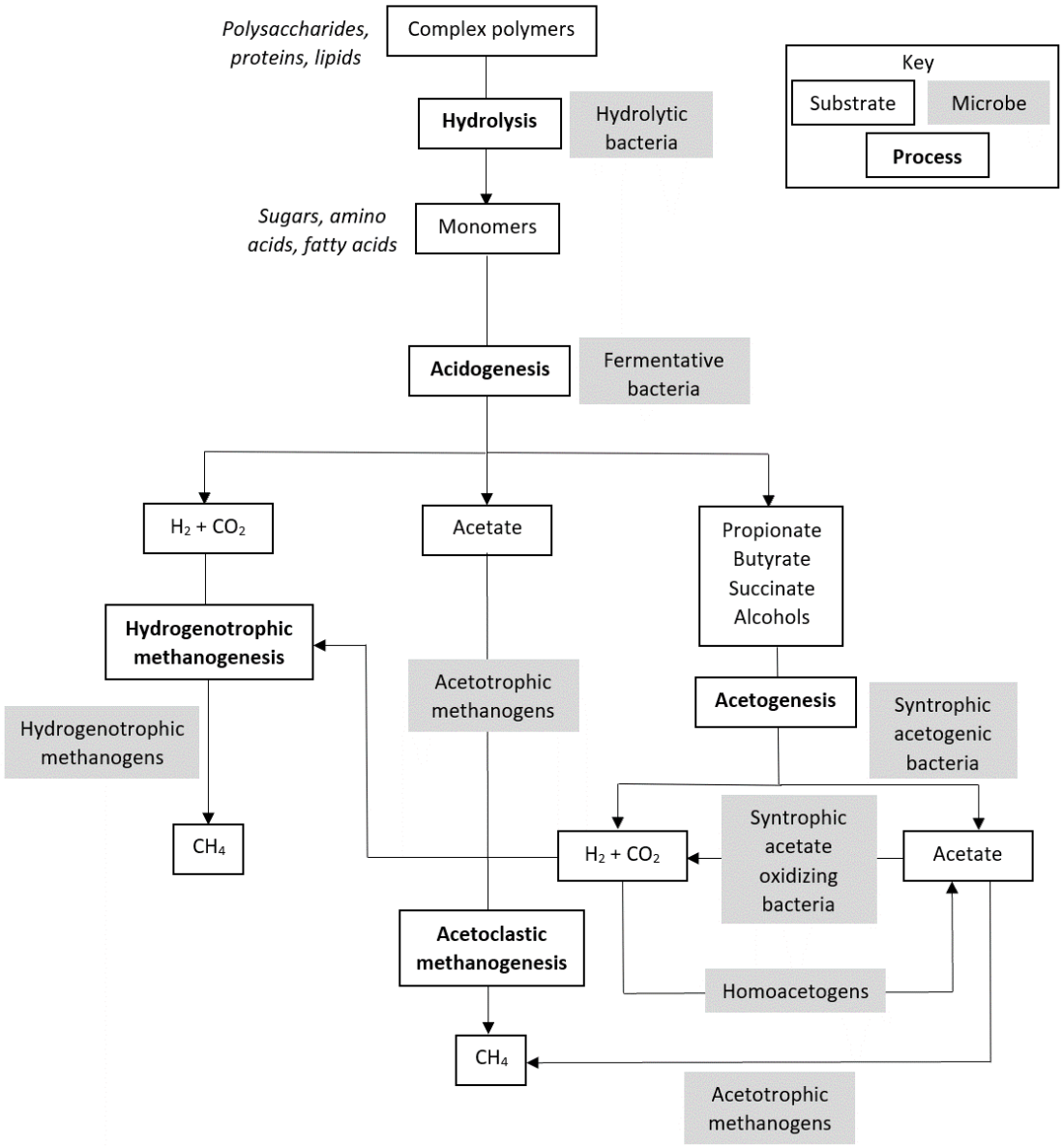

Figure 1. Overall anaerobic digestion process (adapted from Arsova et al., 2010)

Hydrolysis

Hydrolysis is the first stage of AD, where large, inaccessible macromolecules are broken down for use by bacteria in acidogenesis. Hydrolytic bacteria secret extracellular enzymes that convert carbohydrates, lipids, and proteins into simple sugars, long-chain fatty acids, and amino acids, respectively (Rahman et al., 2018). Lipases convert lipids into long-chain fatty acids,

proteases convert proteins into amino acids, and carbohydrates (i.e., cellulose, starch) are converted to monosaccharides by cellulase, amylases, and pectinases (Velmurugan et al., 2014). It is important to note that some carbohydrate molecules, such as lignin, cellulose, and hemicellulose, are more challenging to break down, so enzymes are often added to aid in their hydrolysis (Meegoda et al., 2018). Hydrolytic enzymes are usually activated with trace elements, particularly calcium and magnesium (Gamble et al., 2012; Oumer & Abate, 2017; Pereira et al., 2017).

Hydrolysis is often thought of as the rate-determining step in AD, meaning the overall rate of AD is determined by hydrolysis, the slowest step. However, when FW is used as the sole substrate, especially at a relatively high OLR, the rate of hydrolysis and acidogenesis may be higher than that of methanogenesis, which can lead to VFA accumulation and process failure (P. Wang et al., 2018). Lastly, hydrolysis generally has an optimum temperature between 30-50°C and an optimum pH between 5-7 (Meegoda et al., 2018). The chemical reaction of hydrolysis is displayed in equation 4 (Velmurugan et al., 2014).

$$(C_6H_{10}O_5)n + nH_2O \rightarrow n(C_6H_{12}O_6) \quad \textbf{(4)}$$

Hydrolysis, the rate-limiting step, must be optimized to enhance FW AD performance. The hydrolysis rate of FW is dependent on many factors, including pH, particle size, particle structure, adsorption of enzymes onto FW, and FW characteristics. Hydrolysis of FW can be improved through physical, thermo-chemical, and biological pretreatments and co-digestion with other organic substrates with a higher buffer capacity and optimum nutrient balance (C. Zhang et al., 2014).

pH plays a vital role in hydrolysis performance. Batch AD of kitchen wastes in a two-phase digester showed that pH adjustment could improve hydrolysis and acidogenesis rates (B.

Zhang et al., 2005). A pH adjustment to pH 7 provided optimum working conditions for the AD of kitchen waste compared with pH 5, 9, and 11 (B. Zhang et al., 2005).

Additionally, hydrolytic enzymes required different optimal pH conditions in a two-stage mesophilic AD of solid potato waste (Parawira et al., 2005). Carbohydrates, proteins, and lipids present in FW cannot directly be taken up by the cell. Cells produce hydrolytic enzymes to break down macromolecules into their monomers to facilitate transport into the cell membrane. Some key hydrolytic enzymes are amylase, carboxymethyl cellulase, filter paper cellulase, xylanase, pectinase, and protease. Amylase, carboxymethyl cellulase, and filter paper cellulase had the highest activities, and these enzymes had optimal pH conditions of 5.0, 5.0, and 6.0, respectively. Since enzymatic breakdown is the primary mechanism in hydrolysis, determining enzymatic activity is a direct way to study hydrolysis (Parawira et al., 2005).

Hydrolysis also depends on substrate properties, including particle size. Hydrolysis benefits from FW substrates being in close contact with microorganisms via adsorption since hydrolytic enzymes are secreted into the media (Angelidaki & Sanders, 2004). In addition to the placement of FW substrates, FW particle size is related to hydrolysis. Particle size reduction via mechanical pretreatments aid in the hydrolysis of organic matter due to an increased surface area for adsorption of hydrolytic enzymes (Agyeman & Tao, 2014). Multiple studies found that particle size is one of the most critical factors in FW AD (Izumi et al., 2010; I. S. Kim et al., 2000; Palmowski & Müller, 2000). Digestion of FW pretreated with a meat grinder having different aperture diameters (2.5, 4, and 8 mm) found that the reduction of particle size from 8 to 2.5 mm increased methane production from 10-29% and specific methane yield by 9-34% when co-digested with dairy manure (Agyeman & Tao, 2014). The optimum particle size for FW AD

is 1.02 mm for thermophilic batch digestion (I. S. Kim et al., 2000) and 0.718 mm for mesophilic batch digestion (Izumi et al., 2010).

Other pretreatments of FW that have improved hydrolysis are ultrasonic treatment and biological pretreatment. Ultrasonication in a first stage reactor followed by the second stage had higher biodegradability and the highest methane yield (3.2 L CH_4/L) in a FW AD study (Elbeshbishy & Nakhla, 2011). The optimum conditions in an up-flow anaerobic sludge blanket (UASB) for FW hydrolysis were an enzyme mixture ratio of 1:2:1 (carbohydrase: protease: lipase), 0.2% (w/w FW) of the mixture dose, and a 10 h hydrolysis reaction. (Moon & Song, 2011). Pretreatment of feedstock allows for quicker hydrolysis of material processed by the next stage of AD: acidogenesis.

Acidogenesis

Acidogenesis (or fermentation) is the second stage of AD. Compounds produced in hydrolysis are converted into VFAs and other products, such as ethanol (equation 8) and lactic acid (equation 9), by anaerobic bacteria (Velmurugan et al., 2014). The main VFAs made in this stage are acetic acid (equation 5), propionic acid (equation 6), butyric acid (equation 7), and valeric acid. Acetic acid produced in this stage is directly used in methanogenesis, while the other larger VFAs are further broken down in acetogenesis.

Acidogenesis is generally the quickest AD stage, as acidogenic bacteria have a regeneration time of fewer than 36 h (Meegoda et al., 2018). Consequently, VFA accumulation is often reported as a cause of digester failure (W. Zhang et al., 2020). Additionally, a product of amino acid breakdown during this stage is ammonia, which at high enough concentrations, is also known to inhibit AD systems (Rajagopal et al., 2013). Equations 2-6 display important acidogenesis chemical reactions (Velmurugan et al., 2014).

$$C_6H_{12}O_6 + 2H_2O \rightarrow 2CH_3COOH + 4H_2 + CO_2 \quad \textbf{(5)}$$

$$C_6H_{12}O_6 + 2H_2 \rightarrow 2CH_3CH_2COOH + 2H_2O \quad \textbf{(6)}$$

$$C_6H_{12}O_6 \rightarrow CH_3CH_2CH_2COOH + 2H_2 + 2CO_2 \quad \textbf{(7)}$$

$$C_6H_{12}O_6 \rightarrow 2CH_3CH_2OH + 2CO_2 \quad \textbf{(8)}$$

$$C_6H_{12}O_6 \rightarrow 2CH_3CHOHCOOH \quad \textbf{(9)}$$

As stated earlier, the products of acidogenesis are VFAs known to accumulate and cause AD failure in a system degrading readily biodegradable material, such as FW. The effect of pH on hydrolysis and acidogenesis has been investigated in numerous studies. One study looking at the impact of pH and inorganic nutrient supplementation (Ca, Fe, Co, Ni) on hydrolysis and acidogenesis found that the optimal pH was 7 (in terms of VS removal and sCOD production). A secondary experiment found that reactors supplemented with nutrients showed a higher VFA production and higher hydrolysis rates (in terms of VS removal and sCOD production), implying the importance of nutrient supplementation for hydrolysis and acidogenesis (M. Kim et al., 2003). An optimal pH of 7 was determined in a study digesting kitchen wastes in a two-phase AD system (B. Zhang et al., 2005). At this pH, 86% of total organic carbon (TOC), 82% of COD were solubilized, and a maximum VFA concentration of 36 g/L was achieved by the fourth day. For this study, acidogenesis was the rate-limiting step, most likely due to the long retention time (32 d) (B. Zhang et al., 2005). In R. Wang et al. (2021), VFA content reached a maximum at pH 6, while acetic and formic acid production was highest at a pH of 7 with 78.70% of carbon converted to acetic and formic acids at pH 7. A maximum VFA yield at pH 6 is also in agreement with the reports of (K. Wang et al., 2014) and (J. Jiang et al., 2013).

Trace elements may also play a role in acidogenesis, but their influence is not well studied. Supplementing trace elements (Cr, Cd, Pb, Cu, Zn, Ni) were found to be toxic acetic and

butyric acid. The relative toxicity of trace metals to acetic acid and butyric acid was Cu > Zn > Cr > Cd > Pb > Ni and Cu > Zn > Cr > Cd > Ni > Pb, respectively (C.-Y. Lin, 1993). Cu was the most toxic, and Pb was the least toxic trace element to VFA-producing organisms. Still, the other tested trace metals significantly inhibited the production of butyric acid rather than that of acetic acid (C.-Y. Lin, 1993).

The effects of temperature and HRT on the acidogenesis stage of AD have also been investigated. When the reactor temperature was changed over three hours in 5 °C increments (30 °C to 15 °C) with HRTs of 6, 12, 24, and 48 hrs, the degradation efficiency of the substrate in acidogenesis was significantly affected by the temperature drop at short HRT. However, the stability of the reactor slowly recovered (Cha & Noike, 1997). Additionally, the number of acidogens, homoacetogens, and hydrogenotrophic methanogens were not affected by the rapid temperature drop. Still, a complete washout of acetotrophic methanogens was observed at 15 °C (Cha & Noike, 1997).

Acetogenesis

Acetate, produced from acidogenesis, is a direct substrate for acetotrophic methanogenesis. VFAs with two or more carbons produced from acidogenesis cannot be directly used for methanogenesis. Acetogenesis is the process in which higher VFAs (and other intermediates) are converted into acetate with hydrogen and carbon dioxide as byproducts (Meegoda et al., 2018).

Lipids undergo a different acetogenic pathway from acidogenesis called β-oxidation. β-oxidation produces acetate from long-chain fatty acids (Meegoda et al., 2018). It should also be noted that only long-chain fatty acids with an even amount of carbon can be directly converted into acetate. Long-chain fatty acids with an odd amount of carbons are first converted into

propionate (Meegoda et al., 2018). Equations 7-11 below are the critical chemical reactions for acetogenesis (Velmurugan et al., 2014).

$$CH_3CH_2OH + H_2O \rightarrow CH_3COOH + 2H_2 \quad \textbf{(10)}$$

$$2CH_3CH_2OH + 2CO_2 \rightarrow CH_4 + 2CH_3COOH \quad \textbf{(11)}$$

$$CH_3CH_2COOH + 2H_2O \rightarrow CH_3COOH + 3H_2 + CO_2 \quad \textbf{(12)}$$

$$CH_3CH_2CH_2COOH + 2H_2O \rightarrow 2CH_3COOH + 2H_2 \quad \textbf{(13)}$$

$$CH_3CHOHCOOH + H_2O \rightarrow CH_3COOH + CO_2 + 2H_2 \quad \textbf{(14)}$$

An obligate syntrophic relationship exists between acetogens and methanogens. An example of synthrophy in AD is acetogenesis products as substrates for methanogenesis. Lower hydrogen partial pressure is favored, so thermodynamics favor acetogenesis (Bajpai, 2017). At standard conditions of 1 atm of hydrogen, the conversion between VFA and alcohols to acetate is prevented. A relationship between hydrogen partial pressure and favorable conversion has been determined. For example, the transformation of propionate to acetate and hydrogen does not become favorable until the hydrogen partial pressure decreases below 10^{-4} atm (Mccarty, 1982). Hydrogenotrophic methanogens utilize hydrogen gas to produce methane and maintain a low hydrogen partial pressure in an AD system.

Acetogenesis is a critical stage in AD since it consumes VFAs that can cause system failure when in abundance. This process also produces acetate, hydrogen, and carbon dioxide that can be used as substrates for both hydrogenotrophic and acetotrophic methanogenesis. Optimizing the acetogenesis stage of AD has been widely studied related to different system parameters. Co-digesting FW with pig manure digestate as leachate, containing high microbial quantity and abundance, improved hydrolysis and acidification and enhanced acetogenesis and methanogenesis (Qian et al., 2019). VFAs are an essential intermediate in AD, and their

degradation by acetogens is not fully realized. Amani et al. (2011) investigated the syntrophic AD of VFAs using an enriched acetogenic and methanogenic culture in a mesophilic batch reactor of synthetic wastewater. Optimum conditions for VFA degradation and biogas production were 937.5 mg/L propionic acid, 3275.5 mg/L butyric acid, 2319.5 mg/L acetic acid, 45 h retention time, and 2.2 methanogen:acetogen population ratio. Propionic acid was found to be the most critical parameter because it influenced all responses and reduced the performance of the AD process (Amani et al., 2011).

Temperature is another essential parameter for AD. A maximum methane yield (0.23 L CH_4/g COD_{added}) from FW AD was observed under mesophilic conditions at an OLR of 6.7 g COD/L*d (HRT 30 d). The system failed under thermophilic conditions (M.-S. Kim et al., 2017). Additionally, low concentrations of propionate and acetate in mesophilic conditions indicated successful acetogenesis and methanogenesis. In contrast, syntrophic acetogenesis was the rate-limiting step under the thermophilic condition (M.-S. Kim et al., 2017). The effect of digestate recirculation and temperature on the AD of FW and microbial communities has also been studied (Zamanzadeh et al., 2016). Mesophilic digesters with and without recirculation of digestate were stable with similar performance in terms of methane yield (480 mL CH_4/g VS_{added}). *Methanosaeta* (an acetotrophic methanogen) was the dominant archaea for both. However, *Firmicutes* dominated the mesophilic recirculation system while *Chloroflexi* dominated the mesophilic system without recirculation. The phylum *Firmicutes* contains the genus *Clostridium,* commonly found in most AD systems (Qian et al., 2019). The phylum *Chloroflexi* is also commonly abundant in AD systems (Nelson et al., 2011). *Clostridium* includes proteolytic and saccharolytic bacteria and syntrophic species involved in the degradation of VFAs (Zamanzadeh et al., 2016). *Chloroflexi* is closely related to homoacetogens that actively transcribe genes

involved in sugar fermentations, gluconeogenesis (transformation of non-carbohydrate substrates into glucose), and the Wood-Ljungdahl pathway (Vuillemin et al., 2020). The abundance of *Chloroflexi* in the mesophilic system indicated that an additional abundance of pathways involved in homogenesis was necessary in the absence of recirculation.

Acetogenesis in AD has been studied by using an acetogen-enriched sludge as an inoculum. Using an acetogen-enriched sludge as an inoculum improved the substrate utilization rate and acetate percentage in VFAs compared to the control AD system without adding acetogen-enriched sludge. Additionally, CO_2 sparging from the headspace of the reactors also improved acetate yields by 3.16 times compared to the control (H. Liu et al., 2017).

Methanogenesis

Methanogenesis is the final stage of AD, where methanogens, obligate anaerobic archaea, convert intermediate products into methane and carbon dioxide (Rahman et al., 2018). There are two main pathways for methanogenesis: acetotrophic methanogenesis and hydrogenotrophic methanogenesis. Acetotrophic methanogenesis utilizes acetate as a substrate and accounts for approximately 2/3 of methane production. In contrast, hydrogenotrophic methanogenesis reduces carbon dioxide into methane and accounts for about 1/3 of methane production (Meegoda et al., 2018). Additionally, methanogenesis from methanol, methylamines, and formate has been observed but is much less common.

Methanogenic bacteria require a higher pH than the other three stages in AD and have a slower regeneration time (5-16 days) (Meegoda et al., 2018). The essential chemical reactions for methanogenesis are below (equations 15 and 16) (Velmurugan et al., 2014).

$$CH_3COOH \rightarrow CH_4 + CO_2 \quad \textbf{(15)}$$

$$CO_2 + 4H_2 \rightarrow CH_4 + 2H_2O \quad \textbf{(16)}$$

Methanogenic anaerobes are highly studied since these organisms produce methane, the final product of AD. The distribution of methanogenic communities is dependent on feedstock composition. One study found that FW anaerobic digesters contained a greater abundance of syntrophic acetate oxidizing populations, indicating that co-digestion with FW may improve the functional diversity of AD (de Jonge et al., 2020). Syntrophic microorganisms are of great interest for AD management because these organisms exist in mutualistic partnerships with other microorganisms (Sieber et al., 2012). An example of a syntrophic relationship is between hydrogenotrophic methanogenesis and syntrophic acetate oxidation. The fate of acetate in AD is to either be consumed directly by acetotrophic methanogens or oxidized by acetate-oxidizing bacteria (Dyksma et al., 2020). These pathways are detailed in Figure 2. Syntrophic acetate-oxidizing bacteria produce carbon dioxide and hydrogen gas that are consumed by hydrogenotrophic methanogens. A shift from acetotrophic methanogenesis to hydrogenotrophic methanogenesis via syntrophic acetate oxidation can occur during ammonia stress above 3 g/L (Schnürer & Nordberg, 2008). The shift from the acetotrophic methanogenesis to the syntrophic acetate oxidation pathway resulted in a twofold decrease in biogas and methane yield (Schnürer & Nordberg, 2008). Therefore, the role of syntrophic acetate-oxidizing bacteria is vital in understanding the mechanisms controlling the AD of FW.

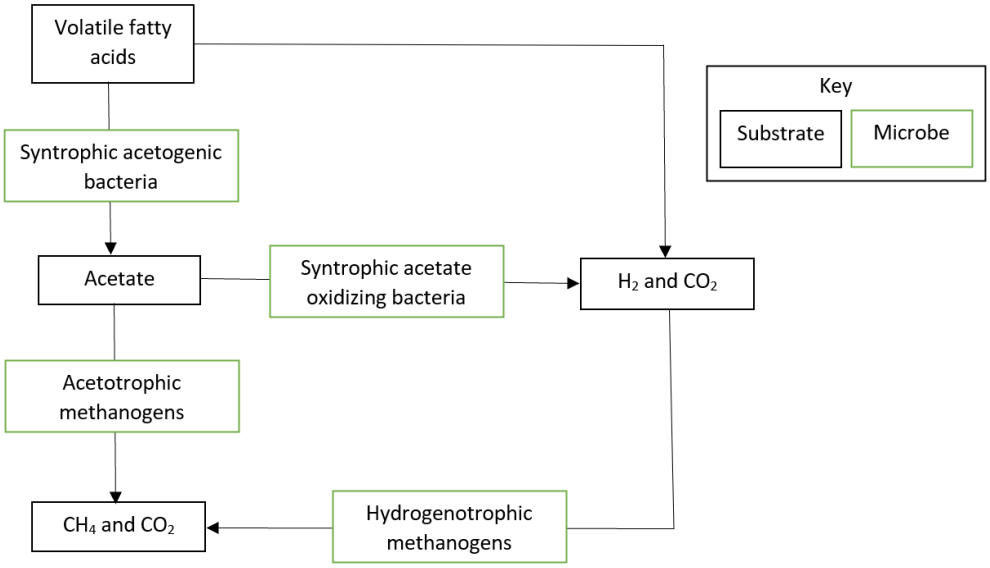

Figure 2. Acetogenic and methanogenic pathways in AD adapted from (Source: Magrí et al., 2019)

The effect of OLR on AD performance has also been studied. Cho et al. (2013) investigated mesophilic dry FW AD performance with increasing OLRs. Microbial analysis of methanogenic communities was also determined. Stable dry AD of FW was achieved through HRT control without alkali agents. At an HRT of 40 days, methane production, methane content, and volatile solids reduction rate were 2.51 ± 0.17 $m^3/m^3/d$, 66 ± 2.1%, and 65.8 ± 1.22%, respectively. The shift from hydrogenotrophic to acetotrophic methanogens resulted in a reduction in genus diversity but indicated an acclimation to dry conditions (Cho et al., 2013).

Trace elements also play an essential role in the methanogenesis stage of AD. FW AD is often inhibited by VFA accumulation, mainly from propionate, and a deficiency of essential trace elements in FW has been cited as the fundamental reason (W. Zhang et al., 2019). Trace element content in the FW AD decreased as new feedstock was added and digestate was removed, limiting the growth of hydrogenotrophic methanogens and *Methanosarcina*. *Methanosarcina* can utilize acetate, methanol, or carbon dioxide to produce methane. In one study, *Methanosarcina* was replaced by *Methanosaeta*, causing a decline in methanogenic

community diversity and ultimately leading to propionate inhibition. Trace element supplementation (Fe, Co, Mo, Ni) improved process stability with the dominant growth of *Methanosarcina* and enhanced methanogenic community diversity (W. Zhang et al., 2019).

FW often contains high concentrations of salt. AD inhibition of acetotrophic methanogens due to high salt concentrations has been observed (Rinzema et al., 1988). Low NaCl levels improved hydrolysis and FW's acidogenesis but inhibited methanogenesis, while high levels of NaCl inhibited both acidogenesis and methanogenesis.

1.5 Essential Trace Elements Used in Metabolic Pathways in AD

A summary of essential microorganisms involved in the four stages of AD is listed and detailed in Table 2. The microbial communities involved in FW AD are of growing interest. Hydrolysis and acidogenesis involve most of the microbial diversity in an AD reactor (de Jonge et al., 2020).

Table 2. Important microorganisms to AD and their metabolic processes (Luo et al., 2019; Müller et al., 2010; Qian et al., 2019)

Stage of AD	**Microbes**	**Metabolic processes**
Hydrolysis	*Clostridium*	Produce cellulase, protease, and hydrolytic enzymes that degrade complex organic matter
Acidogenesis	*Clostridium* *Phodopseudomonas* *Syntrophobacter* *Syntrophus* *Syntrophomonas*	Hydrogen producing – ethanol fermentation pathway Metabolic product: Acetate $C_6H_{12}O_6 + 2H_2O \rightarrow 2CH_3COOH + 2CO_2 + 4H_2$ $CH_3CH_2CH_2COOH + 2H_2O \rightarrow 2CH_3COOH + 2H_2$ $CH_3CH_2CH_2COOH + 2H_2O \rightarrow 2CH_3COOH + CO_2 + 3H_2$
Acidogenesis	*Mycobacterium* *Desulfatibacillum* *Streptosporangium* *Rhodopseudomonas* *Methylobacterium*	Hydrogen producing - ethanol fermentation pathway Metabolic product: ethanol $C_6H_{12}O_6 \rightarrow CH_3CH_2OH + 2CO_2$ $CH_3CH_2OH + 2H_2O \rightarrow CH_3COOH + 2H_2$ $C_6H_{12}O_6 + H_2O \rightarrow CH_3CH_2OH + CH_3COOH + 2CO_2 + 2H_2$
Acidogenesis	*Clostridium* *Bacillus* *Bacteroides* *Syntrophobacter* *Methylobacterium*	Hydrogen producing – butyrate fermentation pathway Metabolic products: acetate, butyrate $C_6H_{12}O_6 \rightarrow CH_3CH_2CH_2COOH + 2CO_2 + 2H_2$ $4C_6H_{12}O_6 \rightarrow CH_3CH_2CH_2COOH + 2CH_3COOH + 8CO_2 + 8H_2$
Acidogenesis	*Rhodopseudomonas* *Pseudomonas* *Mycobacterium*	Hydrogen consuming – propionate fermentation pathway Metabolic products: acetate, propionate $C_6H_{12}O_6 + 2H_2 \rightarrow CH_3CH_2COOH + 2H_2O$

	Streptomyces *Acidovorax*	$3C_6H_{12}O_6 \rightarrow 4CH_3CH_2COOH + 2CH_3COOH + 2CO_2 + 2H_2O$
Acidogenesis	*Clostridium* *Bacillus* *Lactobacillus* *Chloroflexus* *Blastopirellula*	Hydrogen consuming – lactate fermentation pathway Metabolic product: lactate $C_6H_{12}O_6 \rightarrow 2CH_3CH(OH)COOH$ $C_6H_{12}O_6 \rightarrow CH_3CH(OH)COOH + CH_3CH_2OH + CO_2$
Acetogenesis	*Clostridium* *Acetobacterium* *Butyribacterium* *Eubacterium* *Peptostreptococcus* *Sporomusa*	Hydrogen consuming – homoacetogenesis (also referred to as the Wood-Ljungdahl pathway) Metabolic product: acetate $2CO_2 + 4H_2 \rightarrow CH_3COOH + 2H_2O$
Acetogenesis	*Syntrophomonas* *Syntrophus* *Smithella* *Desulfotomaculum thermobenzoicum ssp. thermosyntrophicum*	Hydrogen producing –syntrophic acetogenesis (propionate) Metabolic product: acetate $CH_3CH_2COO^- + 2H_2O \rightarrow CH_3COO^- + CO_2 + 3H_2$ $CH_3CH_2COO^- + 2H_2O + 2CO_2 \rightarrow CH_3COO^- + 3HCOO^- + 3H^+$
Acetogenesis	*Syntrophobacter* *Pelotomaculum*	Hydrogen producing –syntrophic acetogenesis (butyrate) Metabolic product: acetate

		$CH_3CH_2CH_2COO^- + 2H_2O \rightarrow 2CH_3COO^- + H^+ + 2H_2$ $CH_3CH_2CH_2COO^- + 2H_2O + 2CO_2 \rightarrow 2CH_3COO^- + 2HCOO^- + 2H^+$
Methanogenesis	*Euryarchaeota*	Acetate to methane pathway $CH_3COO^- + H^+ \rightarrow CO_2 + CH_4$ H_2/CO_2 to methane pathway $4H_2 + CO_2 \rightarrow CH_4 + 2H_2O$ Methanol to methane pathway $4CH_3OH \rightarrow CH_4 + 2H_2O$ Methanol/hydrogen to methane pathway $CH_3OH + H_2 \rightarrow CH_4 + H_2O$ Formic acid to methane pathway $4HCOO^- + 4H^+ \rightarrow CH_4 + 3CO_2 + 2H_2O$ Carbon monoxide to methane pathway $4CO + 2H_2O \rightarrow CH_4 + 3H_2O$

Hydrolytic Bacteria

Hydrolysis is the first stage of AD where large organic polymers such as starches, cellulose, proteins, and fats are broken down into their respective monomers by enzymes called hydrolases. Hydrolases are enzymes that catalyze covalent bond breakage using water. Some important groups of hydrolases involved in hydrolysis are detailed in Table 3. *Bacteroidetes* and *Firmicutes* are the main phyla of bacteria involved in AD hydrolysis (P. Wang et al., 2018).

Metal-binding is intertwined with the proper functioning of hydrolases. Most of the hydrolases listed in Table 3 are activated by magnesium (Mg) and calcium (Ca) and are inhibited by mecurity. To the author's knowledge, no research has been done on how Ca and Mg affect the hydrolysis of an AD system digesting FW. Based on the literature summarized in Table 3, there is a relationship between the presence of Mg and Ca and the activation of essential hydrolases involved in AD. A literature review synthesizing information regarding trace metal bioavailability in AD signaled a need to understand how Ca and Mg are critical to the optimal operation of AD (Thanh et al., 2016). The information summarized in Table 3 may contain vital information regarding the importance of Ca and Mg in hydrolysis.

Table 3. Hydrolytic enzyme trace element activators/inhibitors

Enzyme	Substrate	Product(s)	Trace element	Source
Proteinase	Proteins	Amino acids	Activator: Calcium (possibly other divalent metal ions)	Gamble et al., 2012
Cellulase	Cellulose	Cellobiose, glucose	Activators: Barium, Magnesium, Calcium, Cobalt Inhibitors: Iron, Nickel, Cadmium, Mercury, Lead	Pereira et al., 2017
Hemicellulase	Hemicellulose	Sugars (i.e., glucose, xylose, mannose, arabinose)	Activators: Magnesium, Calcium Inhibitors: Cadmium, Manganese, Zinc, Silver, Mercury, Lead, Cobalt	Pereira et al., 2017
Amylase	Starch	Glucose	Activators: Cobalt, Maganese Inhibitor: Mercury	Prakash et al., 2011
Lipase	Fats	Fatty acids, glycerol	Activator: Calcium	Hertadi & Widhyastuti, 2015
Pectinase	Pectin	Sugars (i.e., galactose, arabinose, polygalacticuronic acid)	Activators: Calcium, Magnesium (Oumer & Abate, 2017)	Oumer & Abate, 2017

The literature presented in Table 3 regarding activation and inhibition of hydrolases by trace elements was not done concerning AD. Therefore, the role of Ca and Mg in the activation of hydrolases involved in AD still needs to be developed and tested. The vital trace elements required by metalloenzymes in the hydrolytic pathways are summarized in Table 4. Metalloenzymes are enzymes that contain trace elements (metals) essential to active site formation, cofactor functioning, or enzyme structure.

Fermentative Bacteria

Fermentative bacteria degrade hydrolysis products into short-chain organic acids such as propionic acid, butyric acid, acetic acid, alcohols, CO_2, and H_2. It is difficult to distinguish between acidogenic and acetogenic pathways since acetate and hydrogen are produced during both stages (Bajpai, 2017). Both acidogenic and acetogenic bacteria belong to diverse microbial groups that include facultative anaerobes (i.e., can live in anaerobic and aerobic conditions) and obligate anaerobes (i.e., can only live in anaerobic environments). The dominant phylum involved in acidogenesis includes *Bacteroidetes, Chloroflexi, Firmicutes, and Proteobacteria* (P. Wang et al., 2018).

Enzymes in the acetate-ethanol type fermentation (AET) pathway include alcohol dehydrogenase and aldehyde: ferredoxin oxidoreductases. Alcohols are often produced from the digestion of lignocellulose-derived biomass or gases such as H_2, CO_2, and CO. One method for ethanol production in anaerobic digestion is the reduction of intermediate acetyl-CoA with NADH (an electron donor) by aldehyde and alcohol dehydrogenase (Nissen & Basen, 2019). Zinc plays a vital role in alcohol dehydrogenase as it plays a role in catalytic events and helps maintain the enzyme's structural stability (Auld & Bergman, 2008). Another method for alcohol production is through the direct reduction of intermediate organic acids with reduced ferredoxin

(another electron donor). This reaction is catalyzed by aldehyde: ferredoxin oxidoreductases. This oxygen-sensitive enzyme contains tungsten or molybdenum and is found in many anaerobes (Nissen & Basen, 2019). Acetyl-CoA synthase is the enzyme that catalyzes the reaction between acetyl-CoA and acetate in the AET pathway. The active site of this enzyme contains a [4Fe-4S] cluster bridged to a Cu-Ni site (Seravalli et al., 2003). The abundance of acetate in the AET pathway is strongly associated with the functional enzymes in the acetyl-CoA pathway and syntrophic acetogenic pathway (Müller et al., 2010).

There are two distinct pathways to produce propionate in the propionate-type metabolic (PTF) pathway. One pathway is the reduction of pyruvate into lactate via lactate dehydrogenase and then reducing lactate into propionate by propionate dehydrogenase (H.-S. Lee et al., 2008). No information was found regarding trace metal bindings for these two enzymes. Acetate and CO_2 are byproducts of the PTF pathways and can be used by both acetotrophic and hydrogenotrophic methanogens (Zhou et al., 2018). For the butyrate-type metabolic pathway (BTF), pyruvate is converted to acetyl-CoA via pyruvate dehydrogenase, and intermediates are catalyzed by thiolase 3-hydroxybutyrl-CoA dehydrogenase and butyryl-CoA dehydrogenase. Lastly, butyryl-CoA is catalyzed by either phosphotransbutyrylase and butyrate-kinase or by butyryl-CoA: acetate CoA-transferase (Zhou et al., 2018). The products of this pathway are butyrate, acetate, and H_2. A mammalian pyruvate dehydrogenase has been found to have Mg^{2+} dependent catalytic subunits (Roche et al., 2001), and thiolases contain both K^+-activated and K^+-independent members (Marshall & Bruning, 2021). No information was found regarding the other enzymes mentioned above. Lastly, the lactate-type fermentation (LTF) pathway converts glucose or other organic substrates into lactic acid (Zhou et al., 2018). Pyruvate is converted into lactate via lactate dehydrogenase with either two moles of lactate as the product or one mole of

lactate produced along with CO_2 and ethanol (Castillo Martinez et al., 2013). The trace element cobalt is involved in substrate binding and reduction in lactate dehydrogenase (Morpeth & Massey, 1982).

The mixed-acid metabolic pathway (MAF) oxidizes organic monomers into various substrates, such as acetate, propionate, butyrate, valerate, etc., with possible CO_2 and H_2 production (Zhou et al., 2018). This pathway combines the fermentation pathways mentioned previously and is used during acidogenesis with acetate and butyrate as primary metabolites (Zhou et al., 2018).

The known key trace elements required by metalloenzymes in the acidogenesis pathways are summarized in Table 4.

Syntrophic Acetogenic Bacteria

In syntrophic acetogenesis, intermediates produced in acidogenesis (i.e., propionate, butyrate, ethanol, etc.) are converted to acetate, H_2, and CO_2. Synergistic bacteria might play an essential role throughout AD, even though their relative abundance is relatively small, and that relationship is not fully realized. Syntrophic acetogenesis is crucial because it consumes VFAs (i.e., propionic acid) inhibiting methanogenesis even at neutral pH (P. Wang et al., 2018).

Several bacteria are known to degrade propionate and butyrate within a synergistic relationship with methanogens. Syntrophic acetogenic bacteria degrade propionate and other fatty acids that belong to genera *Syntrophobacter, Pelotomaculum, and Smithella propionica. Syntrophomonas, Thermosyntropha,* and *Syntrophus* (Müller et al., 2010; P. Wang et al., 2018). The processes for butyrate and propionate degradation are further detailed in Figure 3. The grey boxes represent enzymes that catalyze the reactions and are abbreviated as follows: PCT, propionate CoA transferase; MCE, methylmalonyl-CoA epimerase; MCM, methylmalonyl-CoA

mutase; SCS, succinyl-CoA synthase; SDH, succinate dehydrogenase; FHT, fumarase (fumarate hydratase); MDH, malate dehydrogenase; ODC, oxaloacetate decarboxylase; PFO, pyruvate: ferredoxin oxidoreductase; PFL, pyruvate formate lyase; POT, propionyl-CoA: oxaloacetate transcarboxylase; BAT, butyryl-CoA: acetateCoA transferase; ACD, acyl-CoA dehydrogenase; ECH, enoyl-CoA hydratase; 3-HCD, 3-hydroxybutyryl-CoA dehydrogenase; ACA, acetyl-CoA acetyltransferase.

Five enzymes require various trace elements in the propionate and butyrate pathways. These enzymes are bolded in Figure 3. The first enzyme is methylmalonyl-CoA mutase, a vitamin-B12-dependent enzyme that catalyzes the formation of methylmalonyl-CoA to succinyl-CoA in the propionate degradation pathway (Figure 3). The trace element cobalt is a necessary component of vitamin -B12. The methylmalonyl-CoA pathway generates one ATP per molecule propionate and three electron pairs by oxidation of succinate to fumarate, oxidation of malate to oxaloacetate, and pyruvate conversion to acetyl-CoA and CO_2. Additionally, the pyruvate conversion to acetyl-CoA and CO_2 can be coupled to proton reduction or CO_2 reduction via pyruvate: ferredoxin oxidoreductases (Müller et al., 2010). It is important to note that pyruvate: ferredoxin oxidoreductase is a microbial enzyme that uses thiamine pyrophosphate, three iron-sulfur clusters [4Fe-4S], and coenzyme A (P. Y.-T. Chen et al., 2018). This alternative enzyme requires the trace element, iron, to function properly.

Another enzyme with a trace element component in the propionate degradation pathway is succinate dehydrogenase. This enzyme participates in the citric acid cycle and electron transport chain in microorganisms and catalyzes the oxidation of succinate to fumarate. This enzyme has four subunits. One subunit contains three iron-sulfur clusters: [2Fe-2S], [4Fe-4S], and [3Fe-4S], meaning it requires iron for proper functioning (Figueroa et al., 2001). Pyruvate

formate-lyase is another iron-sulfur protein within the propionate degradation pathway. Pyruvate formate-lyase catalyzes the conversion of pyruvate to formate and acetyl-CoA (Atteia et al., 2006). Pyruvate formate-lyase depends on iron for activation, and its iron center contains iron-sulfur clusters ($[2Fe\text{-}2S]^{2+}$ and $[4Fe\text{-}4S]^{2+}$) (Broderick et al., 1997).

The enzyme oxaloacetate decarboxylase is a carboxylase that converts oxaloacetate to pyruvate and CO_2 in propionate degradation. The cation Mn^{2+} is required for total enzymatic activity but can also be substituted by Mg^{2+}, Co^{2+}, Ni^{2+} or $Ca^{2+,}$ and the enzyme can be inhibited by Cu^{2+}, Zn^{2+}, coenzyme A and succinate (Jetten & Sinskey, 1995). Therefore, Mn^{2+} is also necessary for the proper functioning of the propionate degradation pathway.

Acetyl-CoA acetyltransferase was identified in the butyrate degradation pathway for containing a metal required for binding. This enzyme is a transferase that catalyzes the chemical reaction of acetoacetyl-CoA into coenzyme A and acetyl-CoA. A potassium ion is bound near the coenzyme A binding site and the catalytic binding site (Haapalainen et al., 2007). However, this enzyme does not require a trace element for proper functioning, as potassium is considered a macronutrient. Enzyme functioning improved 3-fold when potassium ion concentration increased from 0 to 40 mM KCl in a crystallographic and kinetic study (Haapalainen et al., 2007). A high-affinity binding site for a chloride ion was also identified for acetyl-CoA acetyltransferase.

The critical trace elements required by metalloenzymes in the propionate and butyrate degradation pathways are summarized in Table 4.

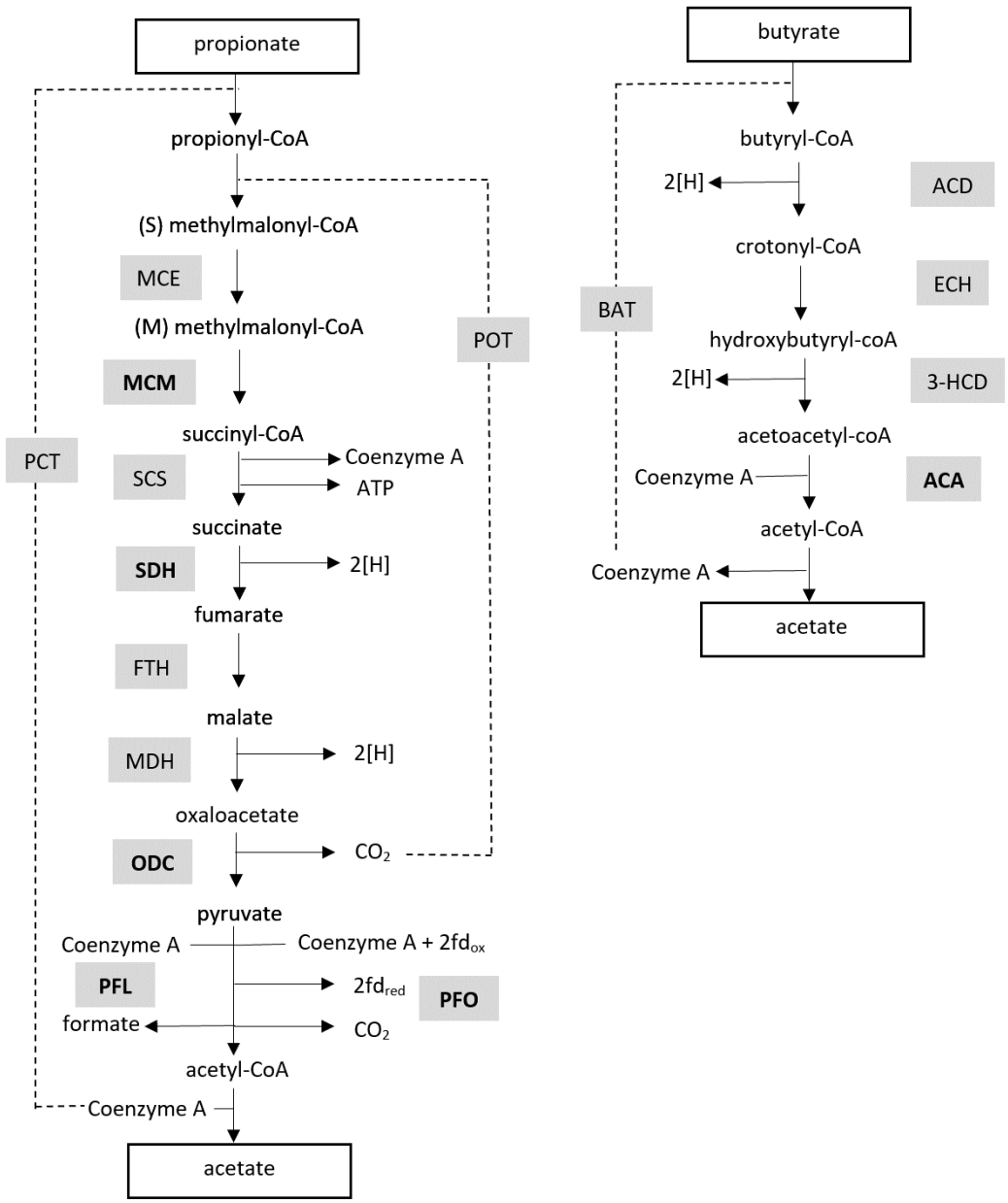

Figure 3. Propionate and butyrate degradation pathways with enzymes identified adapted from (Source: Kuever et al., 2014)

Homoacetogens

Homoacetogens are obligate anaerobes that use H_2 as an electron donor for the stepwise reduction of CO_2 to acetate (Ragsdale & Pierce, 2008). The homoacetogenic fermentation pathway, also referred to as the Wood-Ljungdahl pathway, comprises a methyl branch and a carbonyl branch (Figure 4). In the methyl branch, formate dehydrogenase is the enzyme that

catalyzes the reduction of CO_2 to formate. This enzyme contains the trace elements tungsten and molybdenum (Thanh et al., 2016) as well as iron and selenium (Ljungdhal, 1986). Another critical enzyme in the methyl branch of the Wood-Ljungdahl pathway is methyltransferase. This enzyme catalyzes the transfer of a methyl group and requires Mg^{2+} for activation (Bist & Rao, 2003). Additionally, the enzyme acetate kinase, which catalyzes the transfer of a phosphate from ATP to acetate, requires magnesium binding for proper functioning (Miles et al., 2001). In the carbonyl pathway, CO_2 is reduced to CO by acetyl-CoA synthase. CO is converted into acetyl-CoA, which is either converted to acetate through catabolism or cell carbon by anabolism (Zhou et al., 2018). Acetyl-CoA synthase contains a 4[Fe-4S] cluster bridged to a binuclear Cu-Ni site (Seravalli et al., 2003).

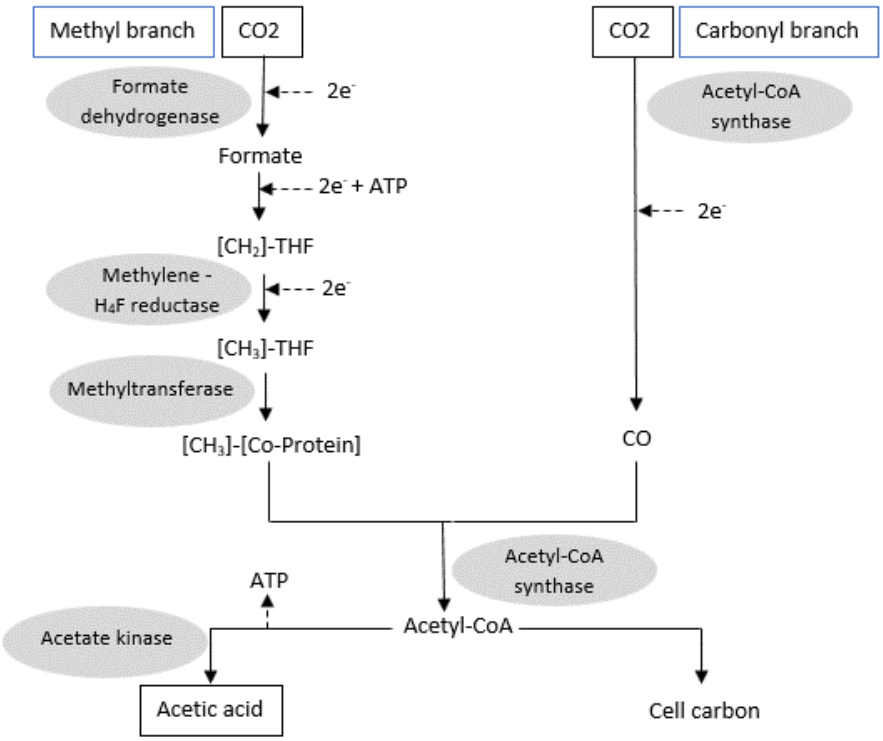

Figure 4. Homoacetogenic metabolic pathways for acetate production (THF, tetrahydrofolate; [Co-Protein], corrinoid enzyme] adapted from (Source: Zhou et al., 2018)

The critical trace elements required by metalloenzymes in the homoacetogenic fermentation pathway are summarized in Table 4.

Syntrophic Acetate Oxidizing Bacteria

The syntrophic acetate oxidizing pathway is an anaerobic process within acetogenesis in which syntrophic acetate oxidizing bacteria oxidize acetate to produce CO_2 and H_2. Currently, known genera capable of syntrophic acetate oxidation are *Thermacetogenium, Pseudothermotoga, Tepidanaerobacter, Chlostridium, and Syntrophaceticus* (Westerholm et al., 2016). Most syntrophic acetate oxidizing bacteria are in the same physiological group as homoacetogens, which are involved in the Wood-Ljungdahl pathway for acetate production (Westerholm et al., 2016). Additionally, syntrophic acetate oxidizing bacteria are slow growers (Hattori, 2008) and have a relatively high ammonia tolerance (H. Wang et al., 2015). In FW AD, where ammonia inhibition is common, it is essential to understand the relationship between trace elements and enzymes used by syntrophic acetate oxidizing bacteria in AD.

It has been suggested that syntrophic acetate oxidizing bacteria use the reverse of the Wood-Ljungdahl pathway for acetate oxidation (Hattori et al., 2005). However, a different pathway combining the methyl branch of the Wood-Ljungdahl and a glycine cleavage system has also been suggested (Nobu et al., 2015). In the reverse Wood-Ljungdahl pathway, the reaction of carbon monoxide converting to carbon dioxide is catalyzed by the enzyme carbon monoxide dehydrogenase, which contains iron, nickel, and zinc (Ljungdhal, 1986). The enzyme formyl tetrahydrofolate synthetase (not featured in Figure 4) is a critical enzyme in the Wood-Ljungdahl pathway that catalyzes the ATP-dependent activation of formate (Westerholm et al., 2016). All synthetic acetate oxidizing bacteria have access to a formyl tetrahydrofolate synthetase-related gene, which shows the importance of this enzyme in the syntrophic acetate

oxidation pathway (Westerholm et al., 2016). This enzyme does not have any known trace element component in its structure. Studies on acetogenic communities in mesophilic AD have revealed community shifts towards more syntrophic acetate oxidizing bacteria due to induced ammonia concentrations (Westerholm et al., 2011). The syntrophic acetate oxidizing pathway coupled with hydrogenotrophic methanogenesis is less efficient than acetotrophic methanogenesis, leading to lower methane production.

Methanogens

The two main pathways involved in methanogenesis are acetotrophic methanogenesis and hydrogenotrophic methanogenesis. Other pathways (i.e., methylotrophic methanogenesis) are not discussed in this document as the pathways involved are similar to the hydrogenotrophic pathway (Choong et al., 2016). Acetotrophic methanogens produce methane directly from acetate and produce approximately 70% methane in a typical AD system, while hydrogenotrophic methanogens produce approximately 30% methane in a digester (Mara & Horan, 2003). Acetotrophic methanogens belong to two genera: *Methanosaeta* and *Methanosarcina* (P. Wang et al., 2018). *Methanosarcina* can use acetate, hydrogen, methanol, and other substrates to produce methane. Commonly identified hydrogenotrophic methanogens in AD include *Methanobacterium, Methanothermobacter, Methanobrevibacter, Methanospirillum,* and *Methanoculleus* (P. Wang et al., 2018).

Metabolic pathways and enzyme reactions are widely studied in methanogenesis. Acetotrophic and hydrogenotrophic pathways undergo separate reactions, but both ultimately form methyl-tetrahydrosarconapterin and methyl-tetrahydromethanopterin. Several metalloenzymes catalyze these reactions (Choong et al., 2016). An enzyme in the acetotrophic pathway is carbon monoxide dehydrogenase/acetyl-coenzyme A synthase (Cdh) complex

enzyme containing iron and nickel (Harrop & Mascharak, 2005). An important metalloenzyme in the hydrogenotrophic pathway is formylmethanofuran dehydrogenase which has two isoenzymes that need molybdenum or tungsten for activation (Hochheimer et al., 1998). The enzyme carbonic anhydrase, which catalyzes the conversion of carbon dioxide to bicarbonate in methanogenesis, requires zinc for proper functioning (Glass & Orphan, 2012). Lastly, the enzyme $CH_3H_4M(S)PT$-coenzyme M methyltransferase contains the cofactor 5-hydroxybenimidazolylcobamide (factor III contains cobalt), while methyl coenzyme M reductase contains two nickel-containing F_{430} cofactors (Ferry, 2010). Hydrogenases are commonly found throughout methanogenesis and acetogenic pathways. This enzyme breaks down hydrogen gas into electrons and protons and contains iron and or nickel (Shima et al., 2002)

The critical trace elements required by metalloenzymes in the methanogenesis pathways are summarized in Table 4.

1.6 Summary of Essential Trace Elements in AD

Trace elements are often components of cofactors and enzymes required in relatively small amounts in biological systems. A deficiency in essential trace elements can limit the growth of microorganisms, can make an AD process unstable, and even cause the system to fail (Thanh et al., 2016). Trace elements are essential to the growth of microorganisms within an anaerobic digester. However, the amount of trace elements necessary to successfully digest without inhibition is still poorly understood. Therefore, it is essential to understand the trace element requirements for FW AD. A summary of trace elements identified as necessary to AD is listed below.

Table 4. Enzymes that require trace elements in various anaerobic digestion pathways

AD Stage	Pathway	Metalloenzyme	Key trace element
Hydrolysis	Protein degradation	proteinase	Ca
	Cellulose degradation	cellulase	Ba, Mg, Ca, Co
	Hemicellulose degradation	hemicellulase	Mg, Ca
	Starch degradation	amylase	Co, Mn
	Lipid degradation	lipase	Ca
	Pectin degradation	pectinase	Ca, Mg
Acidogenesis	Alcohol degradation	Alcohol dehydrogenase	Zn
	Alcohol degradation	aldehyde: ferredoxin oxidoreductases	Mo/W
	Acetate formation	acetyl-CoA synthase	Fe, Cu, Ni
	Butyrate production	pyruvate dehydrogenase	Mg
	Butyrate production	thiolase	K
	Lactate production	lactate dehydrogenase	Co
Acetogenesis	Propionate degradation	methylmalonyl-CoA mutase	Co
	Propionate degradation	pyruvate: ferredoxin oxidoreductases	Fe
	Propionate degradation	succinate dehydrogenase	Fe
	Propionate degradation	Pyruvate formate-lyase	Fe
	Propionate degradation	oxaloacetate decarboxylase	Mn
	Butyrate degradation	acetyl-CoA acetyltransferase	K
	Formate production	formate dehydrogenase	Mo/W, Fe, Se
	homoacetogenesis	methyltransferase	Mg
	homoacetogenesis	acetate kinase	Mg
	homoacetogenesis	acetyl-CoA synthase	Cu, Ni, Fe
	Carbon dioxide formation from carbon monoxide	carbon monoxide dehydrogenase	Fe, Ni, Zn
	hydrogen gas degradation	hydrogenases	Fe or Ni
Methanogenesis	Bicarbonate production from carbon dioxide	carbonic anhydrase	Zn
	CO_2 + MF → CHO-MF + H_2O	formylmethanofuran dehydrogenase	Fe, Mo/W
	MeOH + CoM → CH_3-CoM + H_2O	methyltransferase/factor III	Co
	CH_3-CoM + [H] → CH_4 + CoM	methyl-CoM reductase/F430	Ni
	hydrogen gas degradation	hydrogenase	Fe or Ni

Ca – Calcium, Co – Cobalt, Cu – Copper, Fe – Iron, Mg – Magnesium, Mn – Manganese, Mo – Molybdenum, Ni – Nickel, W – Tungsten, Zn - Zinc

Iron (Fe)

Iron is an essential metal to various enzymes in acidogenesis, acetogenesis, and methanogenesis. Iron is a crucial trace element in AD due to its large reduction capacity, meaning iron can gain electrons from various biochemical processes in AD (Myszograj et al., 2018). In acidogenesis, iron is a component of acetyl-CoA synthase, an enzyme that produces acetate, an essential intermediate in AD. Iron is critical to the proper functioning of enzymes in the propionate degradation pathway (refer to Table 4). Propionate degradation is a significant process in AD systems because propionate accumulation is often an indicator of process failure (Li et al., 2017). Iron is a component of iron-sulfur and iron-nickel clusters in acetyl-CoA synthase (Seravalli et al., 2003), pyruvate: ferredoxin oxidoreductase (Müller et al., 2010), and hydrogenase (Shima et al., 2002). Additionally, iron can act as a binding agent in sulfide precipitation, so it is often added to AD systems to precipitate formed sulfide and control the level of hydrogen sulfide in the biogas (Thanh et al., 2016). There is currently no known relationship between iron and hydrolysis in AD.

Cobalt (Co)

The central known role of cobalt in AD is as a component of vitamin B-12. This corrinoid can bind to coenzyme M methylase, catalyzing methane formation in acetotrophic and hydrogenotrophic methanogenesis (Thanh et al., 2016). Cobalt is critical to the enzyme methyltransferase, which catalyzes the transfer of one methyl group (Ferry, 2010). Additionally, carbon monoxide dehydrogenase, a widely used enzyme during acetogenesis, contains cobalt (Myszograj et al., 2018). Cobalt may play an essential role in activating cellulase, an enzyme that degrades cellulose during hydrolysis (Pereira et al., 2017). Additionally, cobalt is required by

lactate dehydrogenase (H.-S. Lee et al., 2008) in acidogenesis and required by methylmalonyl-CoA mutase during propionate degradation in acetogenesis (Müller et al., 2010).

Nickel (Ni)

Nickel is essential to many anaerobic bacteria when carbon dioxide and hydrogen are the only energy sources. The low molecular weight nickel tetrapyrrole, coenzyme F_{430}, contains nickel. This coenzyme is critical as it is contained within the methyl-coenzyme M reductase enzyme, which reduces methyl coenzyme M to methane in all methanogenic pathways (Ferry, 2010). Carbon monoxide dehydrogenase is a Ni-containing enzyme and may even aid in sulfur-reducing bacteria (Myszograj et al., 2018). Important enzymes containing an iron-nickel cluster are hydrogenase (Shima et al., 2002) and acetyl-CoA synthase (Zhou et al., 2018).

Zinc (Zn)

Zinc is a component of the enzyme formate dehydrogenase and hydrogenase. However, it has not been determined to be an essential trace element for methanogenesis (Myszograj et al., 2018). Additionally, zinc may play an important role in alcohol degradation, as zinc is required for alcohol dehydrogenase (Nissen & Basen, 2019). Zinc also plays a role in acetogenesis since the enzyme carbon monoxide dehydrogenase contains zinc (Ljungdhal, 1986). One study looking at the effect of zinc supplementation (provided as $ZnSO_4$ and $ZnCl_2$) during the anaerobic co-digestion of FW and domestic wastewater found that increasing zinc supplementation from 50 to 100 mg/L Zn^{2+} increased COD removal efficiency by 10% and increased the methane yield by 30-65% (Chan et al., 2019). Zinc was found in high concentrations (50-630 ppm) in 10 methanogenic bacteria (Scherer et al., 1983).

Copper (Cu)

The role of copper within methanogenesis has conflicting observations. While copper has been found in multiple methanogenic bacteria strains, no relationship between copper and biogas production has been determined. Copper has only been studied in trace element mixes, so more studies need to be done to assess the role of copper in biogas production if there is one (Myszograj et al., 2018). However, the enzyme acetyl-CoA synthase contains a binuclear Cu-Ni site (Seravalli et al., 2003).

Manganese (Mn) and Magnesium (Mg)

Manganese and magnesium play an essential role in acetogenesis and may be necessary for hydrolysis and acidogenesis. Manganese and magnesium can stabilize methyltransferase in bacteria that produce methane (Bist & Rao, 2003; Myszograj et al., 2018). In kinase reactions, manganese is often interchangeable with magnesium (Miles et al., 2001; Myszograj et al., 2018). However, it is still unclear if either manganese or magnesium are directly related to biogas production. In butyrate production, the enzyme pyruvate dehydrogenase has Mg^{2+} dependent catalytic subunits (Roche et al., 2001). Lastly, magnesium and manganese may play an essential role in hydrolases. Cellulase, hemicellulase, amylase, and pectinase are activated by manganese, magnesium, or both (Pereira et al., 2017). The relationship between magnesium/manganese and hydrolases should be studied further concerning the AD process.

Tungsten (W) and Molybdenum (Mo)

The enzyme formate dehydrogenase uses tungsten and molybdenum, catalyzing formate production by propionate oxidizers (Thanh et al., 2016). Some methanogenic bacteria have different forms of enzymes that contain tungsten and molybdenum for the same purpose. *Methanobacterium thermoautotrophicum* has two formylmethanofuran dehydrogenase iso-

enzymes, a W-containing form and a Mo-containing form (Thanh et al., 2016). The tungsten enzyme is made when either tungsten or molybdenum is available. However, if the growth medium contains molybdenum, the tungsten enzyme will have molybdenum instead of tungsten (Myszograj et al., 2018). The enzyme aldehyde: ferredoxin oxidoreductases is a Mo- or W-containing enzyme found in many anaerobes that play an important role in alcohol degradation (Nissen & Basen, 2019).

Molybdenum may inhibit sulfate-reducing bacteria, which limits the formation of necessary sulfides. However, studies have shown that molybdenum can stimulate methane production, but the requirement for both molybdenum and tungsten is higher in hydrogenotrophic methanogenesis when compared to acetotrophic methanogenesis. (Myszograj et al., 2018). This is most likely due to the enzyme formylmethanofuran dehydrogenase. This enzyme is used in the hydrogenotrophic methanogenic pathway and requires either molybdenum or tungsten for activation (Hochheimer et al., 1998).

Selenium (Se)

Selenium is not a strict trace metal, but it is vital for AD systems and is a component of several anaerobic bacterial enzymes and certain bacterial nucleic acids. A relationship between the stimulatory effect of selenium on growth was discovered. Selenium causes increased formate dehydrogenase (FDH) activity in *Methanococcus vannielii*, a strict anaerobic microorganism. Ultimately, decreased selenium levels in the influent can cause growth limitations in some methanogens, decrease microbial activity, and even lead to process failure (Thanh et al., 2016). In one study treating food industry waste to determine the effects of Co, Ni, Mo, B, Se, and W on biogas production, it was determined that the highest methane production was linked to the addition of selenium, tungsten, and cobalt (Feng et al., 2010b).

Other metals (Ca, K, Ba)

The roles of calcium, potassium, and barium in AD are still not clear. However, calcium seems to play an essential role in the activation of various hydrolases, including proteinase (Gamble et al., 2012), cellulase (Pereira et al., 2017), and hemicellulase (Pereira et al., 2017). Additionally, barium (Ba) may play a role in activating cellulase (Pereira et al., 2017). The specific role of calcium, magnesium, manganese, and barium in the hydrolysis of FW in AD still needs to be studied and classified. Thiolases contain K+-activated and K+-independent members (Marshall & Bruning, 2021). Thiolase catalyzes a reaction in butyrate production in acidogenesis. However, there is no studied relationship between the thiolase activation in butyrate production and potassium (K).

1.7 Objectives

Based on the current knowledge of metalloenzymes used in the four stages of AD, a lack of essential trace elements is expected to inhibit the FW AD process at various stages. However, there are no conclusive results on the impact of trace element supplementation on the activation of metalloenzymes utilized during hydrolysis in the literature. Additionally, there is still a lack of knowledge regarding the complex synergistic relationships between microorganisms and the metalloenzymes used in the four stages of AD. Trace elements are often added into AD systems without thoroughly understanding their effects on specific enzymes. The cause of the mixed results from trace element supplementation into the AD of FW is most likely due to differing FW compositions, inoculum characteristics and associated microbial community, and operating conditions (mesophilic vs. thermophilic, HRT, OLR, etc.).

The first part of this study (Ch 2 & 3) assessed the effect of trace element supplementation (Mg, Ca, Co, Fe, Cu, Ni, Mn, Se, Zn, Mo) on FW AD process productivity

(methane yield and organic matter destruction) using the gas density-based biomethane potential (BMP) method. The trace element mixture was designed to target the four main metabolic pathways in AD based on the literature. The findings in this study contribute to the knowledge of what roles trace elements play in the AD of FW and how adding trace elements required by enzymes used in different stages of the AD process affects process productivity (methane yield, VS destruction).

The latter part of this study (Ch 4) calculated the greenhouse gas reduction potential of anaerobically digesting multiple FW streams in Montgomery, VA. The purpose of this work was to generate an estimate of the total mass of FW in Montgomery, VA, use the results from the BMP analyses to inform the design of a theoretical community digester, and predict the greenhouse gas reduction potential of anaerobically digesting the FW instead of sending it to landfill. Equations for calculating greenhouse gas reduction were adapted from the Climate Action Reserve Organic Waste Digestion Project Protocol (Climate Action Reserve, 2014). The Excel spreadsheet used to calculate greenhouse gas reduction in this study has the potential to be used by other FW AD systems.

2. Materials and Methods

2.1 Feedstock and Inoculum Collection and Preparation

The FW was collected from the Southgate Food Processing Center at Virginia Tech, Blacksburg, VA. On a wet basis, it contained 17% whole wheat bread, 22% fruit (strawberries, Roma tomatoes), and 61% vegetables (potato skins, green cabbage, red cabbage, celery – stalks and leaves, green bell peppers, red bell peppers, red onions – flesh and skins). The FW was prepared by mixing two parts FW with one part DI water (mass basis). The mixture was homogenized into a slurry for 30 seconds using a Waring Commercial blender (Model CB15, Torrington, Connecticut). The FW slurry was diluted, prepared, and stored in 1 L plastic bottles, according to Table 5. Section 2.4 outlines analytical methods for each parameter.

Table 5. Dilutions, pretreatment, and storage of food waste slurry for analytical methods

Parameter	Dilution	Pretreatment	Storage
TS, VS, pH	1	None	Analyzed immediately
Alkalinity	2	None	Freezer storage at -20 °C
sCOD	100	Centrifuged (14,000 rpm for 20 min) Filtered (0.45 µm filer membrane)	Refrigeration at 4 °C
tCOD	100	None	Refrigeration at 4 °C

TS – Total solids

VS – Volatile solids

tCOD – Total chemical oxygen demand

sCOD – Soluble chemical oxygen demand

VFAs – Volatile fatty acids

The inoculum used was collected from the effluent of a secondary mesophilic (35°C) anaerobic digester at a local Water Resource Recovery Facility that has been active for 35 years (Montgomery County, VA). This digester treats primary sludge (OLR: 980 mg VS/L/day, HRT: 30 days) and thickened waste sludge from the aeration tank (OLR: 670 mg VS/L/day, HRT: 43 days). The inoculum was collected with three 2 L plastic containers, prepared using the same dilutions and pretreatments listed in Table 5 (columns 2 and 3), but was stored at ambient temperature (~ 20 °C) for a maximum of 5 days until use.

2.2 Experimental Design of Biomethane Potential Tests

The biomethane potential (BMP) test of FW was conducted using the gas density-based BMP method. This approach is based on measuring bottle mass loss and vented biogas volume in each sampling event. With both measurements, biogas density and composition were determined. The three treatments used in the BMP tests are described in Table 6. Treatment 1 (IR) contained inoculum only, treatment 2 (FR) contained inoculum and FW, and treatment 3 (FT) contained inoculum, FW, and 10 mL of the trace element solution. Table 7 outlines the details of the trace element solution. Treatments were prepared based on the VS concentration of the FW slurry and inoculum (inoculum-to-substrate ratio of 1.6:1). The mass of FW slurry and inoculum added was calculated using an online biogas app (OBA) (S. D. Hafner et al., 2018).

Table 6. The experimental design for the BMP test

Treatment	**Inoculum**	**Food waste**	**Trace element**
IR (IR1, IR2, IR3)	✓	n.a.	n.a.
FR (FR1, FR2, FR3)	✓	✓	n.a.
FT (FT1, FT2, FT3)	✓	✓	✓

n.a. – not applicable

Nine 1000 mL glass bottles with two connectors (Simax, Czech Republic) were used for the BMP tests (total volume: 1150 mL) (Figure 5). Each of the three caps was wrapped with Teflon tape to ensure an airtight seal to prevent leakage of biogas. The working volume for treatments IR and FR was 425 mL (headspace volume: 725 mL), and the working volume for treatment FT was 435 mL (headspace volume: 715 mL). Inoculum, FW slurry, and DI water were weighed using an electronic scale (PM4800 DeltaRange® scale, Mettler Toledo, Greifensee, Switzerland). For the IR treatment, 400 g of inoculum and 25 g of DI water were weighed and funneled into each bottle. For the FR and FT treatments, 400 g of inoculum was weighed, mixed with 25 g of FW, and then funneled into each bottle. Lastly, 10 mL of the trace element solution (Table 7) was pipetted into the FT treatments.

The headspace of each bottle was flushed to remove oxygen and ensure anaerobic conditions with N_2 gas from a gas cylinder (UN1066, GTS-Welco, Allentown, PA) attached to a pressure regulator to provide low pressure (Restek, Bellefonte, PA). Norprene tubing (6.4 mm ID) connected the pressure regulator to the headspace of each bottle, and the headspace was flushed for 30 seconds. Each bottle was capped (1 GL 45 cap, 2 GL 25 caps + 2 rubber septa) and weighed twice after venting with N_2 gas. The average of the two masses for each type of reactor was considered the "initial mass" for that respective bottle. Bottles were placed in a reciprocating incubator shaker (C25KC, New Brunswick Scientific, Edison, NJ) set at 37°C and 25 rpm.

Figure 5. BMP test bottle

Table 7. Mass of trace elements in the 1 L inorganic trace element salt solution

Trace element	Inorganic trace element salt	Salt mass (mg)	Trace element mass (mg)	Trace element concentration (mmole/L)
Iron	Iron (II) chloride pentahydrate, $FeCl_2*4H_2O$	356	100	1.79
Nickel	Nickel (II) acetate tetrahydrate, $C_4H_6NiO_4*4H_2O$	42.4	10	0.17
Selenium	Sodium selenite, Na_2SeO_3	11	5.0	0.06
Molybdenum	Ammonium molybdate tetrahydrate, $(NH_4)_6Mo_7O_{24}*4H_2O$	64.4	5.0	0.05
Magnesium	Magnesium chloride hexahydrate, $MgCl_2*6H_2O$	41.8	5.0	0.21
Calcium	Calcium chloride hexahydrate, $CaCl_2*6H_2O$	16.4	3.0	0.07
Zinc	Zinc gluconate hydrate, $C_{12}H_{24}O_{14}Zn$	28	4.0	0.06
Copper	Copper (II) sulfate pentahydrate, $CuSO_4*5H_2O$	9.8	2.5	0.04
Manganese	Manganese (II) chloride, $MnCl_2$	5.7	2.5	0.05
Cobalt	Cobalt (II) nitrate hexahydrate, $Co(NO_3)_2*6H_2O$	9.9	2.0	0.03

2.3 Incubation and Biogas Collection

The ambient pressure and temperature were recorded to standardize biogas volume. It was assumed that the collected biogas inside the syringe was at ambient temperature. A manometer (Figure 6) allowed the pressure to be kept nearly identical to the ambient value. The ambient pressure (in kPa) was measured using a barometer app (Barometer Plus), and the temperature was measured using a multiparameter meter (WTW Multi 3420, Cole-Parmer, Vernon Hills, IL).

The procedures for biogas collection were (1) remove one treatment from the incubator, (2) swirl the first bottle for 10 seconds, (3) weight bottle (pre-venting mass), (4) release biogas and measure biogas volume, (5) weight bottle (post-venting mass), (6) repeat until all bottles were measured. Masses were measured using an electronic scale (PM4800 DeltaRange® scale, Mettler Toledo, Greifensee, Switzerland). IR treatment bottles were removed from the incubator, and the first replicate (IR1) was gently swirled for 10 seconds. This allowed the contents to mix and encouraged CO_2 to equilibrate between the solution and the headspace. To prevent mass loss during mixing, effort was made to avoid contact between the liquid and septum. Before venting, each bottle was weighed and recorded as "pre-venting mass."

The biogas volume was measured using a 100 mL syringe, a manometer made from clear polyvinyl chloride (PVC) tubing (10 mm ID), smaller diameter tygon tubing (6.4 mm ID), plastic hose barb (hose fitting 1: 10 mm, hose fitting 2: 6.4 mm), a 21-gauge needle, and a three-way plastic valve (Figure 6). The manometer was filled with water and closed at one end to minimize water loss. Smaller diameter tubing connected the manometer to the three-way valve. Additionally, the small diameter tubing connected the syringe to the three-way valve and connected the three-way valve to the needle attached to the BMP reactor.

First, the valve connection was opened from the needle to the syringe, which allowed the biogas to flow into the syringe. After a maximum of 70 mL of biogas was collected, the valve connection was opened from the syringe to the manometer, and the syringe plunger was adjusted until the water levels were equal in the manometer. This volume was read and recorded off the syringe. The syringe was disconnected, and the biogas was pushed out into an exhaust snorkel. If the water levels were equal without any adjustment, biogas collection was ended as it was assumed the pressure in the headspace was at ambient pressure. If an adjustment was needed, the syringe was reattached, and the process was repeated.

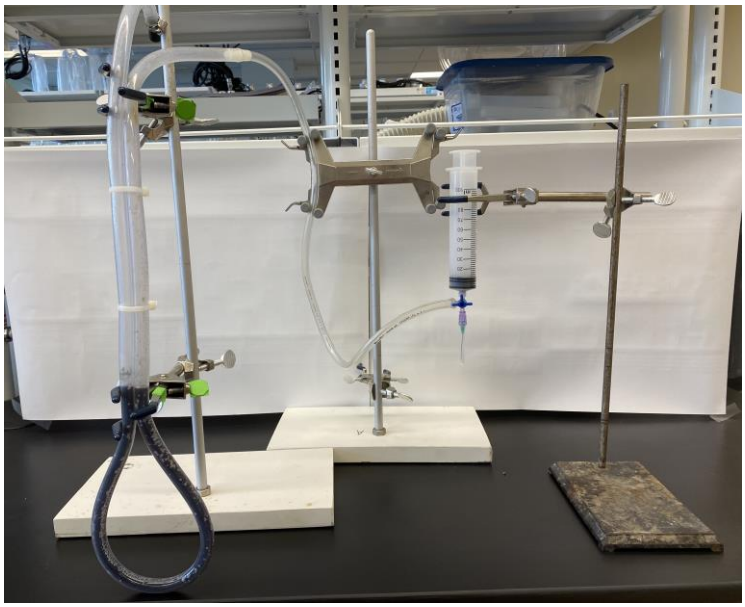

Figure 6. Biogas collection set up to measure biogas volume

After venting was completed, the bottle was weighed and recorded as “post-venting” mass. These steps were repeated for the next replicates (IR2, IR3). After all replicates were mixed, weighed, vented, and weighed again, the bottles were placed back in the incubator. These steps were repeated for each treatment (FR, FT). To minimize the uncertainty of headspace temperature used in calculations, the time the reactors spent outside of the incubator was kept as short as possible

The experiment ran for a period of 30 days. Biogas volumes were measured on days 1, 2, 3, 4, 5, 6, 8, 11, 14, 17, 20, 25, 30. At the end of the 30 days, samples from all treatments were taken and analyzed for TS, VS, tCOD, sCOD, and pH.

2.4 Sample Analysis and Data Processing

Samples of the FW slurry, inoculum, and the resultant digestate produced after the BMP test were analyzed for TS, VS, pH, tCOD, and sCOD. Alkalinity was also determined for the inoculum. Indicative values for an inoculum of good quality for digester performance were pH > 7.0 and < 8.5 and alkalinity > 3 g $CaCO_3$/L (Holliger et al., 2016). The FW slurry and inoculum were prepared according to Table 5. The digestate was kept at room temperature until all tests could be performed (2 days) and was prepared with the same dilutions and pretreatments listed in Table 5.

Total solids (TS) and volatile solids (VS) were analyzed according to Standard Methods (APHA, 2012). For TS analysis, roughly 10 g of the raw sample was placed in a crucible and dried in an oven at 105 °C for 24 hrs. The weight of the crucible without the sample (CW), the weight of the crucible with the wet sample (WSW), and the weight of the crucible and dried sample (DSW) were used to calculate TS (equation 17). For VS analysis, the dried solids were placed in a furnace at 550 °C for 1 hour and weighed to determine VS. The weight of the crucible and ash sample (ASW) was used to calculate VS (equation 18).

Total Solids Percentage (%) = $\frac{DSW-CW}{WSW-CW} * 100$ **(17)**

Volatile Solids on wet basis (%) = $\frac{DSW-ASW}{WSW-CW} * 100$ **(18)**

Total and soluble chemical oxygen demand (tCOD and sCOD) was analyzed according to the Hach Method 8000 (Hach, Loveland, CO). To determine tCOD, 2 mL of diluted sample (100 x dilution) was placed in a Hach HR COD digestion reagent vial (2415915, Hach, Loveland,

CO), digested for 2 hours at 150 °C (COD Reactor Model 45600, Hach, Loveland, CO), and analyzed on a spectrophotometer (DR2800, Hach, Loveland, CO). To determine sCOD, 20 mL of the diluted sample (100 x dilution) was added into a 25 mL centrifuge tube and centrifuged for 20 minutes at 14,000 rpm (5804R, Eppendorf, Hauppauge, NY). The supernatant was vacuum filtered using 0.45 µm filter paper (Filter RW03, Millipore, Billerica, MA). Then, 2 mL of the filtrate was placed in a Hach HR COD digestion reagent vial (2415915, Hach, Loveland, CO), digested for 2 hours at 150 °C (COD Reactor Model 45600, Hach, Loveland, CO), and analyzed on a spectrophotometer (DR2800, Hach, Loveland, CO).

Total alkalinity was analyzed by the burette titration method (APHA, 2012; Method 8221, Hach, Loveland, CO). To determine total alkalinity, 25 mL of the sample was mixed with 25 mL of DI water (2 x dilution). Then, 0.2 N sulfuric acid standard solution was added to a 25 mL burette to the zero mark, and the sample was titrated until pH 4.5 was reached. The total alkalinity was calculated based on the volume of sulfuric acid added to achieve a pH of 4.5, the normality of the acid (0.2 N), the volume of sample (25 mL), and a conversion factor in changing the normality into units of $CaCO_3$ (50,000) (Method 8221, Hach, Loveland, CO) (Equation 16). pH was measured using a multiparameter meter (WTW Multi 3420, Cole-Parmer, Vernon Hills, IL).

$$Total\ alkalinity\ \left(\frac{mg}{L}\ as\ CaCO_3\right) = \frac{mL\ sulfuric\ acid\ added * 0.2\ N * 50{,}000}{25\ mL} \quad \textbf{(19)}$$

To determine the pH of the FW slurry and the digestate, 20 g of the sample was mixed with 40 mL of DI water, stirred for 1 minute, allowed to rest for 30 minutes, and then measured by placing an electrode in the supernatant of the solution. To determine the pH of the inoculum, 40 mL of the sample was constantly stirred using a magnetic stirrer and magnetic stir plate. The pH

was immediately measured using a multiparameter meter (WTW Multi 3420, Cole-Parmer, Vernon Hills, IL).

Waste Stabilization

VS reduction (% VSR) was calculated for both treatments (FR and FT) to determine the amount of organic matter degraded during the 30-day digestion period. The following equation was used to calculate % VSR:

$$\% \, VSR = \frac{VS_{influent} - VS_{effluent}}{VS_{influent}} * 100 \quad \textbf{(20)}$$

Where,

$VS_{influent}$ is the VS of the mixture at day 0 (% wet basis) and $VS_{effluent}$ is the VS of the digestate at day 30 (% wet basis). $VS_{influent}$ was calculated (not measured) based on the mass of FW added, VS of FW measured, the mass of inoculum added, and the VS of inoculum measured. The following equation was used to calculate $VS_{influent}$:

$$VS_{influent} = \frac{(m_{FW,added} * VS_{FW}) + (m_{inoculum,added} * VS_I) + (m_{trace\ elements} * VS_{TE})}{m_{FW,added} + m_{inoculum,added} + m_{trace\ elements}} \quad \textbf{(21)}$$

Where,

$m_{FW,added}$ is the mass of FW added, VS_{FW} is the VS of FW measured (% wet mass), $m_{inoculum,added}$ is the mass of inoculum added, VS_I is the VS of the inoculum measured (% wet mass), $m_{trace\ elements}$ is the mass of the trace element solution added, and VS_{TE} is the VS of the trace element solution. It is important to note that the mass of trace element solution added was 10 g and it was assumed the trace element solution did not contain VS, TS, tCOD, or sCOD. Similar equations were used to determine the TS reduction (% TSR) of both treatments (FR and FT):

$$\% \, TSD = \frac{TS_{influent} - TS_{effluent}}{TS_{influent}} * 100 \quad \textbf{(22)}$$

$$TS_{influent} = \frac{(m_{FW,added} * TS_{FW}) + (m_{inoculum,added} * TS_I) + (m_{trace\ elements} * TS_{TE})}{m_{FW,added} + m_{inoculum,added} + m_{trace\ elements}} \quad \textbf{(23)}$$

Additionally, tCOD reduction was calculated for the FR and FT treatments. tCOD reduction was calculated to determine the amount of organic matter degraded over the 30-day period. The sCOD reduction was not calculated, as sCOD may increase overtime if more material is degraded and there is a higher proportion of soluble material available. The following equations were used to calculate tCOD (% tCODR):

$$\%\ tCODR = \frac{tCOD_{influent} - tCOD_{effluent}}{tCOD_{influent}} * 100 \quad \textbf{(24)}$$

$$tCOD_{influent} = \frac{(m_{FW,added} * tCOD_{FW}) + (m_{inoculum,added} * tCOD_I) + (m_{trace\ elements} * tCOD_{TE})}{m_{FW,added} + m_{inoculum,added} + m_{trace\ elements}} \quad \textbf{(25)}$$

Where the units of tCOD input into the equations were in mg/L.

Mole Fraction of Methane in Biogas

The equations used to calculate the mole fraction of methane in biogas were taken from (Hafner et al., 2020). Biogas density (ρ_b, g/mL) was estimated using the following equation:

$$\rho_b = \frac{\Delta m_b}{V_b} - c_{H_2O} \quad \textbf{(26)}$$

Where,

Δm_b is mass loss (g), V_b is the standardized biogas volume (mL) and c_{H_2O} is the water vapor content in the vented biogas (g/L).

The water vapor content (c_{H_2O}, g/L) used in equation 26 was estimated using the following equation:

$$c_{H_2O} = M_{H_2O} * \frac{p_{H_2O}}{p_{hs} - p_{H_2O}} * \frac{1}{v_b} \quad \textbf{(27)}$$

Where,

M_{H_2O} is the molar mass of water (18.02 g/mol), p_{H_2O} is the water vapor partial pressure (kPa), p_{hs} is the pressure of biogas in the bottle headspace prior to venting (kPa), and v_b is the molar volume of biogas at standard conditions (22,300 mL/mol). The headspace pressure, p_{hs}, is calculated from the ratio of vented biogas volume to headspace volume multiplied by the ambient pressure.

The p_{H_2O}, assumed to be at saturation, is calculated using the following Magnus-form equation:

$$p_{H_2O} = 0.61094 * e^{\frac{17.625*T_{hs}}{243.04+T_{hs}}} \quad \textbf{(28)}$$

Where,

T_{hs} is the headspace temperature at the time of venting (°C). The estimated headspace temperature during biogas venting was estimated as 30°C. The standardized biogas volume (V_b) used in equation 26 was calculated using the following equation:

$$V_b = V_{meas} * \frac{(p_{meas} - p_{H_2O})}{101.325\ kPa} * \frac{273.15\ K}{(T_{hs}+273.15)} \quad \textbf{(29)}$$

Where,

V_{meas} is measured volume (mL) (corrected for water vapor, temperature and pressure), p_{meas} is the measured ambient air pressure (kPa), p_{H_2O} is water vapor pressure (kPa) (calculated in equation 19), and T_{hs} is the gas temperature at the time of volume measurement, assumed to be 37°C. This equation combines Boyle's, Charles's, and Dalton's laws.

The molar mass of the biogas (M_b, g/mol) was calculated using the following equation:

$$M_b = \rho_b * v_b \quad \textbf{(30)}$$

The mole fraction of methane in biogas (x_{CH_4}, dimensionless) was calculated based on the following equation:

$$x_{CH_4} = \frac{M_{CO_2} - M_b}{M_{CO_2} - M_{CH_4}} \quad \textbf{(31)}$$

M_{CH_4} is the molar mass of CH_4 (16.04 g/mol), M_{CO_2} is the molar mass of CO_2 (44.01 g/mol), and M_b is the molar mass of biogas (g/mol), calculated in equation 30. It is assumed that the biogas contained only CH_4 and CO_4.

Calculation of BMP

BMP is expressed in standardized CH_4 volume per unit of mass of feedstock organic matter (VS) (mL CH_4/g VS). Specific methane production (SMP) refers to CH_4 yield from a particular feedstock. BMP is SMP over a particular duration. BMP of the feedstock (FW) was calculated by subtracting the CH_4 production (determined from blank reactors, mL) from the total CH_4 production from feedstock and inoculum (mL), normalized by feedstock VS mass. The equations used to calculate BMP and SMP were taken from (Hafner et al., 2020).

The blank treatment assessed the methane produced from the inoculum only. It was assumed that the volume of methane produced from the blank was the same volume of methane produced from the inoculum in the FW treatments (FR and FT). Therefore, methane produced from FW in the FR and FT treatments was calculated by subtracting off the average methane produced from the blank treatment.

The average methane produced from the blank reactors ($v_{CH4,I,j,t}$, mL) was calculated using the following equation,

$$\bar{v}_{CH4,I,t} = \frac{\sum_{j=1}^{k} v_{CH4,I,j,t}}{3} \quad \textbf{(32)}$$

Where,

$v_{CH_4,I,j,t}$ is the methane produced from the blank reactors (mL/g) and 3 is the number of IR replicates.

The CH_4 produced from the treatment reactors (FR and FT, net CH_4 production) ($V_{CH_4,S,i,t,net}$, mL) was calculated using the following equation.

$$V_{CH_4,S,i,t,net} = V_{CH_4,S,i,t} - \bar{v}_{CH_4,I,t} \quad \textbf{(33)}$$

Where,

$V_{CH_4,S,i,t}$ is the cumulative standardized volume of CH_4 produced in reactor *i* containing inoculum and feedstock at time *t* (mL), $\bar{v}_{CH_4,I,t}$ is the cumulative standardized volume of CH_4 produced in reactor *j* with inoculum only (mL). This calculation was done for each day (t) that a measurement was taken (1, 2, 3, 4, 5, 6, 8, 11, 14, 17, 20, 25, 30).

SMP (mL/g) for an individual reactor was calculated by normalizing CH_4 production ($V_{CH_4,S,i,t,net}$, mL) by feedstock VS mass ($m_{VS,S,i}$, g). BMP was directly calculated by dividing the SMP at day 30 by k, the number of replicates.

$$\text{SMP} = \frac{V_{CH_4,S,i,t,net}}{m_{VS,S,i}} \quad \textbf{(34)}$$

$$BMP = \frac{\sum_{i=1}^{n} SMP}{k} \quad \textbf{(35)}$$

2.5 Statistical Analysis

Statistical analyses were performed using JMP Pro 16® desktop software (SAS Institute Inc., Cary, NC). The data were tested for normality and a one-way analysis of variance (ANOVA) was used to test treatment effects. A Tukey's multiple comparison test was performed to test the differences in means of TS reduction, VS reduction, tCOD reduction, methane fraction, average cumulative biogas produced, average cumulative methane produced, specific methane potential, and biomethane potential of the IR, FR, and FT treatments. Significance level (α) was set at 0.05.

3. Results and Discussion

3.1 Food Waste, Inoculum, and Digestate Characteristics

The FW and inoculum were characterized for the BMP test before being mixed. The FW and inoculum were characterized by the following tests: pH, TS, VS, tCOD, sCOD. The inoculum was also tested for total alkalinity. The FW and inoculum characteristics of interest are expressed as mean (± standard deviation) in Table 8.

Table 8. Mean (± standard deviation) characteristics of the food waste feedstock and inoculum

Parameter	**Units**	**Food waste feedstock**	**Inoculum**
pH	--	5.06 (± 0.01)	7.81 (± 0.04)
TS	% wet basis	10.6 (± 0.1)	1.33 (± 0.01)
VS	% wet basis	10.1 (± 0.1)	1.01 (± 0.01)
VS/TS	%	95.1 (±0.07)	75.6 (± 0.4)
tCOD	g/L	110 (± 7)	18.8 (± 0.3)
sCOD	g/L	55.4 (± 16.7)	0.61 (± 0.22)
Total alkalinity	mg/L $CaCO_3$	--	4540 (± 122)

TS – Total solids

VS – Volatile solids

tCOD – Total chemical oxygen demand

sCOD – Soluble chemical oxygen demand

VFAs – Volatile fatty acids

The FW characteristics were within the range compared to the literature; for instance, pH is reported to be (3.9 -6.1) (Agyeman & Tao, 2014; Elbeshbishy et al., 2012; K. Wang et al., 2014; B. Zhang et al., 2005), VS/TS (80% – 97%) (Ren et al., 2018; Wulansari & Kristanto, 2015; B. Zhang et al., 2005; R. Zhang et al., 2007), tCOD (91 g/L -166 g/L) (Elbeshbishy et al., 2012, p.; Wulansari & Kristanto, 2015; B. Zhang et al., 2005), and sCOD (25 g/L - 60 g/L) (Elbeshbishy et al., 2012; K. Wang et al., 2014; B. Zhang et al., 2005).

The high VS/TS ratio (organic content), tCOD and sCOD indicated that the FW would be highly degradable and, therefore, a desirable feedstock for AD. The total alkalinity of the FW was assumed to be zero since total alkalinity is negligible below a pH of 4.5. The inoculum characteristics exhibited very similar values to those found in the literature (Bayr & Rintala, 2012; Bohutskyi et al., 2016; Elbeshbishy et al., 2012). The inoculum was of good quality since the alkalinity exceeded 3,000 mg/L $CaCO_3$ and the pH was between 7.0-8.5 (Holliger et al., 2016). The inoculum did not contain large granules. Therefore, it was not blended or diluted before the BMP test to avoid any disturbance to the microbial communities. Additionally, the inoculum was not pre-incubated as there is no significant difference in methane yield using the pre-incubated versus non-incubated inocula (Elbeshbishy et al., 2012).

3.2 Waste Stabilization

TS and VS Reductions

The feedstock and effluent characteristics are presented in Table 9. The average reductions in TS for the IR, FR, and FT treatments were 12%, 38%, and 40%, respectively, and the average reductions in VS for the IR, FR, and FT treatments were 14%, 45%, and 47%, respectively. There was a difference ($p<0.05$) in the TS reduction and VS reduction between the three treatments. The TS and VS reduction of the IR treatment was significantly different than

that of the FR and FT treatments, but no difference was detected between the FR and FT treatments.

The values for VS reduction in this study were lower than values found in the literature. VS reduction of FW is generally 70-80% since FW is a highly biodegradable material (J. Lin et al., 2011; R. Zhang et al., 2007). VS reduction depends greatly on particle size. It has been studied that decreasing the substrate particle size from 3.2 mm to 1.3 mm increased VS reduction from 35.2% to 60.3% (Hills & Nakano, 1984). The FW in this study was initially blended with water; however, the resulting mixture was not sieved. Larger particles in the FW may have contributed to the lower TS reduction and, therefore, VS reduction as microorganisms had a more challenging time breaking down the larger particle sizes (Izumi et al., 2010).

tCOD Reduction

The average tCOD reduction for the FR and FT treatments was 39% and 42%, respectively. The average tCOD reduction for the IR treatment was negative, therefore it was not compared to the FR and FT treatments. There was no difference ($p>0.05$) between the tCOD reductions between the FR and FT treatments. The sCOD accounted for an average of 16% and 17% of the tCOD of the feedstock for treatments FR and FT, respectively. The sCOD was 4% and 5% of the tCOD of the digestate for treatments FR and FT, respectively. The decrease of the sCOD fraction in the tCOD over the 30-day digestion period shows that most of the FW degraded was in the soluble form. While the value for tCOD reduction was low, it is compatible with the findings from TS and VS reduction in this study and is potentially due to the large particle sizes in the FW feedstock.

pH

The mean digestate pH from the three treatments (IR, FR, and FT) were not different ($p > 0.05$) from each other. The pH of the AD system was not controlled, as the bottles were sealed for the duration of the digestion (30 days). However, many inferences can be made from the digestate pH of the treatments. The ideal pH range for AD is narrow (6.8-7.2), and the ideal pH for methanogenesis is 7.0 (Ward et al., 2008). The pH of the digestate for the IR, FR, and FT treatments were 7.95, 7.92, and 7.86, respectively. The digestate pH for all treatments was higher than the ideal range for AD, specifically, methanogenesis. Excessively alkaline pH (> 7.5) values can lead to the disintegration of microbial granules and potential process failure (Sandberg & Ahring, 1992, p.). Additionally, free ammonia is considered the leading cause of inhibition of methanogenesis. A study found that the free ammonia in an anaerobic digester (pH 7, 35 °C) was < 1% of the total ammonia. However, when the pH was raised to 8, the free ammonia increased to 10% of the total ammonia (Fernandes et al., 2012; Rajagopal et al., 2013). Total nitrogen concentration was not measured in this study. However, assumptions about free ammonia can be made from the digestate pH values. The pH of the digestate of each treatment at the end of the 30 days was roughly 8. This coincides with the decrease in biogas production (<1% cumulative biogas production) towards the end of the 30 days. It is possible that free ammonia was accumulating by the end of the digestion period, causing high pH and inhibiting methanogenesis.

Table 9. Mean (± standard deviation) characteristics of the IR, FR, FT treatments

Parameter	Feedstock			Digestate		
	IR	**FR**	**FT**	**IR**	**FR**	**FT**
pH	--	--	--	7.95 (± 0.08)	7.92 (± 0.16)	7.86 (± 0.16)
TS (%)	1.25 *	1.89 *	1.84 *	1.10 (± 0.31)	1.20 (± 0.05)	1.10 (± 0.04)
VS (%)	0.95 *	1.55 *	1.51 *	0.82 (± 0.12)	0.85 (± 0.04)	0.80 (± 0.04)
tCOD (g/L)	17.72 (± 0.004) *	24.29 (± 0.08)*	23.72 (± 0.04)*	22.72 (± 8.02)	14.79 (± 1.78)	13.59 (± 0.86)
sCOD (g/L)	0.58 (± 0.0001) *	3.96 (± 0.14)*	3.78 (± 0.02)*	0.63 (± 0.10)	0.59 (± 0.05)	0.62 ± 0.03)

* Indicates calculated value based on food waste and inoculum characteristics, not measured in lab

TS – Total solids

VS – Volatile solids

tCOD – Total chemical oxygen demand

sCOD – Soluble chemical oxygen demand

VFAs – Volatile fatty acids

3.3 Biogas and Methane Production

The replicate FT2 was excluded from the analysis. The total amount of biogas produced from FT2 was less than the total biogas produced from the IR treatment. The average cumulative standardized (101.325 kPa, 273.15 K) biogas produced was 310 mL, 1534 mL, and 2168 mL for the IR, FR, and FT treatments, respectively. The average total standardized (101.325 kPa, 273.15 K) methane produced from the same treatments were 227 mL, 933 mL, and 1146 mL, respectively. The total standardized biogas and methane produced for the FR and FT treatments were corrected for IR by subtracting off the average cumulative biogas and methane produced by the IR treatment from the FR and FT treatment.

3.4 Biogas Production

The average cumulative volumes of biogas produced from treatments IR, FR, and FT are presented in Figure 7. The average cumulative biogas produced from the IR treatment was lower than the biogas produced from the FR and FT treatments. This result makes sense as the IR treatments did not contain any FW.

Biogas Produced from the Treatments

The average cumulative biogas produced by the IR, FR and FT treatments over the 30-day period was 310 (± 154) mL, 1534 (± 316 mL), and 2168 (± 482) mL, respectively. There was sufficient evidence to conclude that there was a treatment difference in the mean cumulative biogas produced ($p < 0.05$) after 30 days. Additionally, the average cumulative biogas produced from the IR treatment differed from the average cumulative biogas produced from the FR and FT treatments. This makes sense as no FW was added to the IR treatment. Therefore, there would be significantly less biogas produced than treatments with FW added.

No difference was detected between the average cumulative biogas produced from the FR treatment and the average cumulative biogas produced from the FT treatment after 30 days. However, the average total biogas produced from the FR treatment was 41% lower than the average total biogas produced from the FT treatment. In the literature, adding trace elements into anaerobic digesters treating FW has increased the production of biogas (and methane). For instance, the addition of Fe, Se, Ni, and Co increased the biomethane production of FW AD by 39.2%, 34.1%, 26.4%, and 23.8%, respectively (Ariunbaatar et al., 2016c). However, the results of externally adding trace elements into FW AD are highly dependent on the initial concentration of trace elements in the feedstock and inoculum. No information was collected regarding the trace element content in the inoculum or the FW. In the future, that information should be measured to understand the entire picture of the initial trace element content in the feedstock and inoculum.

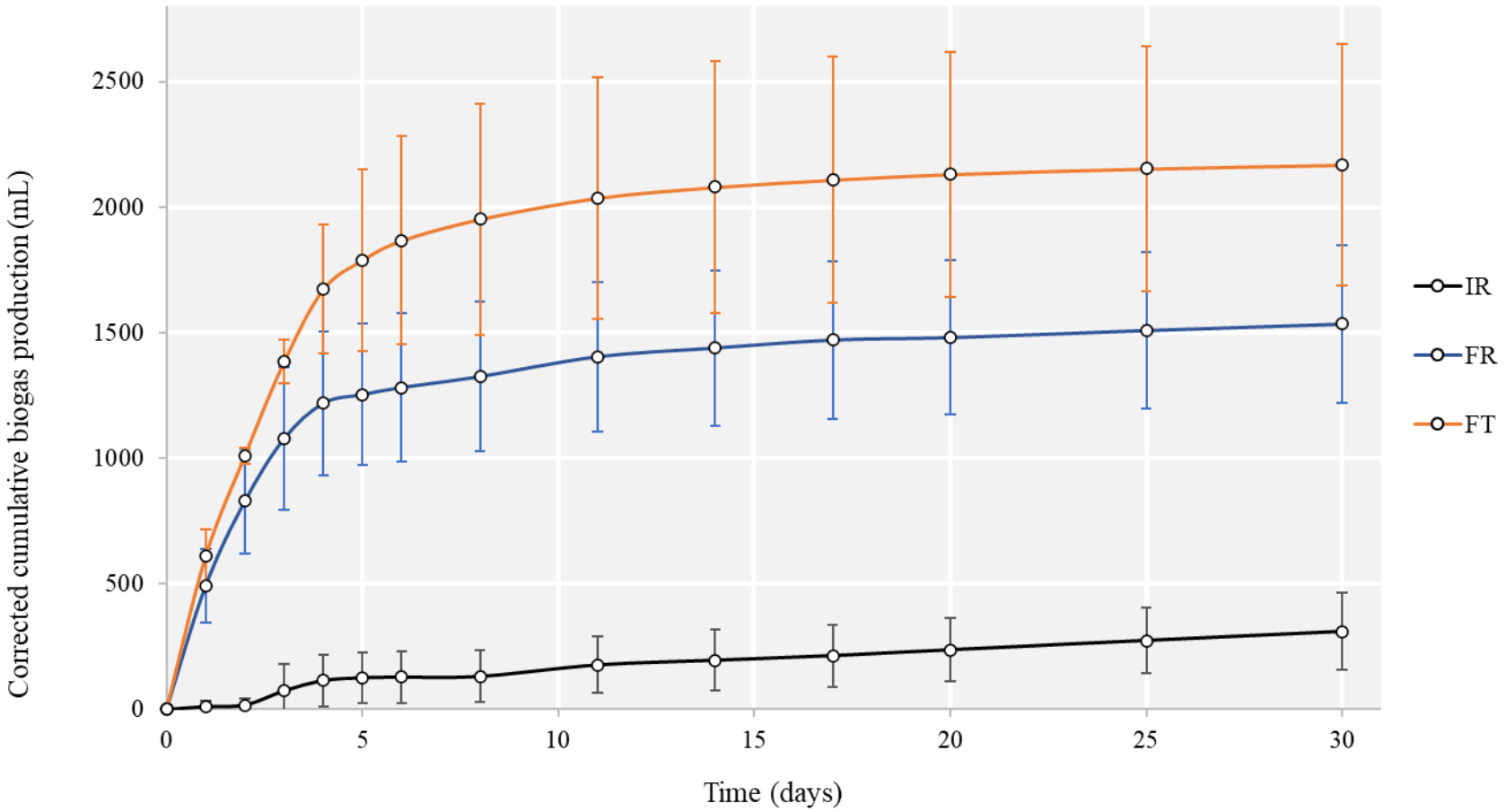

Figure 7. Average cumulative biogas produced from IR (inoculum only), FR (inoculum + food waste), and FT (inoculum + food waste + trace element solution) treatments over 30 days

3.5 Methane Fraction

The average methane fraction of the biogas after 30 days was 0.73 (± 0.04), 0.63 (± 0.16), and 0.55 (± 0.001) for the IR, FR, and FT treatments, respectively. The average calculated headspace pressure over the 30 days was 113 kPa. The estimated headspace temperature and pressure did not affect the calculated methane fraction value (Justesen et al., 2019). The methane fraction in biogas usually ranges between 45% and 75%, with most of the remainder as carbon dioxide (*An Introduction to Biogas and Biomethane – Outlook for Biogas and Biomethane*, n.d.). There was high variability in the data (i.e., high standard deviation) regarding the mole fraction of methane in the FR treatment. Additionally, there was no statistical significance between the average methane fraction of the IR, FR, and FT treatments ($p > 0.05$). Therefore, there was insufficient evidence to suggest a treatment difference in the mean methane fraction.

The calculation for mole fraction of methane was dependent on the cumulative mass loss (pre-venting mass – post-venting mass) and the cumulative standardized (101.325 kPa and 273.15 K) biogas volume. The gas-density based BMP method assumed that the remaining fraction of biogas was composed of carbon dioxide. Therefore, the fraction of other gases (water vapor, ammonia, hydrogen sulfide) was assumed to be zero. This assumption was another source of error while using the gas-density based BMP method for calculating the methane fraction in the biogas produced.

3.6 Methane Production and Yield

The cumulative volume of methane produced from all three treatments is shown in Figure 8. The average methane produced over the 30 days was 227 (±113) mL, 933 (± 162) mL, and 1146 (± 267) mL from the IR, FR, and FT treatments, respectively. There was sufficient evidence to conclude that there was a treatment difference in the mean cumulative methane

produced ($p < 0.05$) after 30 days. The average total methane production of the FT treatment was 23% higher than the average total methane production of the FR treatment. The average total methane produced from the IR treatment differed from the average total methane produced from the FR treatment. Still, no difference was detected between the average total methane produced from the FR treatment and the average total methane produced from the FT treatment.

The methane yield (SMP) of the three treatments over the 30 days is shown in Figure 9. Figure 9 includes the SMP of the inoculum only treatment (mL CH_4/g inoculum VS added), which is not commonly shown in the literature. It is shown here for a complete assessment, as the IR treatment was one of the three treatments in this experiment. The trend of the SMP curves for the FR and FT treatments have similar patterns to the literature (i.e., goal-seeking curve shape). The IR treatment followed less of a goal-seeking curve, as the methane yield plateaued and then increased through day 30. The average SMP by day 2 was 56% and 49% of the SMP by day 30 for the FR and FT treatments, respectively. For the FR and FT treatments, the SMP curve began to level by day 11, meaning the methane yield was not increasing but instead slowing down and tapering off in a goal-seeking pattern. The experimental data (Figure 9) suggested that the FT treatment had a higher average SMP than the FR treatment, indicating that trace element addition did stimulate methane production.

Lastly, the BMP of both the FR and FT treatments was calculated as the average SMP on day 30. The BMP of the IR, FR, and FT treatment was 56.1 (± 27.9) mL CH_4/g VS added (VS from inoculum only), 363 (± 77) mL CH_4/g VS added, and 447 (± 100) mL CH_4/g VS added, respectively. A difference was detected between the mean BMP of the IR, FR, and FT treatments ($p < 0.05$). Therefore, there was sufficient evidence to suggest a treatment difference in BMP.

The results from this experiment indicate that trace elements have a stimulating effect on biogas and methane produced in FW AD. Leakage was kept to a minimum during this experiment, as leakage would increase variability in the results. High variability is often expected when working with biological systems, which is reflected in the results of this experiment. The origin of the variability cannot be known. However, it could be due to the diverse consortia of microorganisms present in AD systems. Although the inoculum was the same for each treatment, different microorganisms may have dominated across treatments or in the same treatment due to the dynamic nature of AD. It is hypothesized that lower methane production was attributed to the system having a higher proportion of microorganisms using the syntrophic acetate oxidation and hydrogenotrophic methanogenesis pathways, as these pathways are less efficient in producing methane compared with acetotrophic methanogenesis (Schnürer & Nordberg, 2008). However, further microbial analysis (i.e., 16S sequencing) needs to be done to understand how microbial communities are affected by supplementing trace elements.

In addition, chemical oxygen demand (COD) was related to the produced CH_4 volume. COD measures the amount of oxygen required to oxidize organic material into water and carbon dioxide. In methane oxidation, one mole of CH4 combines with 2 moles of O_2 to produce one mole of CO2 and 2 moles of H_2O. The relation between COD and volume of CH_4 for this system was calculated using CH_4 density at 30 °C (0.637 kg/m^3), the stoichiometric coefficients of the balanced methane oxidation equation (2 mol O_2: 1 mol CH_4), and the molar masses of O_2 (32 g/mol) and CH_4 (16.04 g/mol). For this AD system, 1 g COD = 0.39 L CH_4. In practice, this theoretical COD of CH_4 is not achievable and would likely be lower as not all COD is biodegradable, making it difficult to convert all COD to CH_4.

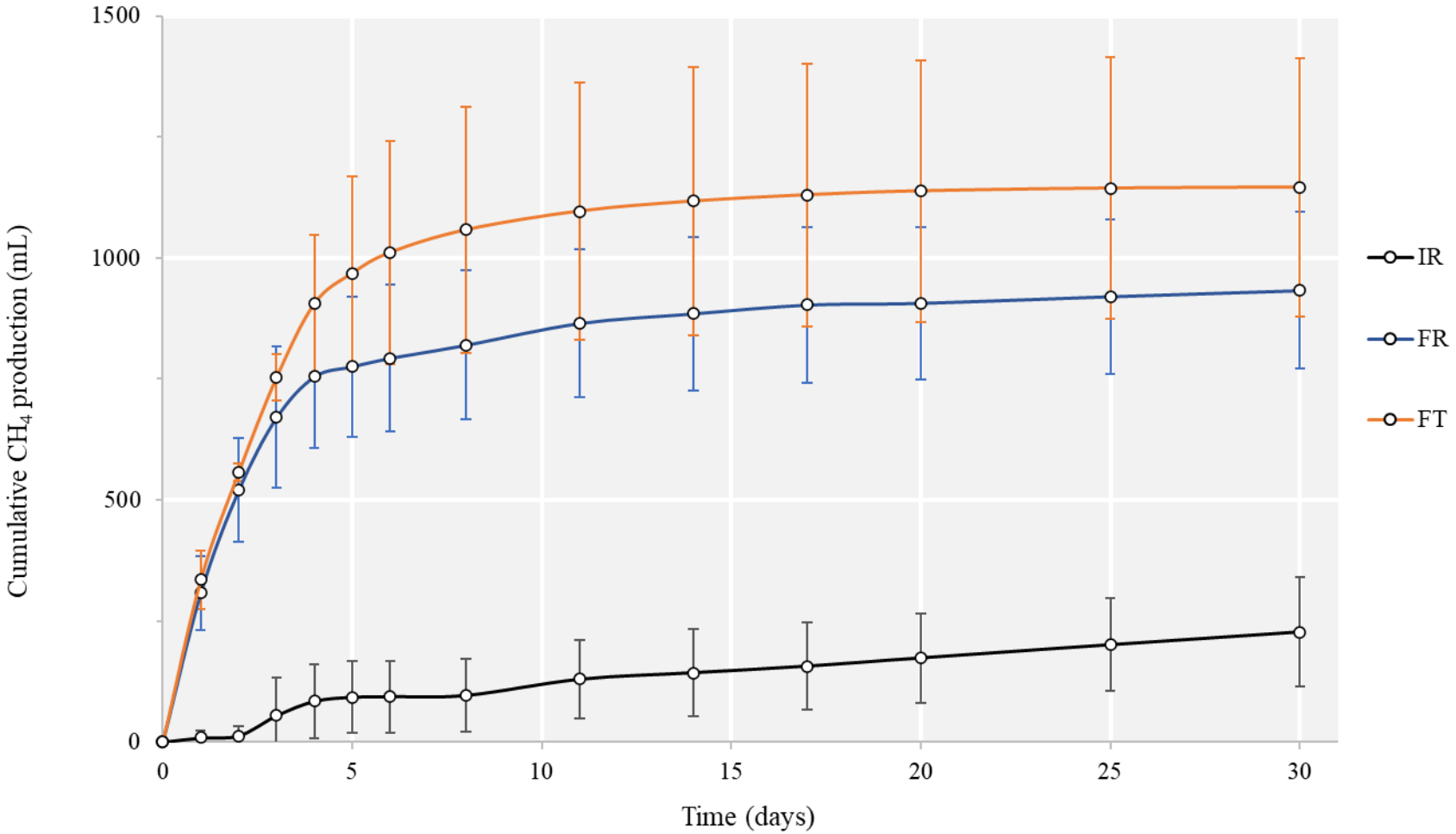

Figure 8. Cumulative methane produced from IR (inoculum only), FR (inoculum + food waste), and FT (inoculum + food waste + trace element solution) treatments over 30 days

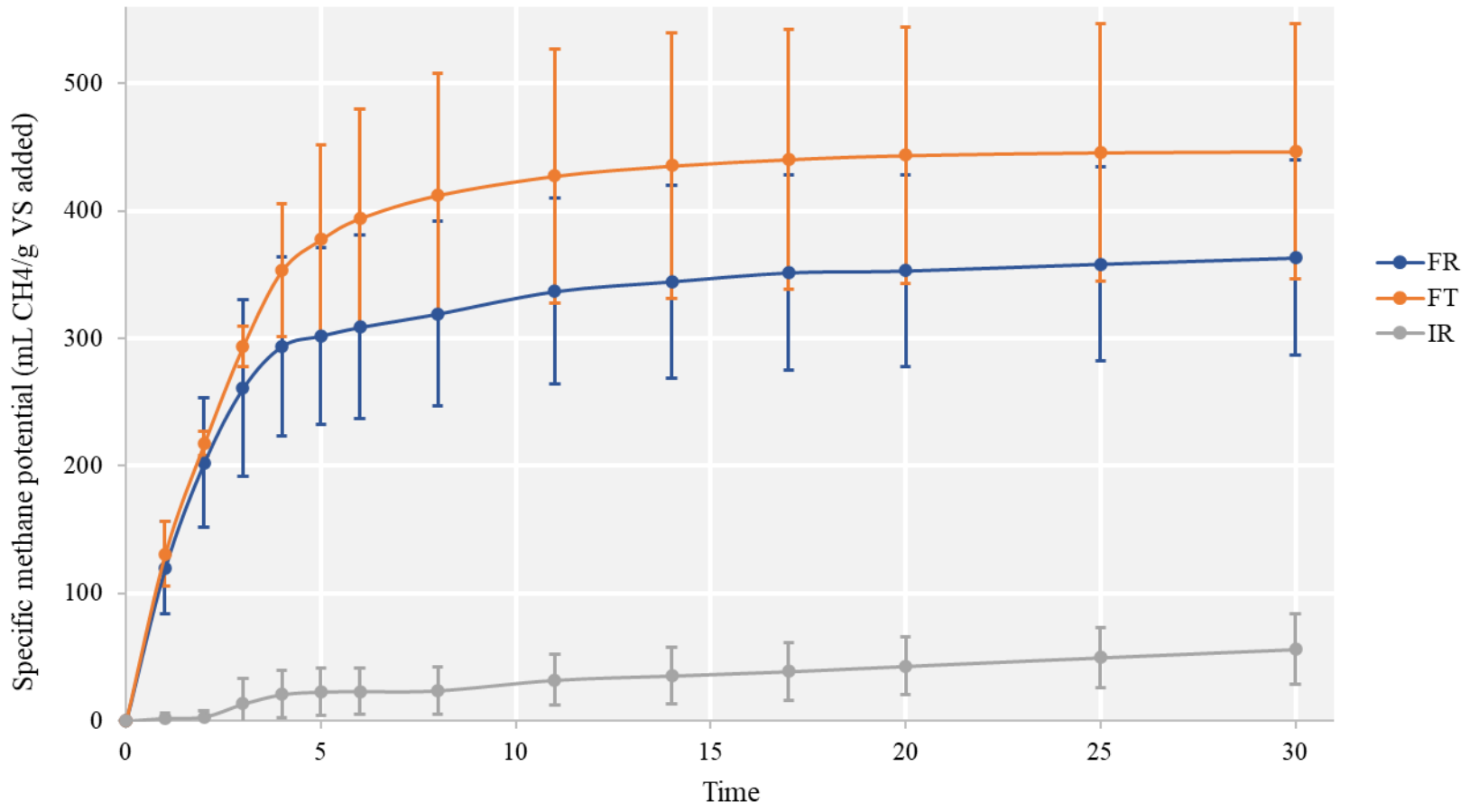

Figure 9. Specific methane potential of the IR (inoculum only), FR (inoculum + food waste), and FT (inoculum + food waste + trace element solution) treatments

3.7 Limitations and Future Work

The results from this experiment have limitations that must be addressed to move forward and provide insight into future experiments involving trace element supplementation in FW AD. The large size of the bottles used (1150 mL working volume) was an issue during this experiment. A larger bottle relates to a heavier bottle, meaning a scale with a higher capacity is needed. Scales with a higher capacity often have lower accuracy, decreasing the pre-venting and post-venting mass accuracy. Again, the gas density-based BMP method requires high accuracy in mass measurements, which were hindered by the heavier bottles used in this experiment. Therefore, if performing the gas density-based BMP method, it is recommended that a smaller bottle is used to increase the accuracy of the mass measurements.

This experiment was limited by the number of bottles available for use. If more bottles were available, a positive control (i.e., microcrystalline cellulose) with three replicates would have been set up to allow for the BMP test to be validated appropriately. Microcrystalline cellulose has a well-known and standard BMP range (340 – 395 mL_{CH4}/kgVS) compared to the experimental values (Holliger et al., 2016). The experiment would be further validated if the measured values were within the known range for microcrystalline cellulose. Water-only bottles were not set up in this experiment but should be set up in future experiments using the gas density-based BMP method. Water-only bottles are set up the same way as other BMP bottles but only contain water. The leakage detection limit can be estimated from the measured mass change in water-only bottles over the BMP testing period (Justesen et al., 2019). Measured leakage in treatments larger than the calculated detection limit indicates significant leakage. The water-only bottles further validate the results of a gas density-based BMP test.

Lastly, a future experiment could include creating trace element mixes targeting different AD process stages. This experiment would consist of an inoculum-only treatment (IR) and four FW and inoculum blends with different trace element blends (S1, S2, S3, S4). S1 would contain Ca, Co, and Mg to target hydrolysis. S2 would contain Ca, Co, Cu, Fe, Mg, and Ni to target hydrolysis and acidogenesis. S3 would contain Ca, Co, Cu, Fe, Mg, Mn, Ni, and Se to target hydrolysis, acidogenesis, and acetogenesis. Last, S4 would contain Ca, Co, Cu, Fe, Mg, Mn, Mo, Ni, Se, and Zn to target hydrolysis, acidogenesis, acetogenesis, and methanogenesis. This experiment would aim to identify how different trace element blends stimulate (or hinder) methane yield in batch FW AD systems.

4. Estimating the Potential Greenhouse Gas Reduction from Food Waste Streams in Montgomery, VA Using Anaerobic Digestion

4.1 Section Overview

The purpose of this work was to (1) estimate the total amount of FW produced in Montgomery, VA, annually, (2) use the BMP analyses from Ch 3 to inform the design of a theoretical community digester in Montgomery, VA, and (3) use that information to predict the greenhouse gas (GHG) reductions of anaerobically digesting the FW instead of sending it to landfill. FW produced per year (tonnes, t/year) was estimated from ten sectors: food manufacturing, hospitality, hospitals, correctional facilities, college and universities, K-12 institutions (publicly supported grade school before college), grocery retail, restaurants/food services, residential, food wholesale. The FW from each sector was then summed and used to calculate GHG reductions associated with sending FW to landfills. In addition, the energy produced from the digester and the number of houses that could be powered by the digester annually was estimated.

Additionally, a theoretical community anaerobic digester treating FW was designed to determine GHG emissions associated with running and operating the AD system. Fossil fuels from transportation were not included, and it was assumed that the digester was powered from the biogas produced and not grid electricity. Estimated inputs included methane destruction efficiency of biogas destruction devices (turbine, boiler, flare, etc.), methane released from venting, and emissions associated with digestate storage. The GHG emissions from the AD system in addition to the GHG emissions associated with sending FW to landfill determined the GHG reductions associated with the AD system.

It was hypothesized that anaerobically digesting FW instead of sending it to landfill in Montgomery, VA would substantially reduce GHG emissions. It was expected that the AD system would produce some GHG emissions, but the emissions would be insignificant compared to the GHG emissions from sending FW to landfills (without landfill gas capture). Additionally, the results from this study could be used to inform the GHG reduction potential of similar communities, and the Excel spreadsheet created for this study could be applied to other FW AD systems.

4.2 Greenhouse Gas Emission Overview

GHGs emitted into the atmosphere from human activities are the most significant driver of climate change (*AR5 Climate Change 2013*, 2013). GHGs are gases that trap heat in the atmosphere. The four main GHGs are carbon dioxide, methane, nitrous oxide, and fluorinated gases. Fluorinated gases include hydrofluorocarbons, perfluorocarbons, sulfur hexafluoride, and nitrogen trifluoride. The overview of U.S. GHG emissions in 2019 is summarized in Figure 10. The total U.S. GHG emissions in 2019 were 6,558 million metric tons of CO_2 equivalent (tCO_2e).

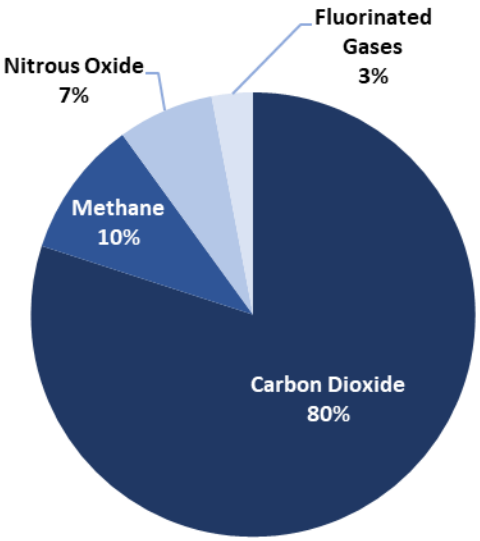

Figure 10. Overview of U.S. greenhouse gas emissions in 2019 (adapted from US EPA, 2015b)

The effect of each GHG on climate change depends on three factors: concentration (abundance) in the atmosphere, time in the atmosphere, and impact on the atmosphere. While carbon dioxide has a larger abundance in the atmosphere than methane (Figure 10), methane has a larger global warming potential (GMP) which means methane absorbs more energy (per pound) and contributes more to warming the planet than carbon dioxide (US EPA, 2015c).

Moreover, the emissions of these gases into the atmosphere must be minimized as much as possible. In 2019, 17% of methane emissions in the U.S. came from landfills (US EPA, 2015a). Municipal solid waste (MSW) landfills consist of everyday items people use and throw away, such as food residue, garden waste, paper, metal, glass, textiles, and plastic. MSW landfills are the third largest source of human-related methane emissions in the United States (~15% of all methane emissions) (US EPA, 2016). In perspective, methane emissions from MSW landfills in 2019 were approximately equivalent to GHG emissions from more than 21.6 million passenger vehicles driven for one year (US EPA, 2016).

The composition of MSW varies but consists of a high proportion of organic matter, i.e., food residues and paper and garden wastes. The organic fraction of municipal solid waste (OFMSW) represents 70% of the waste composition in an MSW landfill, with a moisture content of around 85-90% (Albanna, 2013). Once in landfills, OFMSW breaks down uncontrollably into landfill gas that is emitted into the atmosphere. Landfill gas comprises roughly 50% methane and 50% carbon dioxide, both of which are GHGs (US EPA, 2016). The OFMSW could instead be diverted from landfills and anaerobically digested. AD prevents the emission of methane and carbon dioxide into the atmosphere and instead captures these gases for direct use as heating and electricity, or it can be upgraded into renewable natural gas (RNG).

FW is generated from the whole food supply chain, including production, processing, distribution, storage, sale, preparation, cooking, and serving (Xu et al., 2018). Generally, FW collected from production and processing is more nutrient-rich and higher quality. Therefore, it is easier to divert this waste to animal feed or chemical processing. FW from consumers has the lowest recycling rate due to logistics, health and safety concerns, and poor traceability (Xu et al., 2018). The typical composition of FW generated from the consumer stage (preparation, cooking, and serving) is summarized in Table 10. Table 10 shows a typical composition of FW components at the consumer stage, but it is often more informative to look at available data regarding the specific FW stream of interest.

Table 10. The composition of food waste generated from the consumer stage (Xu et al., 2018)

Food group	Composition of consumer FW (%)
Cereals	52%
Fruits and vegetables	21%
Dairy	12%
Meat	6%
Roots and tubers	6%
Oil	2%
Fish	1%

4.3 Quantifying Greenhouse Gas (GHG) Emission Reductions

Quantifying GHG emission reductions aims to determine whether a new process produces less GHG emissions than the original process. It was assumed that the current treatment process for FW was landfilling. The new proposed treatment process for FW handling was an AD system. It was essential to establish baseline emissions before GHG emission reductions were determined for this particular AD system. GHG emission reductions were quantified by comparing actual project emissions to baseline emissions from anaerobic waste management (Climate Action Reserve, 2014). Baseline emissions were defined as the estimated GHG emissions from sources within the defined project boundary (dotted box in Figure 11) that would occur without the AD system. The baseline emissions for this project were the emissions associated with disposing FW at a landfill. Project emissions arise from sources associated with the FW AD project within the GHG Assessment Boundary. The project emissions include fossil fuels and electricity consumed by the AD system, the efficiency of methane destruction devices,

methane released from venting, and emissions associated with digestate storage. The general formula for this project's net GHG emission reductions is as follows,

$$GHG\ emission\ reductions = Baseline\ emissions - Project\ emissions \quad \textbf{(36)}$$

The GHG Assessment Boundary in Figure 11 outlines the GHG sources, sinks, and reservoirs (SSRs) that were assessed to determine the GHG reductions from the AD of FW. The grey boxes represent SSRs included for both the baseline and the project. These SSRs were outside the GHG Assessment Boundary, so they were not included in any calculations. The blue boxes represent SSRs associated with the AD system. Temporary FW storage emissions were excluded from the GHG Assessment Boundary because it was assumed the FW was stored appropriately with negligible GHG emissions. Additionally, thermal energy and electricity grid use was excluded since the assessment does not cover the displacement of GHG emissions from using biogas instead of fossil fuels. Lastly, the white box represents baseline emissions associated with FW disposal at a landfill.

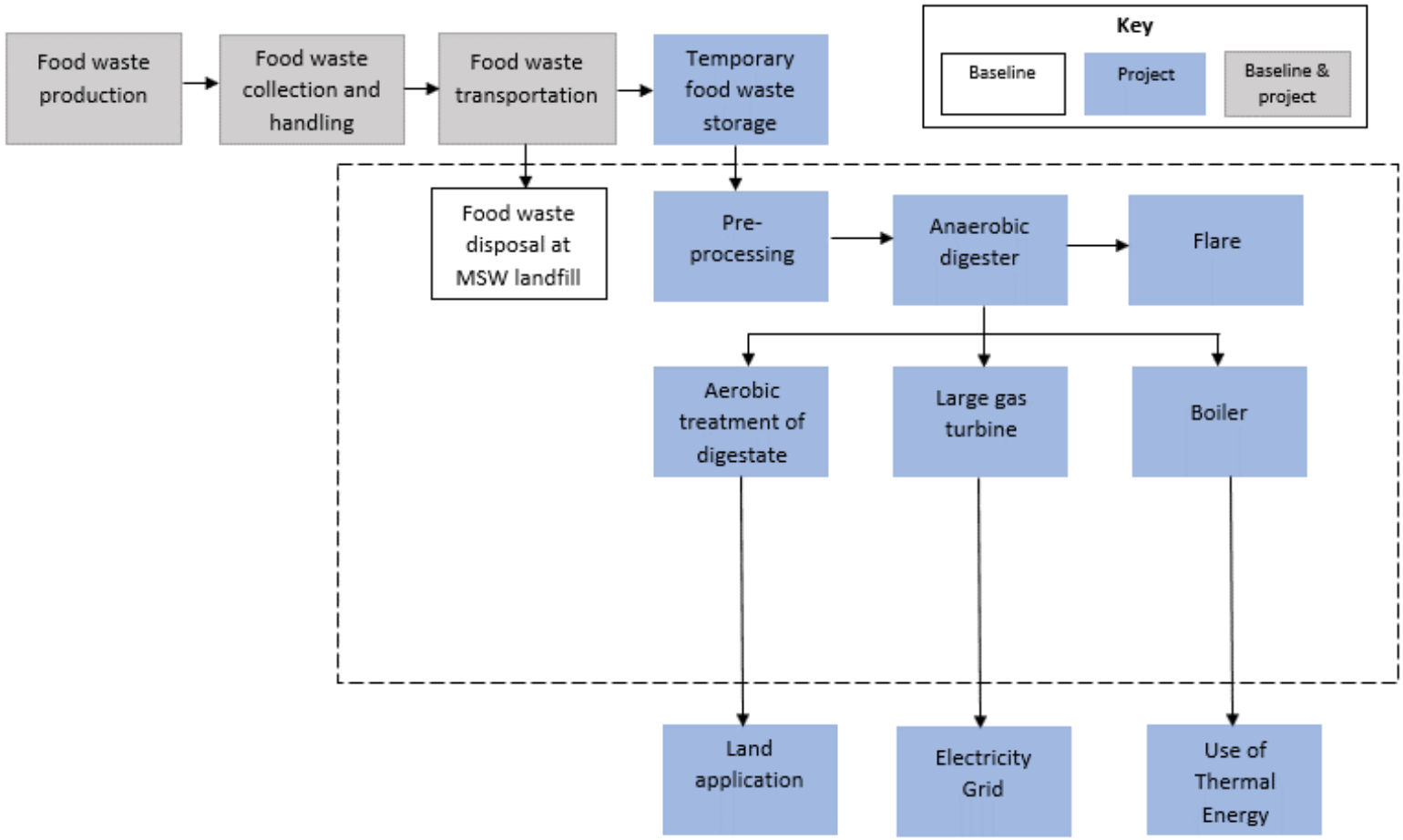

Figure 11. GHG Assessment Boundary adapted from (Source: Climate Action Reserve, 2014)

4.4 Food Waste Streams in Montgomery, VA

The main FW streams in Montgomery, VA were summarized into ten categories: food manufacturing, hospitality, hospitals, correctional facilities, colleges and universities, K-12 institutions, grocery retail, restaurants/food service, residential, and food wholesale. These categories were created in alignment of the 2018 Wasted Food Report published by the EPA in 2020 (US EPA, 2020). The 2018 Wasted Food Report document outlined average wasted food generation factors based on studies conducted in state and municipal governments, industry groups, universities, and an extensive literature review. Each sector's generation factor has units based on facility-specific characteristics (revenue, number of employees, etc.). The relevant generation factors to this project are listed in Table 11. The generation factors were used to calculate estimates of FW produced in one year (tonnes/year) from the different sectors in Montgomery, VA. Assumptions and estimates are explicitly listed when used. It was assumed that all FW produced in Montgomery, VA was sent to landfill unless otherwise stated.

Table 11. Estimated FW produced in Montgomery, VA based on average wasted food generation factors (US EPA, 2020)

Sector	Generation factor	Units of generation factor	Estimated food waste produced in Montgomery, VA (tonnes/year)
Food manufacturing	0.095	lbs/sales $/year	7,445
Hospitality	1137.83	lbs/employee/year	259
Hospitals	653.14	lbs/bed/year	68.5
Correctional facilities	1.12	lbs/inmate/year	21.1
Colleges and Universities	0.01	tons/student/year	189
K-12 institutions	26.3	lbs/student/year	119
Grocery retail	2.04	tons/employee/year	1801
Restaurants/food service	3,050.67 (full service) 2,751.33 (limited service)	lbs/employee/year lbs/employee/year	5,107
Residential	338	lbs/household/year	5,425
Food wholesale	120.68	tons/facility/year	219
Total	--	--	**20,652**

Food Manufacturing

In the scope of this project, food manufacturing included animal food manufacturing, grain and oilseed milling, sugar and confectionery product manufacturing, fruit and vegetable preserving and specialty food manufacturing, dairy product manufacturing, animal slaughtering and processing, bakeries and tortilla manufacturing, and other food manufacturing (snack food manufacturing, coffee and tea manufacturing, flavoring syrup and concentrate manufacturing, seasoning and dressing manufacturing, perishable prepared food manufacturing) as defined by the United States Census Bureau (U.S. Census Bureau, 2022). The industry code (NAICS) for overall food manufacturing is 311. This study's scope did not cover beverage manufacturing (soft drink and ice manufacturing, breweries, wineries, distilleries) due to limited public information available.

Revenue from food manufacturing was estimated using the 2018-2020 Statistics for All Manufacturing by State provided by the United States Census Bureau (US Census Bureau, 2021a). This data contained information regarding food manufacturing at the state level, not the county level. The food manufacturing sales in Virginia in 2020 was $14,955,198,000 (US Census Bureau, 2021a), and the population of Virginia and Montgomery County, VA were 8,631,393 and 99,721, respectively in 2020 (*U.S. Census Bureau QuickFacts*, n.d.). The revenue of food manufacturing in Montgomery, VA was estimated assuming that the food manufacturing revenue in Virginia was proportional to food manufacturing revenue in Montgomery County based on population estimates. This revenue estimated the FW produced per year in food manufacturing in Montgomery, VA. The estimated amount of FW produced from food manufacturing in Montgomery, VA is listed in Table 11.

$$\frac{Revenue\ from\ food\ manufacturing\ in\ Virginia}{Population\ of\ Virginia} = \frac{\boldsymbol{Revenue\ from\ food\ manufacturing\ in\ Montgomery,VA}}{Population\ of\ Montgomery,VA} \quad \textbf{(37)}$$

Hospitality

The hospitality industry involves travel accommodation, including hotels and motels (NAICS code: 7211). There are currently no casino hotels in Virginia. The average FW generation factor for the hospitality industry is based on the number of employees. The County Business Patterns by Industry: 2019 provided by the U.S. Census Bureau estimated 501 employees in the hospitality industry in Montgomery, VA in 2019 (US Census Bureau, 2021b). The estimated amount of FW produced from the hospitality industry in Montgomery, VA is listed in Table 11.

Hospitals

There are currently two hospitals in Montgomery, VA: Carilion New River Valley Medical Center and Lewisgale Hospital Montgomery. The amount of FW produced by hospitals in Montgomery, VA was estimated using the relevant generation factor based on the total number of hospital beds. American hospital directory, a publicly available website on hospital statistics, indicated that Carilion New River Valley Medical Center has 130 staffed beds and Lewisgale Hospital Montgomery has 92 (*American Hospital Directory - Individual Hospital Statistics for Virginia*, 2021). There are 222 hospital beds in Montgomery, VA and the estimated amount of FW produced from hospitals in Montgomery, VA is listed in Table 11.

Correctional Facilities

Correctional facilities include jails, prisons, and juvenile detention facilities. Montgomery, VA has two correctional facilities: Montgomery County Jail and New River Valley Juvenile Detention Home. The generation factor for correctional facilities was based on the number of inmates per day. It was assumed that both the facilities were always at capacity. The capacity of Montgomery County Jail and New River Valley Juvenile Detention home are 90

and 24 inmates, respectively (*Montgomery County Jail - Christiansburg, VA*, n.d.; *New River Valley Juvenile Detention Home*, n.d.). The estimated amount of FW produced from the correctional facilities in Montgomery, VA is listed in Table 11.

Colleges and Universities

The only university in Montgomery, VA is Virginia Tech. As of Fall 2021, Virginia Tech had 34,656 on-campus students at the Blacksburg, VA campus. The generation factor for estimating FW from colleges and universities was based on the number of students. The estimated FW produced from colleges and universities in Montgomery, VA using the generation factor is 346.6 tons/year. However, Virginia Tech has waste management practices in place to address FW produced on the Blacksburg campus. According to the Virginia Tech 2020-21 Sustainability Annual Report, approximately 138 tons of FW was diverted from landfill in 2020. 118 tons were sent to a composting facility (Royal Oaks Farm LLC, Evington, VA). The remaining mass of FW was donated to hunger relief agencies in the New River Valley (*Virginia Tech 2020-21 Sustainability Annual Report*, n.d.). No data was recorded regarding FW sent to the landfill from Virginia Tech Dining Services. Therefore, the estimate using the generation factor was used. The amount of waste diverted from landfills from Virginia Tech (138 tons) was subtracted from the total amount of FW estimated from the generation factor (346.6 tons). The estimated amount of FW produced from Virginia Tech is listed in Table 11.

K-12 Institutions

There are currently 21 public K-12 institutions in Montgomery, VA, with 10,016 students (*Montgomery County Public Schools*, n.d.). The FW generated by K-12 schools was estimated based on the number of students attending those institutions. The estimated amount of FW produced by K-12 institutions in Montgomery, VA is listed in Table 11.

Grocery Retail

FW produced from grocery retail (NAICS code: 4451) in Montgomery, VA was estimated based on the number of grocery store employees using the County Business Patterns by Industry: 2019 released by the U.S. Census Bureau (US Census Bureau, 2021b). The estimated number of employees in grocery retail in Montgomery, VA was 973, and this value was then used to calculate the amount of FW produced by grocery retail in Table 11.

Restaurants/Food Service

The U.S. Census Bureau defines full-service restaurants (NAICS code: 722513) and limited services restaurants (NAICS code: 722513) separately. Full-service restaurants are food services where patrons order and are served while seated (i.e., waiter, waitress service) and pay after eating. Limited-service restaurants are food services where patrons order or select items and pay before eating. The FW produced from restaurants/food services was estimated based on the number of employees using the County Business Patterns by Industry: 2019 released by the U.S. Census Bureau (US Census Bureau, 2021b). The number of employees at full-service restaurants and limited-service restaurants in Montgomery, VA was estimated at 2,346 and 1,491, respectively. The estimated amount of FW produced from restaurants/food services in Montgomery, VA is listed in Table 11.

Residential

An estimate for FW produced by the residential sector was based on the number of households in Montgomery, VA. An estimate for the number of households in Montgomery, VA in 2016-2020 (35,388) was provided by Quickfacts from the U.S. Census Bureau (*U.S. Census Bureau QuickFacts*, n.d.). The estimated amount of FW produced from the residential sector in Montgomery, VA is listed in Table 11.

Food Wholesale

The amount of FW produced from food wholesale (NAICS Code: 4244) was based on the number of facilities in Montgomery, VA (2 facilities). Food wholesale included general line grocery wholesale, packaged frozen food wholesale, dairy product (except dried or canned) wholesale, poultry and poultry product wholesale, confectionary wholesale, fish and seafood wholesale, meat and meat product wholesale, fresh fruit and vegetable wholesale, and other grocery and related product wholesale. This estimate was based on the most recent data from the U.S. Census Bureau Wholesale Trade: Geographic Area Series: Summary Statistics for the U.S., States, Metro Area, Counties, and Place: 2012 (US Census Bureau, 2012). The estimated amount of FW produced from food wholesale in Montgomery, VA is listed in Table 11.

Summary

The percentage of FW produced from each of the ten sectors in Montgomery, VA was compared to national FW percentages in 2018 (Table 12) (US EPA, 2020). The national data also included FW from sectors not included in Montgomery, VA data, including office buildings (3.95%), nursing homes (0.44%), military installations (0.06%), and sports venues (0.04%). These sectors were not included in the FW estimate due to insufficient data regarding FW in those sectors in Montgomery, VA. However, the U.S. data provide a comparison between the national estimate and the estimate calculated for Montgomery, VA. The estimated FW produced in Montgomery, VA by sector closely matches the estimated FW produced in the U.S. by sector, which indicates that the estimate for the total amount of FW produced in Montgomery, VA is plausible and was used to calculate baseline emissions.

Table 12. Percent of FW produced in each sector in Montgomery, VA and nationally (US EPA, 2020)

Sector	% of total (Montgomery, VA)	% of total (2018 U.S. data)
Food manufacturing	36.05%	38.68%
Hospitality	1.25%	1.18
Hospitals	0.32%	0.29%
Correctional facilities	0.10%	0.43%
Colleges and universities	0.92%	0.60%
K-12 institutions	0.58%	1.21%
Grocery retail	8.72%	8.43%
Restaurants/Food services (full and limited)	24.73%	16.60%
Residential	26.27%	24.24%
Food wholesale	1.06%	3.85%
Other	--	4.49%

4.5 Large-scale Theoretical Complete Mix Anaerobic Digester Sizing

A complete mix anaerobic digester with a working volume of approximately 2,346,000 L (total volume ~ 3,395,000 L) was proposed to treat the FW produced from multiple sectors in Montgomery County, VA. The design parameters for the digester were informed by the BMP test detailed in Ch 3. The calculations to determine the working and total volume of the theoretical anaerobic digester, organic loading rate, and daily methane produced from the digester are presented in Appendix A.

BMP

The BMP test results informed the large-scale community digester's retention time, organic loading rate (OLR), pH, and temperature. Retention time is the time the FW remains in the digester before being removed. It was assumed that the retention time for the large-scale community digester would be 15 days. It was determined by the BMP analyses that the cumulative methane production was < 1% of the total methane production by day 15, indicating that would be a sufficient retention time for the large-scale digester. The retention time determined (15 days) was also used to determine the organic loading rate of the large-scale digester. As described in Ch 1, the OLR has units of kg VS/m^3*day and is a main factor that influences the amount of biogas produced during AD. The volatile solids (VS) of FW (10.12%) were also used to calculate the OLR of the community digester.

In addition, two other essential factors in AD design are pH and temperature. As this section's purpose is not to detail all AD design parameters, it is assumed that the digester will have pH controls in place (as FW generally has an acidic pH). Having a pH control in place would keep the digestion at a pH of 7-7.5 to avoid process failure. The temperature would be controlled at a mesophilic (37°C) temperature as that was done for the BMP analyses.

Additionally, it was assumed that for the large-scale digester, the FW slurry would be prepared similarly to the BMP analyses (two parts FW mixed with one-part water). It was also assumed that for the calculations in Appendix A, 1 L = 1 kg. Lastly, the working volume was assumed to be 75% of the total digester volume, and the headspace was 25% of the total digester volume.

Anaerobic Digester

A stand-alone digester would be built to process FW, and more specifically, the digester would be considered a multi-source FW digester since it processes FW from multiple sectors (Pennington, 2021). The digester would treat approximately 21,000 tonnes of FW per year (Table 12) as feedstock to produce biogas and digestate. First, the FW would be fed into a mixing blender tank to homogenize the material originating from different sources. The FW would then be pumped into the complete mix anaerobic digester that would be kept airtight to prevent biogas leakage. The biogas produced would be used to produce electricity and heating. Surplus biogas would be flared to prevent the escape of methane into the atmosphere. The digestate would be transported to a local composting facility to be aerobically composted to stabilize the material and eventually be used as a soil amendment or fertilizer.

4.6 GHG Reduction Calculations

GHG reductions were calculated in a Microsoft Excel 2019 spreadsheet using the guidance of the Climate Action Reserve Organic Waste Digestion Project Protocol document (Climate Action Reserve, 2014). All calculations (Equation 38- 44) used were taken and adapted from this protocol with the permission of the Climate Action Reserve. It was assumed that the FW collected from all sources in Montgomery, VA would have similar characteristics (BMP, methane fraction) as the FW analyzed for the BMP test (collected from Virginia Tech).

Calculated Baseline Emissions

The mass used in the calculations for baseline emissions was in metric tons (tonnes, t). The calculation for baseline emissions was based on the estimated total weight of the FW (tonnes, wet basis) produced over a year. It was assumed that all FW would be sent to landfills without the AD system. Equation 38 represents the baseline emission calculation, and equation 39

represents the estimate of the fraction of methane generated that is emitted to the atmosphere over a 10-year horizon (Climate Action Reserve, 2014):

$$BE = 0.9 * W_{FW} * (1 - WTE) * 36.9 * \rho_{CH_4} * FE_{FW} * 28 \quad \textbf{(38)}$$

Where,

0.9 is a model correction factor to account for FW composition variabilities and uncertainties, W_{FW} is the weight of FW produced in one year (20,652 tonnes), WTE is the fraction of FW that would have been incinerated at a waste-to-energy plant instead of being landfilled (0.13, Virginia value) (Table B.2., Climate Action Reserve Organic Waste Digestion Project Protocol, Version 2.1, Virginia value), 36.9 is the methane potential of FW on a wet basis (m^3 CH_4/tonne FW) based on BMP analyses) (Equation 5.4., Climate Action Reserve Organic Waste Digestion Project Protocol, Version 2.1), ρ_{CH_4} is the density of methane (0.000674 tCH_4/m^3), FE_{FW} is the fraction of methane generated that is emitted into the atmosphere over ten years (0.642, calculated in equation 41), and 28 is the global warming potential of methane (tCO_2e/tCH_4) (Myhre et al., n.d.). Equation 41 details how the fraction of methane generated that is emitted into the atmosphere was calculated:

$$FE_{FW} = \sum_{x=1}^{10}\left[e^{-k_{FW}(x-1)} * (1 - e^{-k_{FW}}) * (1 - (WTE * LCE_x))\right] * (1 - 0.1) \quad \textbf{(39)}$$

Where,

The value k_{FW} is the decay rate of FW, which is calculated based on the climate in the region of interest (Montgomery, VA), LCE_x is the fraction of methane captured and destroyed by a landfill gas collection system in year x, and 0.1 is a fraction of methane oxidized in the cover soil. The decay rate of FW, 0.144 yr^{-1}, was based on mean annual precipitation in Montgomery VA (wet, 25-50 in) (Barlaz et al., 2009). LCE_x was calculated using a conservative and standardized method to determine landfill gas collection efficiency from the Climate Action

Reserve Organic Waste Digestion Project Protocol (Climate Action Reserve, 2014). This method assumes that the fraction of methane collected from a landfill gas system increases over time. Lastly, (1-0.1) is a corrective factor that considers methane oxidation by methane-oxidizing bacteria in the soil. This type of bacteria solely uses methane as an energy source and acts as a sink for methane emissions.

Equations 38 and 39 were used to calculate the GHG emissions associated with sending FW to landfills in Montgomery, VA.

Calculated Project Emissions

Project emissions are associated with operating the AD system. Project emissions include emissions from the anaerobic digester, methane released from venting events, and emissions from the aerobic treatment of solid digestate.

Fossil fuel combustion and grid delivered electricity. Emissions associated with nonrenewable energy consumed onsite at the AD system were considered outside the scope of this analysis. Firstly, emissions related to the transportation of FW to the AD system and the transportation of compost from the AD system were not considered within the boundaries of this project. It was assumed the transportation of FW to the AD system was the same as the transportation to a landfill. Additionally, it was assumed that the transportation of the compost produced from the AD system was the same as the transportation of commercial fertilizer to the same site. Therefore, transportation fossil fuel use was not considered in this analysis.

It was also assumed that the large-scale digester did not consume electricity from the electrical grid. Instead, the digester would consume electricity produced from the biogas, eliminating the electricity grid's need.

Anaerobic digester emissions. Emissions from the anaerobic digester arise from the methane destruction efficiencies of the large gas turbine, boiler, and enclosed flare, and from venting events. There are four equations associated with anaerobic digester emissions, and the calculations used were from the Organic Waste Digestion Project Protocol (Climate Action Reserve, 2014).

$$PE_{AD\ system} = 28 * 12 * (CH_{4_{meter,monthly}} * \left(\frac{1}{BCE} - BDE\right) + CH_{4_{vented,monthly}}) \quad \textbf{(40)}$$

Where,

The value $PE_{AD\ system}$ is the methane emissions from the anaerobic digester system in one year, 28 is the global warming potential of methane, 12 is the number of months in a year, $CH_{4_{meter,monthly}}$ is the quantity of methane collected and metered by the anaerobic digester in one month, BCE is the methane collection efficiency of the enclosed complete-mix anaerobic digester (0.98, referenced from Table B.6. in the Organic Waste Digestion Project Protocol), BDE is the weighted methane destruction efficiency of the turbine, boiler, and enclosed flare (calculated in Equation 42), and $CH_{4_{vented,monthly}}$ is the quantity of methane that is emitted into the atmosphere due to venting events per month (calculated in Equation 43). It was assumed that for the calculation of methane emissions from the digester system, the total monthly volumetric flow of biogas to the turbine, boiler, and flare was the same, and the percentage of biogas going to the turbine (86%), the boiler (10%), and the flare (4%) remained constant over the year. Equation 41 was used to calculate $CH_{4_{meter,monthly}}$ detailed below,

$$CH_{4_{meter,monthly}} = Q_{monthly} * CH_{4_{fraction}} * 0.04230 * 0.000454 \quad \textbf{(41)}$$

Where,

The value $Q_{monthly}$ is the total monthly volumetric flow of biogas, $CH_{4_{fraction}}$ is the average fraction of methane in the biogas, 0.04230 is the density of methane at standard

conditions (101.325 kPa, 273.15 K, units: lbs CH_4/scf), and 0.000454 is a conversion factor from lbs to metric tons. The value for the fraction of methane was taken from the experimental value detailed in Ch 3 for the FR treatment (0.63). The weighted methane destruction efficiency of the turbine, boiler, and the flare is detailed in Equation 42:

$$BDE = \frac{(BDE_{engine} * Q_{engine}) + (BDE_{boiler} * Q_{boiler}) + (BDE_{flare} * Q_{flare})}{Q_{monthly}} \quad \textbf{(42)}$$

Where,

The values BDE_{engine}, BDE_{boiler}, and BDE_{flare} are the methane destruction efficiencies of the turbine, the boiler, and the flare, respectively, and Q_{engine}, Q_{boiler}, and Q_{flare} are the flows of biogas (scf/month) to the turbine, the boiler, and the flare, respectively. The biogas destruction efficiencies for the large gas turbine (0.995), the boiler (0.98), and the enclosed flare (0.995) were taken from Table B.7. in the Organic Waste Digestion Project Protocol (Climate Action Reserve, 2014). The flows of biogas to each biogas destruction device were calculated by multiplying the total monthly flow of biogas ($Q_{monthly}$) by the percentage biogas going to each device (86% to the turbine, 10% to the boiler, 4% to the flare). It was assumed that the biogas metering system internally corrected temperature and pressure of the biogas to standard conditions (101.325 kPa, 273.15 K).

Venting events occur when the system needs to be temporarily shut down due to the failure of equipment in the AD system. Venting events emit biogas directly into the atmosphere and must be accounted for in the GHG reduction calculations. The quantity of methane emitted due to venting events was calculated by Equation 43 taken from the Organic Waste Digestion Project Protocol (Climate Action Reserve, 2014).

$$CH_{4_{vented,monthly}} = \left(HS_{AD} + \left(Q_{daily} * t\right)\right) * CH_{4_{fraction}} * 0.04230 * 0.000454 \quad \textbf{(43)}$$

Where,

The value HS_{AD} represents the maximum headspace storage of the anaerobic digester, Q_{daily} is the estimated daily flow of biogas from the system, t is the number of days that the biogas is vented in one month, $CH_{4_{fraction}}$ is the average fraction of methane in the biogas, 0.04230 is the density of methane at standard conditions (101.325 kPa, 273.15 K, units: lbs CH_4/scf), and 0.000454 is a conversion factor from lbs to metric tons. As venting is not common under normal digester conditions, it was conservatively assumed that three days in a month, biogas was vented to the atmosphere.

Aerobic treatment of solid digestate. Solid digestate treatment is essential as the material is further processed, and aerobic treatment improves the digestate's usability as a fertilizer or land amendment (Aguirre-Villegas et al., 2019). The digestate in this AD system would be treated at an offsite composting facility. The emissions associated with digestate transport to the digestion facility are assumed to be the same as those associated with commercial fertilizer transport to the same site.

The treatment of solid digestate may result in methane and nitrous oxide emissions. However, it is often hard to predict the amount of these GHGs emitted. Therefore, a conservation value (0.06 tCO_2e/ t (wet weight) of digestate aerobically treated) for the methane and nitrous oxide emission factor from Table 5.2. in the Organic Waste Digestion Project Protocol was assumed (Climate Action Reserve, 2014). The emissions associated with the aerobic treatment of the solid digestate are detailed in Equation 44.

$$PE_{AT} = W_{digestate} * EF_{composting} \quad \textbf{(44)}$$

Where,

PE_{AT} are the project emissions associated with the aerobic treatment of the solid digestate, $W_{digestate}$ is the weight of the digestate treated over the one-year period, and

$EF_{composting}$ is the estimated emissions factor associated with sending the digestate to a composting facility. A default value of 20% of the wet weight of FW entering the digester was assumed for the value of $W_{digestate}$ and 0.06 tCO_2e/ t digestate was assumed as the value of $EF_{composting}$.

Equations 40-44 were used to calculate the GHG emissions associated with the theoretical large-scale community digester in Montgomery, VA.

4.7 GHG Reduction Results and Implications

The calculated baseline emission total was 7,226 tCO_2e/year, and the project emission total was 694 tCO_2e/year. Therefore, the GHG reduction for treating FW in Montgomery, VA is estimated at 6,532 tCO_2e/year. Table 13 summarizes the baseline and project emissions associated with the large-scale community digester. Project emissions were broken down into operational emissions of the AD system and the emissions from digestate treatment.

From an environmental perspective, implementing a large-scale community digester would mitigate GHG emissions in Montgomery, VA. The captured biogas would potentially create energy in the form of electricity, heating, or vehicle fuel for the community. Assuming methane has an energy potential of 38.3 MJ/m^3 CH_4, one home consumes approximately 10,800 kWh/year, and electricity generation has a 60% efficiency, approximately 7,370 kWh/day could be produced by the digester, which is enough energy to power 149 homes. Additionally, 4130 tonnes/year of digestate (20% of FW mass) would be composted, potentially being used as a soil amendment or fertilizer, partially eliminating the demand for commercialized fertilizer. Overall, the results from the theoretical analysis on a large-scale community digester in Montgomery, VA show that the large majority of emissions produced from FW going to landfills can be eliminated by anaerobically digesting the FW instead. The simplified design of the large-scale digester

(excluding fossil fuel and electrical grid use) demonstrates that AD is a promising technology for reducing GHG emissions.

Table 13. Baseline and project GHG emissions

Baseline or Project Emissions	**Subcategory**	**GHG emissions (tCO_2e/year)**
Baseline	Emissions from sending FW to landfill	7,226
Project	Emissions from anaerobic digester system	447
Project	Emissions from aerobic treatment of digestate	248

BMP Analysis Contribution

The BMP analyses discussed in Ch 3 were used to inform the decisions of the large-scale AD design for Montgomery, VA. An important implication of conducting a BMP test is being able to inform a large-scale sizing for a digester. Firstly, BMP analyses are done to determine the maximum theoretical methane potential (yield) of a substrate. It is important to note that BMP is the maximum *potential* of the substrate. The methane potential of continuous operation of a large-scale digester is often lower than that of the BMP (Koch et al., 2020). Continuous operation of a large-scale digester will yield different results than what a BMP test can predict. However, the BMP test performed in this study allowed for a rough estimate of AD sizing parameters for the community digester. The BMP test provided data to predict a reasonable OLR (0.75 kg VS/m^3*day), retention time (15 days), and daily methane production (693 m^3 CH_4/day)

for the large-scale digester. These design parameters were ultimately used to estimate project emissions. The baseline emissions were calculated based on the methane potential of FW on a wet basis determined from the BMP test of FW (36.9 m^3/tonne of FW wet basis).

It is also important to note the limitations of using BMP results to inform a large-scale, continuously run digester. Firstly, the objective of the BMP analyses done in Ch 3 was to determine the effect of supplementing trace elements on the BMP and organic matter destruction during FW AD. However, BMP test results do not provide direct or clear insight into whether a trace element supplement would be beneficial in continuous AD. This is due to the fact that BMP studies have a single feeding event while continuous operation has continuous feeding that may lead to trace element washout or accumulation (Koch et al., 2020). Therefore, the FR treatment data was used to inform the large-scale digester, and it is assumed that the large-scale digester would not have supplemented trace elements. However, multiple studies have shown that trace element supplementation in continuous AD of FW has improved AD process stability and productivity (L. Zhang et al., 2012; L. Zhang & Jahng, 2012; W. Zhang et al., 2015). A follow-up economic analysis would need to be performed to determine if supplementing trace elements would be cost-effective for the AD system.

Overall, this study (1) estimated the total amount of FW produced in Montgomery, VA, (2) informed the design of a theoretical community anaerobic digester with the BMP analyses done in Ch 3, and (3) estimated the GHG reductions from anaerobically digesting the FW instead of sending it to landfill. The results show that GHG reduction would be 6,532 tCO_2e/year. The digester would produce approximately 693 m^3 CH_4/day, which could generate enough electricity to power 149 homes in Montgomery, VA. Additionally, a co-benefit of the AD process would be digestate production (4130 tonnes/year), which could be used as a soil amendment or fertilizer

for the surrounding farms in Montgomery, VA. Further research would include an economic analysis to determine the upfront cost and payback period for implementing a large-scale community digester in Montgomery, VA.

5. Conclusions

Based on the results of this study, it can be concluded that supplementing trace elements (iron, copper, magnesium, manganese, selenium, manganese, zinc, cobalt, nickel, molybdenum) may affect the methane yield of anaerobic digesters treating FW. This study showed that supplementing trace elements in a BMP assay treating FW, on average, increased the average total cumulative biogas produced by 41% and the average total cumulative methane produced by 23%. There was no significant difference in the organic waste destruction between treatments. However, the TS and VS reduction was lower than the values found in the literature for the FR and FT treatments. It was postulated that since the FW was not sieved, larger particles may have reduced the organic waste destruction for the digestion in this study. Trace element supplementation into FW digestion has varied results in the literature, and this study contributed further knowledge to this research area. However, further research is necessary to understand the relationship between trace elements and the metabolic pathways used in AD. Additionally, more work needs to be performed to understand further the effect of this supplement of trace elements on the continuous AD of FW.

Sustainable management of FW is a worldwide problem with environmental, economic, and social implications. Environmentally, keeping FW out of landfills reduces greenhouse gas emissions that contribute to climate change. The EPA Food Recovery Hierarchy prioritizes ways to prevent FW from most to least preferred as source reduction, feed hungry people, feed animals, industrial uses (including AD), composting, landfill/incineration (US EPA, 2015b). Anaerobic digesters treating FW are much less common than digesters treating

wastewater or manure. However, there is great potential for implementing FW AD on a larger scale.

The results of the theoretical design of a community anaerobic digester showed that anaerobically digesting FW instead of sending it to landfill would theoretically reduce GHG emissions by 6,532 tCO_2e/year in Montgomery, VA. Additionally, an estimated 693 m^3 CH_4/day would be produced from this digester, which could power 149 homes in Montgomery, VA. The digester's 4130 tonnes/year of digestate could be used as a soil amendment or fertilizer by farmers after being aerobically composted. The BMP analyses performed in this work were vital in estimating the sizing parameters used to calculate the project emissions from implementing a community digester. Further research is needed to determine the economic analysis of installing an anaerobic digester in Montgomery, VA to see if this project would be economically viable.

References

Aguirre-Villegas, H. A., Larson, R. A., & Sharara, M. A. (2019). Anaerobic digestion, solid-liquid separation, and drying of dairy manure: Measuring constituents and modeling emission. *Science of The Total Environment*, *696*, 134059. https://doi.org/10.1016/j.scitotenv.2019.134059

Agyeman, F. O., & Tao, W. (2014). Anaerobic co-digestion of food waste and dairy manure: Effects of food waste particle size and organic loading rate. *Journal of Environmental Management*, *133*, 268–274. https://doi.org/10.1016/j.jenvman.2013.12.016

Akturk, A. S., & Demirer, G. N. (2020). Improved Food Waste Stabilization and Valorization by Anaerobic Digestion Through Supplementation of Conductive Materials and Trace Elements. *Sustainability*, *12*(12), 5222. https://doi.org/10.3390/su12125222

Albanna, M. (2013). Anaerobic Digestion of the Organic Fraction of Municipal Solid Waste. In A. Malik, E. Grohmann, & M. Alves (Eds.), *Management of Microbial Resources in the Environment* (pp. 313–340). Springer Netherlands. https://doi.org/10.1007/978-94-007-5931-2_12

Amani, T., Nosrati, M., Mousavi, S. M., & Kermanshahi, R. K. (2011). Study of syntrophic anaerobic digestion of volatile fatty acids using enriched cultures at mesophilic conditions. *International Journal of Environmental Science & Technology*, *8*(1), 83–96. https://doi.org/10.1007/BF03326198

American Hospital Directory—Individual Hospital Statistics for Virginia. (2021, July 26). Individual Hospital Statistics for Virginia. https://www.ahd.com/states/hospital_VA.html

An introduction to biogas and biomethane – Outlook for biogas and biomethane: Prospects for organic growth – Analysis. (n.d.). IEA. Retrieved April 4, 2022, from

https://www.iea.org/reports/outlook-for-biogas-and-biomethane-prospects-for-organic-growth/an-introduction-to-biogas-and-biomethane

Angelidaki, I., & Ahring, B. K. (1993). Thermophilic anaerobic digestion of livestock waste: The effect of ammonia. *Applied Microbiology and Biotechnology*, *38*(4), 560–564. https://doi.org/10.1007/BF00242955

Angelidaki, I., & Sanders, W. (2004). Assessment of the anaerobic biodegradability of macropollutants. *Re/Views in Environmental Science & Bio/Technology*, *3*(2), 117–129. https://doi.org/10.1007/s11157-004-2502-3

AR5 Climate Change 2013: The Physical Science Basis — IPCC. (2013). https://www.ipcc.ch/report/ar5/wg1/

Ariunbaatar, J., Esposito, G., Yeh, D. H., & Lens, P. N. L. (2016a). Enhanced Anaerobic Digestion of Food Waste by Supplementing Trace Elements: Role of Selenium (VI) and Iron (II). *Frontiers in Environmental Science*, *4*, 8. https://doi.org/10.3389/fenvs.2016.00008

Ariunbaatar, J., Esposito, G., Yeh, D., & Lens, P. (2016b). Enhanced Anaerobic Digestion of Food Waste by Supplementing Trace Elements: Role of Selenium (VI) and Iron (II). *Frontiers in Environmental Science*, *4*, 8. https://doi.org/10.3389/fenvs.2016.00008

Ariunbaatar, J., Esposito, G., Yeh, D., & Lens, P. (2016c). Enhanced Anaerobic Digestion of Food Waste by Supplementing Trace Elements: Role of Selenium (VI) and Iron (II). *Frontiers in Environmental Science*, *4*, 8. https://doi.org/10.3389/fenvs.2016.00008

Arsova, L., Themelis, N., & Chandran, K. (2010). *Anaerobic digestion of food waste: Current status, problems and an alternative product*.

Atteia, A., van Lis, R., Gelius-Dietrich, G., Adrait, A., Garin, J., Joyard, J., Rolland, N., & Martin, W. (2006). Pyruvate formate-lyase and a novel route of eukaryotic ATP synthesis in Chlamydomonas mitochondria. *The Journal of Biological Chemistry*, *281*(15), 9909–9918. https://doi.org/10.1074/jbc.M507862200

Auld, D. S., & Bergman, T. (2008). Medium- and short-chain dehydrogenase/reductase gene and protein families: The role of zinc for alcohol dehydrogenase structure and function. *Cellular and Molecular Life Sciences: CMLS*, *65*(24), 3961–3970. https://doi.org/10.1007/s00018-008-8593-1

Bajpai, P. (2017). Basics of Anaerobic Digestion Process. In P. Bajpai (Ed.), *Anaerobic Technology in Pulp and Paper Industry* (pp. 7–12). Springer. https://doi.org/10.1007/978-981-10-4130-3_2

Banks, C. J., Chesshire, M., Heaven, S., & Arnold, R. (2011). Anaerobic digestion of source-segregated domestic food waste: Performance assessment by mass and energy balance. *Bioresource Technology*, *102*(2), 612–620. https://doi.org/10.1016/j.biortech.2010.08.005

Bardi, M. J., & Aminirad, H. (2020). Synergistic effects of co-trace elements on anaerobic co-digestion of food waste and sewage sludge at high organic load. *Environmental Science and Pollution Research*, *27*(15), 18129–18144. https://doi.org/10.1007/s11356-020-08252-y

Barlaz, D. M., Thompson, V., & Choate, A. (2009). *WARM component-specific decay rate methods*. https://www.epa.gov/sites/default/files/2016-03/documents/warm_decay_rate_structure_10_30_2009.pdf

Bayr, S., & Rintala, J. (2012). Thermophilic anaerobic digestion of pulp and paper mill primary sludge and co-digestion of primary and secondary sludge. *Water Research*, *46*(15), 4713–4720. https://doi.org/10.1016/j.watres.2012.06.033

Bist, P., & Rao, D. N. (2003). Identification and Mutational Analysis of Mg2+ Binding Site in EcoP15I DNA Methyltransferase. *Journal of Biological Chemistry*, *278*(43), 41837–41848. https://doi.org/10.1074/jbc.M307053200

Blasius, J. P., Contrera, R. C., Maintinguer, S. I., & Alves de Castro, M. C. A. (2020). Effects of temperature, proportion and organic loading rate on the performance of anaerobic digestion of food waste. *Biotechnology Reports*, *27*, e00503. https://doi.org/10.1016/j.btre.2020.e00503

Bohutskyi, P., Kligerman, D. C., Byers, N., Nasr, L. K., Cua, C., Chow, S., Su, C., Tang, Y., Betenbaugh, M. J., & Bouwer, E. J. (2016). Effects of inoculum size, light intensity, and dose of anaerobic digestion centrate on growth and productivity of Chlorella and Scenedesmus microalgae and their poly-culture in primary and secondary wastewater. *Algal Research*, *19*, 278–290. https://doi.org/10.1016/j.algal.2016.09.010

Broderick, J. B., Duderstadt, R. E., Fernandez, D. C., Wojtuszewski, K., Henshaw, T. F., & Johnson, M. K. (1997). Pyruvate Formate-Lyase Activating Enzyme Is an Iron−Sulfur Protein. *Journal of the American Chemical Society*, *119*(31), 7396–7397. https://doi.org/10.1021/ja9711425

Burke, D. (2001). *Dairy Waste Anaerobic Digestion Handbook: Options for Recovering Beneficial Products From Dairy Manure*. Environmental Energy Company. http://www.build-a-biogas-plant.com/PDF/DigesterBiogasHandbook.pdf

Capson-Tojo, G., Girard, C., Rouez, M., Crest, M., Steyer, J.-P., Bernet, N., Delgenès, J.-P., & Escudié, R. (2019). Addition of biochar and trace elements in the form of industrial FeCl3 to stabilize anaerobic digestion of food waste: Dosage optimization and long-term study. *Journal of Chemical Technology & Biotechnology*, *94*(2), 505–515. https://doi.org/10.1002/jctb.5797

Capson-Tojo, G., Moscoviz, R., Ruiz, D., Santa-Catalina, G., Trably, E., Rouez, M., Crest, M., Steyer, J., Bernet, N., Delgenès, J., & Escudié, R. (2018). Addition of granular activated carbon and trace elements to favor volatile fatty acid consumption during anaerobic digestion of food waste. *Bioresource Technology*. https://doi.org/10.1016/j.biortech.2018.03.097

Castillo Martinez, F. A., Balciunas, E. M., Salgado, J. M., Domínguez González, J. M., Converti, A., & Oliveira, R. P. de S. (2013). Lactic acid properties, applications and production: A review. *Trends in Food Science & Technology*, *30*(1), 70–83. https://doi.org/10.1016/j.tifs.2012.11.007

Cha, G. C., & Noike, T. (1997). Effect of rapid temperature change and HRT on anaerobic acidogenesis. *Water Science and Technology*, *36*(6), 247–253. https://doi.org/10.1016/S0273-1223(97)00529-5

Chan, P., de Toledo, R., lu, H., & Shim, H. (2019). *Effect of Zinc Supplementation on Biogas Production and Short/Long Chain Fatty Acids Accumulation During Anaerobic Co-digestion of Food Waste and Domestic Wastewater*. *10*, 3885–3895. https://doi.org/10.1007/s12649-018-0323-9

Chen, H., Wang, W., Xue, L., Chen, C., Liu, G., & Zhang, R. (2016). Effects of Ammonia on Anaerobic Digestion of Food Waste: Process Performance and Microbial Community. *Energy & Fuels*, *30*(7), 5749–5757. https://doi.org/10.1021/acs.energyfuels.6b00715

Chen, P. Y.-T., Aman, H., Can, M., Ragsdale, S. W., & Drennan, C. L. (2018). Binding site for coenzyme A revealed in the structure of pyruvate:ferredoxin oxidoreductase from Moorella thermoacetica. *Proceedings of the National Academy of Sciences*, *115*(15), 3846–3851. https://doi.org/10.1073/pnas.1722329115

Chen, Y., Cheng, J. J., & Creamer, K. S. (2008). Inhibition of anaerobic digestion process: A review. *Bioresource Technology*, *99*(10), 4044–4064. https://doi.org/10.1016/j.biortech.2007.01.057

Cho, S.-K., Im, W.-T., Kim, D.-H., Kim, M.-H., Shin, H.-S., & Oh, S.-E. (2013). Dry anaerobic digestion of food waste under mesophilic conditions: Performance and methanogenic community analysis. *Bioresource Technology*, *131*, 210–217. https://doi.org/10.1016/j.biortech.2012.12.100

Choong, Y., Norli, I., Abdullah, A., & Yhaya, M. (2016). *Impacts of trace element supplementation on the performance of anaerobic digestion process: A critical review*. *209*, 369–379. https://doi.org/10.1016/j.biortech.2016.03.028

Climate Action Reserve. (2014). *Organic Waste Digestion Project Protocol* (p. 108).

Climenhaga, M. A., & Banks, C. J. (2008). Anaerobic digestion of catering wastes: Effect of micronutrients and retention time. *Water Science and Technology*, *57*(5), 687–692. https://doi.org/10.2166/wst.2008.092

de Jonge, N., Davidsson, Å., la Cour Jansen, J., & Nielsen, J. L. (2020). Characterisation of microbial communities for improved management of anaerobic digestion of food waste. *Waste Management*, *117*, 124–135. https://doi.org/10.1016/j.wasman.2020.07.047

Deepanraj, B., Sivasubramanian, V., & Jayaraj, S. (2015). Experimental and kinetic study on anaerobic digestion of food waste: The effect of total solids and pH. *Journal of Renewable and Sustainable Energy*, *7*(6), 063104. https://doi.org/10.1063/1.4935559

Duan, N., Zhang, D., Lin, C., Zhang, Y., Zhao, L., Liu, H., & Liu, Z. (2019). Effect of organic loading rate on anaerobic digestion of pig manure: Methane production, mass flow, reactor scale and heating scenarios. *Journal of Environmental Management*, *231*, 646–652. https://doi.org/10.1016/j.jenvman.2018.10.062

Dyksma, S., Jansen, L., & Gallert, C. (2020). Syntrophic acetate oxidation replaces acetoclastic methanogenesis during thermophilic digestion of biowaste. *Microbiome*, *8*(1), 105. https://doi.org/10.1186/s40168-020-00862-5

Elbeshbishy, E., & Nakhla, G. (2011). Comparative study of the effect of ultrasonication on the anaerobic biodegradability of food waste in single and two-stage systems. *Bioresource Technology*, *102*(11), 6449–6457. https://doi.org/10.1016/j.biortech.2011.03.082

Elbeshbishy, E., Nakhla, G., & Hafez, H. (2012). Biochemical methane potential (BMP) of food waste and primary sludge: Influence of inoculum pre-incubation and inoculum source. *Bioresource Technology*, *110*, 18–25. https://doi.org/10.1016/j.biortech.2012.01.025

Facchin, V., Cavinato, C., Fatone, F., Pavan, P., Cecchi, F., & Bolzonella, D. (2013). *Effect of trace element supplementation on the mesophilic anaerobic digestion of foodwaste in batch trials: The influence of inoculum origin*. *70*, 71–77. https://doi.org/10.1016/j.bej.2012.10.004

Feng, X., Karlsson, A., Svensson, B., & Bertilsson, S. (2010a). *Impact of trace element addition on biogas production from food industrial waste—Linking process to microbial communities* (No. 1). *74*(1), 226–240. https://doi.org/10.1111/j.1574-6941.2010.00932.x

Feng, X., Karlsson, A., Svensson, B., & Bertilsson, S. (2010b). *Impact of trace element addition on biogas production from food industrial waste—Linking process to microbial communities*. *74*(1), 226–240. https://doi.org/10.1111/j.1574-6941.2010.00932.x

Fernandes, T. V., Keesman, K. J., Zeeman, G., & van Lier, J. B. (2012). Effect of ammonia on the anaerobic hydrolysis of cellulose and tributyrin. *Biomass and Bioenergy*, *47*, 316–323. https://doi.org/10.1016/j.biombioe.2012.09.029

Ferry, J. G. (2010). The chemical biology of methanogenesis. *Planetary and Space Science*, *58*(14), 1775–1783. https://doi.org/10.1016/j.pss.2010.08.014

Figueroa, P., León, G., Elorza, A., Holuigue, L., & Jordana, X. (2001). Three different genes encode the iron-sulfur subunit of succinate dehydrogenase in Arabidopsis thaliana. *Plant Molecular Biology*, *46*(2), 241–250. https://doi.org/10.1023/a:1010612506070

Forster-Carneiro, T., Pérez, M., & Romero, L. I. (2008). Influence of total solid and inoculum contents on performance of anaerobic reactors treating food waste. *Bioresource Technology*, *99*(15), 6994–7002. https://doi.org/10.1016/j.biortech.2008.01.018

Gamble, M., Künze, G., Brancale, A., Wilson, K. S., & Jones, D. D. (2012). The role of substrate specificity and metal binding in defining the activity and structure of an intracellular subtilisin. *FEBS Open Bio*, *2*, 209–215. https://doi.org/10.1016/j.fob.2012.07.001

Gao, A., Tian, Z., Wang, Z., Wennersten, R., & Sun, Q. (2017). Comparison between the Technologies for Food Waste Treatment. *Energy Procedia*, *105*, 3915–3921. https://doi.org/10.1016/j.egypro.2017.03.811

Glass, J., & Orphan, V. (2012). Trace Metal Requirements for Microbial Enzymes Involved in the Production and Consumption of Methane and Nitrous Oxide. *Frontiers in Microbiology*, *3*, 61. https://doi.org/10.3389/fmicb.2012.00061

Haapalainen, A. M., Meriläinen, G., Pirilä, P. L., Kondo, N., Fukao, T., & Wierenga, R. K. (2007). Crystallographic and Kinetic Studies of Human Mitochondrial Acetoacetyl-CoA Thiolase: The Importance of Potassium and Chloride Ions for Its Structure and Function,. *Biochemistry*, *46*(14), 4305–4321. https://doi.org/10.1021/bi6026192

Hafner, S.D.; Justesen, C.G.; Thorsen, R.; Astals, S.; Holliger, C.; Koch, K.;, Weinrich, S., Calculation of methane production from gas density-based measurements. Standard BMP Methods document 204, version 1.7. Available online: https://www.dbfz.de/en/BMP (accessed on April 13, 2022).

Hafner, S., Astals, S., Holliger, C., Justesen, C., Koch, K., & Mortensen, J. (2021). *Gas density-based BMP measurement: Standard BMP Methods document 304, version 2.3*. https://www.dbfz.de/en/BMP

Hafner, S. D., Koch, K., Carrere, H., Astals, S., Weinrich, S., & Rennuit, C. (2018). Software for biogas research: Tools for measurement and prediction of methane production. *SoftwareX*, *7*, 205–210. https://doi.org/10.1016/j.softx.2018.06.005

Harnadek, C. M. W., Guilford, N. G. H., & Edwards, E. A. (2015). Chemical Oxygen Demand Analysis of Anaerobic Digester Contents. *STEM Fellowship Journal*, *1*(2), 2–5. https://doi.org/10.17975/sfj-2015-008

Harrop, T. C., & Mascharak, P. K. (2005). Structural and spectroscopic models of the A-cluster of acetyl coenzyme a synthase/carbon monoxide dehydrogenase: Nature's Monsanto

acetic acid catalyst. *Coordination Chemistry Reviews*, *249*(24), 3007–3024. https://doi.org/10.1016/j.ccr.2005.04.019

Hattori, S. (2008). Syntrophic Acetate-Oxidizing Microbes in Methanogenic Environments. *Microbes and Environments*, *23*(2), 118–127. https://doi.org/10.1264/jsme2.23.118

Hattori, S., Galushko, A. S., Kamagata, Y., & Schink, B. (2005). Operation of the CO Dehydrogenase/Acetyl Coenzyme A Pathway in both Acetate Oxidation and Acetate Formation by the Syntrophically Acetate-Oxidizing Bacterium Thermacetogenium phaeum. *Journal of Bacteriology*, *187*(10), 3471–3476. https://doi.org/10.1128/JB.187.10.3471-3476.2005

Hertadi, R., & Widhyastuti, H. (2015). Effect of Ca2+ Ion to the Activity and Stability of Lipase Isolated from Chromohalobacter japonicus BK-AB18. *Procedia Chemistry*, *16*, 306–313. https://doi.org/10.1016/j.proche.2015.12.057

Hills, D. J., & Nakano, K. (1984). Effects of particle size on anaerobic digestion of tomato solid wastes. *Agricultural Wastes*, *10*(4), 285–295. https://doi.org/10.1016/0141-4607(84)90004-0

Hochheimer, A., Hedderich, R., & Thauer, R. K. (1998). The formylmethanofuran dehydrogenase isoenzymes in Methanobacterium wolfei and Methanobacterium thermoautotrophicum: Induction of the molybdenum isoenzyme by molybdate and constitutive synthesis of the tungsten isoenzyme. *Archives of Microbiology*, *170*(5), 389–393. https://doi.org/10.1007/s002030050658

Holliger, C., Alves, M., Andrade, D., Angelidaki, I., Astals, S., Baier, U., Bougrier, C., Buffière, P., Carballa, M., de Wilde, V., Ebertseder, F., Fernández, B., Ficara, E., Fotidis, I., Frigon, J.-C., de Laclos, H. F., Ghasimi, D. S. M., Hack, G., Hartel, M., … Wierinck, I.

(2016). Towards a standardization of biomethane potential tests. *Water Science and Technology*, *74*(11), 2515–2522. https://doi.org/10.2166/wst.2016.336

Izumi, K., Okishio, Y., Nagao, N., Niwa, C., Yamamoto, S., & Toda, T. (2010). Effects of particle size on anaerobic digestion of food waste. *International Biodeterioration & Biodegradation*, *64*(7), 601–608. https://doi.org/10.1016/j.ibiod.2010.06.013

Jetten, M. S. M., & Sinskey, A. J. (1995). Purification and properties of oxaloacetate decarboxylase fromCorynebacterium glutamicum. *Antonie van Leeuwenhoek*, *67*(2), 221–227. https://doi.org/10.1007/BF00871217

Jiang, J., Zhang, Y., Li, K., Wang, Q., Gong, C., & Li, M. (2013). Volatile fatty acids production from food waste: Effects of pH, temperature, and organic loading rate. *Bioresource Technology*, *143*, 525–530. https://doi.org/10.1016/j.biortech.2013.06.025

Jiang, Y., Heaven, S., & Banks, C. J. (2012). Strategies for stable anaerobic digestion of vegetable waste. *Renewable Energy*, *44*, 206–214. https://doi.org/10.1016/j.renene.2012.01.012

Justesen, C. G., Astals, S., Mortensen, J. R., Thorsen, R., Koch, K., Weinrich, S., Triolo, J. M., & Hafner, S. D. (2019). Development and Validation of a Low-Cost Gas Density Method for Measuring Biochemical Methane Potential (BMP). *Water*, *11*(12), 2431. https://doi.org/10.3390/w11122431

Kim, I. S., Kim, D. H., & Hyun, S.-H. (2000). Effect of particle size and sodium ion concentration on anaerobic thermophilic food waste digestion. *Water Science and Technology*, *41*(3), 67–73. https://doi.org/10.2166/wst.2000.0057

Kim, M., Gomec, C. Y., Ahn, Y., & Speece, R. E. (2003). Hydrolysis and acidogenesis of particulate organic material in mesophilic and thermophilic anaerobic digestion.

Environmental Technology, *24*(9), 1183–1190. https://doi.org/10.1080/09593330309385659

Kim, M.-S., Kim, D.-H., & Yun, Y.-M. (2017). Effect of operation temperature on anaerobic digestion of food waste: Performance and microbial analysis. *Fuel*, *209*, 598–605. https://doi.org/10.1016/j.fuel.2017.08.033

Koch, K., Hafner, S. D., Weinrich, S., Astals, S., & Holliger, C. (2020). Power and Limitations of Biochemical Methane Potential (BMP) Tests. *Frontiers in Energy Research*, *8*. https://www.frontiersin.org/article/10.3389/fenrg.2020.00063

Kuever, J., Visser, M., Loeffler, C., Boll, M., Worm, P., Sousa, D., Plugge, C., Schaap, P., Muyzer, G., Cardoso Pereira, I., Parshina, S., Goodwin, L., Kyrpides, N., Detter, J., Woyke, T., Chain, P., Davenport, K., Rohde, M., Spring, S., & Stams, A. (2014). Genome analysis of Desulfotomaculum gibsoniae strain GrollT a highly versatile Gram-positive sulfate-reducing bacterium. *Standards in Genomic Sciences*, *9*, 821–839. https://doi.org/10.4056/sigs.5209235

Lee, D.-J., Lee, S.-Y., Bae, J.-S., Kang, J.-G., Kim, K.-H., Rhee, S.-S., Park, J.-H., Cho, J.-S., Chung, J., & Seo, D.-C. (2015). Effect of Volatile Fatty Acid Concentration on Anaerobic Degradation Rate from Field Anaerobic Digestion Facilities Treating Food Waste Leachate in South Korea. *Journal of Chemistry*, *2015*, 1–9. https://doi.org/10.1155/2015/640717

Lee, H.-S., Salerno, M. B., & Rittmann, B. E. (2008). Thermodynamic Evaluation on H2 Production in Glucose Fermentation. *Environmental Science & Technology*, *42*(7), 2401–2407. https://doi.org/10.1021/es702610v

Li, Y., Zhang, Y., Sun, Y., Wu, S., Kong, X., Yuan, Z., & Dong, R. (2017). The performance efficiency of bioaugmentation to prevent anaerobic digestion failure from ammonia and propionate inhibition. *Bioresource Technology*, *231*, 94–100. https://doi.org/10.1016/j.biortech.2017.01.068

Lin, C.-Y. (1993). Effect of heavy metals on acidogenesis in anaerobic digestion. *Water Research*, *27*(1), 147–152. https://doi.org/10.1016/0043-1354(93)90205-V

Lin, J., Zuo, J., Gan, L., Li, P., Liu, F., Wang, K., Chen, L., & Gan, H. (2011). Effects of mixture ratio on anaerobic co-digestion with fruit and vegetable waste and food waste of China. *Journal of Environmental Sciences*, *23*(8), 1403–1408. https://doi.org/10.1016/S1001-0742(10)60572-4

Liotta, F., d'Antonio, G., Esposito, G., Fabbricino, M., van Hullebusch, E. D., Lens, P. N., Pirozzi, F., & Pontoni, L. (2014). Effect of total solids content on methane and volatile fatty acid production in anaerobic digestion of food waste. *Waste Management & Research*, *32*(10), 947–953. https://doi.org/10.1177/0734242X14550740

Liu, C., Yuan, X., Zeng, G., Li, W., & Li, J. (2008). Prediction of methane yield at optimum pH for anaerobic digestion of organic fraction of municipal solid waste. *Bioresource Technology*, *99*(4), 882–888. https://doi.org/10.1016/j.biortech.2007.01.013

Liu, H., Shi, J., Zhan, X., Zhang, L., Fu, B., & Liu, H. (2017). Selective acetate production with CO2 sequestration through acetogen-enriched sludge inoculums in anaerobic digestion. *Biochemical Engineering Journal*, *121*, 163–170. https://doi.org/10.1016/j.bej.2017.02.008

Ljungdhal, L. G. (1986). The Autotrophic Pathway of Acetate Synthesis in Acetogenic Bacteria. *Annual Review of Microbiology*, *40*(1), 415–450. https://doi.org/10.1146/annurev.mi.40.100186.002215

Lukitawesa, Patinvoh, R. J., Millati, R., Sárvári-Horváth, I., & Taherzadeh, M. J. (2020). Factors influencing volatile fatty acids production from food wastes via anaerobic digestion. *Bioengineered*, *11*(1), 39–52. https://doi.org/10.1080/21655979.2019.1703544

Luo, L., Kaur, G., & Wong, J. W. C. (2019). A mini-review on the metabolic pathways of food waste two-phase anaerobic digestion system. *Waste Management & Research*, *37*(4), 333–346. https://doi.org/10.1177/0734242X18819954

Magrí, A., Fernández, B., Prenafeta-Boldú, F. X., & Ruiz-Sánchez, J. (2019). Coupling Syntrophic Acetate Oxidation and Anaerobic Ammonium Oxidation When Treating Nitrogen-Rich Organic Wastes for Energy Recovery and Nitrogen Removal: Overview and Prospects. In H. Treichel & G. Fongaro (Eds.), *Improving Biogas Production: Technological Challenges, Alternative Sources, Future Developments* (pp. 117–147). Springer International Publishing. https://doi.org/10.1007/978-3-030-10516-7_6

Mara, D., & Horan, N. J. (2003). *Handbook of Water and Wastewater Microbiology*. Elsevier.

Marshall, A. C., & Bruning, J. B. (2021). Engineering potassium activation into biosynthetic thiolase. *Biochemical Journal*, *478*(15), 3047–3062. https://doi.org/10.1042/BCJ20210455

Mccarty, P. (1982). *ONE HUNDRED YEARS OF ANAEROBIC TREATMENT*. http://pascal-francis.inist.fr/vibad/index.php?action=getRecordDetail&idt=PASCAL83X0082338

Meegoda, J. N., Li, B., Patel, K., & Wang, L. B. (2018). A Review of the Processes, Parameters, and Optimization of Anaerobic Digestion. *International Journal of Environmental Research and Public Health*, *15*(10), 2224. https://doi.org/10.3390/ijerph15102224

Menon, A., Wang, J.-Y., & Giannis, A. (2017). *Optimization of micronutrient supplement for enhancing biogas production from food waste in two-phase thermophilic anaerobic digestion*. *59*, 465–475. https://doi.org/10.1016/j.wasman.2016.10.017

Miles, R. D., Iyer, P. P., & Ferry, J. G. (2001). Site-directed Mutational Analysis of Active Site Residues in the Acetate Kinase from Methanosarcina thermophila *. *Journal of Biological Chemistry*, *276*(48), 45059–45064. https://doi.org/10.1074/jbc.M108355200

Montgomery County Jail—Christiansburg, VA. (n.d.). Retrieved March 22, 2022, from https://www.countyoffice.org/montgomery-county-jail-christiansburg-va-127/

Montgomery County Public Schools. (n.d.). Retrieved March 22, 2022, from https://www.usnews.com/education/k12/virginia/districts/montgomery-co-pblc-schs-111182

Moon, H. C., & Song, I. S. (2011). Enzymatic Hydrolysis of FoodWaste and Methane Production Using UASB Bioreactor. *International Journal of Green Energy*, *8*(3), 361–371. https://doi.org/10.1080/15435075.2011.557845

Morpeth, F. F., & Massey, V. (1982). Metal binding to D-lactate dehydrogenase. *Biochemistry*, *21*(6), 1318–1323. https://doi.org/10.1021/bi00535a033

Müller, N., Worm, P., Schink, B., Stams, A. J. M., & Plugge, C. M. (2010). Syntrophic butyrate and propionate oxidation processes: From genomes to reaction mechanisms. *Environmental Microbiology Reports*, *2*(4), 489–499. https://doi.org/10.1111/j.1758-2229.2010.00147.x

Myhre, G., Shindell, D., Bréon, F.-M., Collins, W., Fuglestvedt, J., Huang, J., Koch, D., Lamarque, J.-F., Lee, D., Mendoza, B., Nakajima, T., Robock, A., Stephens, G., Zhang, H., Aamaas, B., Boucher, O., Dalsøren, S. B., Daniel, J. S., Forster, P., … Shine, K. (n.d.). *8 Anthropogenic and Natural Radiative Forcing*. 82.

Myszograj, S., Stadnik, A., & Płucuennik-Koropczuk, E. (2018). *The Influence of Trace Elements on Anaerobic Digestion Process*. *28*(4), 105–115. http://dx.doi.org/10.2478/ceer-2018-0054

Nelson, M. C., Morrison, M., & Yu, Z. (2011). A meta-analysis of the microbial diversity observed in anaerobic digesters. *Bioresource Technology*, *102*(4), 3730–3739. https://doi.org/10.1016/j.biortech.2010.11.119

New River Valley Juvenile Detention Home. (n.d.). New River Valley Juvenile Detention Home. Retrieved March 22, 2022, from https://www.nrvjdh.org/

Nissen, L. S., & Basen, M. (2019). The emerging role of aldehyde:ferredoxin oxidoreductases in microbially-catalyzed alcohol production. *Journal of Biotechnology*, *306*, 105–117. https://doi.org/10.1016/j.jbiotec.2019.09.005

Nobu, M. K., Narihiro, T., Rinke, C., Kamagata, Y., Tringe, S. G., Woyke, T., & Liu, W.-T. (2015). Microbial dark matter ecogenomics reveals complex synergistic networks in a methanogenic bioreactor. *The ISME Journal*, *9*(8), 1710–1722. https://doi.org/10.1038/ismej.2014.256

Oumer, O. J., & Abate, D. (2017). Characterization of Pectinase from Bacillus subtilis Strain Btk 27 and Its Potential Application in Removal of Mucilage from Coffee Beans. *Enzyme Research*, *2017*, 7686904. https://doi.org/10.1155/2017/7686904

Palmowski, L. M., & Müller, J. A. (2000). Influence of the size reduction of organic waste on their anaerobic digestion. *Water Science and Technology*, *41*(3), 155–162. https://doi.org/10.2166/wst.2000.0067

Paramaguru, G., Kannan, M., Lawrence, P., & Thamilselvan, D. (2017). Effect of total solids on biogas production through anaerobic digestion of food waste. *Desalination and Water Treatment*, *63*, 63–68.

Parawira, W., Murto, M., Read, J. S., & Mattiasson, B. (2005). Profile of hydrolases and biogas production during two-stage mesophilic anaerobic digestion of solid potato waste. *Process Biochemistry*, *40*(9), 2945–2952. https://doi.org/10.1016/j.procbio.2005.01.010

Parker, N., Williams, R., Dominguez-Faus, R., & Scheitrum, D. (2017). Renewable natural gas in California: An assessment of the technical and economic potential. *Energy Policy*, *111*, 235–245. https://doi.org/10.1016/j.enpol.2017.09.034

Parra-Orobio, B., Donoso-Bravo, A., Ruiz-Sánchez, J., Valencia-Molina, K., & Torres-Lozada, P. (2018). *Effect of inoculum on the anaerobic digestion of food waste accounting for the concentration of trace elements*. *71*, 342–349. https://doi.org/10.1016/j.wasman.2017.09.040

Pennington, M. (2021). *Anaerobic Digestion Facilities Processing Food Waste in the United States (2017 & 2018)* (EPA/903/S-21/001; p. 56). EPA. https://www.epa.gov/sites/default/files/2021-02/documents/2021_final_ad_report_feb_2_with_links.pdf

Pereira, J. de C., Giese, E. C., SouzaMoretti, M. M. de, Gomes, A. C. dos S., Perrone, O. M., Boscolo, M., Silva, R. da, Gomes, E., & Martins, D. A. B. (2017). Effect of Metal Ions,

Chemical Agents and Organic Compounds on Lignocellulolytic Enzymes Activities. In *Enzyme Inhibitors and Activators*. IntechOpen. https://doi.org/10.5772/65934

Prakash, O., Jaiswal, N., & Pandey, R. (2011). Effect of Metal Ions, EDTA and Sulfhydryl Reagents on Soybean Amylase Activity. *Asian Journal Fo Biochemistry*, *6*(3), 282–290. https://doi.org/10.3923/ajb.2011.282.290

Procházka, J., Dolejš, P., Máca, J., & Dohányos, M. (2012). Stability and inhibition of anaerobic processes caused by insufficiency or excess of ammonia nitrogen. *Applied Microbiology and Biotechnology*, *93*(1), 439–447. https://doi.org/10.1007/s00253-011-3625-4

Qian, M., Li, Y., Zhang, Y., Sun, Z., Wang, Y., Feng, J., Yao, Z., & Zhao, L. (2019). Efficient acetogenesis of anaerobic co-digestion of food waste and maize straw in a HSAD reactor. *Bioresource Technology*, *283*, 221–228. https://doi.org/10.1016/j.biortech.2019.03.032

Ragsdale, S. W., & Pierce, E. (2008). Acetogenesis and the Wood–Ljungdahl pathway of CO2 fixation. *Biochimica et Biophysica Acta (BBA) - Proteins and Proteomics*, *1784*(12), 1873–1898. https://doi.org/10.1016/j.bbapap.2008.08.012

Rahman, Md. M., Lee, Y. S., Tamiri, F. M., & Hong, M. G. J. (2018). Anaerobic Digestion of Food Waste. In N. Horan, A. Z. Yaser, & N. Wid (Eds.), *Anaerobic Digestion Processes: Applications and Effluent Treatment* (pp. 105–122). Springer. https://doi.org/10.1007/978-981-10-8129-3_7

Rajagopal, R., Massé, D. I., & Singh, G. (2013). A critical review on inhibition of anaerobic digestion process by excess ammonia. *Bioresource Technology*, *143*, 632–641. https://doi.org/10.1016/j.biortech.2013.06.030

Ren, Y., Yu, M., Wu, C., Wang, Q., Gao, M., Huang, Q., & Liu, Y. (2018). A comprehensive review on food waste anaerobic digestion: Research updates and tendencies. *Bioresource Technology*, *247*, 1069–1076. https://doi.org/10.1016/j.biortech.2017.09.109

Reungsang, A., Pattra, S., & Sittijunda, S. (2012). Optimization of Key Factors Affecting Methane Production from Acidic Effluent Coming from the Sugarcane Juice Hydrogen Fermentation Process. *Energies*, *5*(11), 4746–4757. https://doi.org/10.3390/en5114746

Rinzema, A., van Lier, J., & Lettinga, G. (1988). Sodium inhibition of acetoclastic methanogens in granular sludge from a UASB reactor. *Enzyme and Microbial Technology*, *10*(1), 24–32. https://doi.org/10.1016/0141-0229(88)90094-4

Roche, T. E., Baker, J. C., Yan, X., Hiromasa, Y., Gong, X., Peng, T., Dong, J., Turkan, A., & Kasten, S. A. (2001). Distinct regulatory properties of pyruvate dehydrogenase kinase and phosphatase isoforms. *Progress in Nucleic Acid Research and Molecular Biology*, *70*, 33–75. https://doi.org/10.1016/s0079-6603(01)70013-x

Salminen, E. A., & Rintala, J. A. (2002). Semi-continuous anaerobic digestion of solid poultry slaughterhouse waste: Effect of hydraulic retention time and loading. *Water Research*, *36*(13), 3175–3182. https://doi.org/10.1016/S0043-1354(02)00010-6

Sandberg, M., & Ahring, B. K. (1992). Anaerobic treatment of fish meal process waste-water in a UASB reactor at high pH. *Applied Microbiology and Biotechnology*, *36*(6), 800–804. https://doi.org/10.1007/BF00172198

Sawayama, S., Tada, C., Tsukahara, K., & Yagishita, T. (2004). Effect of ammonium addition on methanogenic community in a fluidized bed anaerobic digestion. *Journal of Bioscience and Bioengineering*, *97*(1), 65–70. https://doi.org/10.1016/S1389-1723(04)70167-X

Scherer, P., Lippert, H., & Wolff, G. (1983). Composition of the major elements and trace elements of 10 methanogenic bacteria determined by inductively coupled plasma emission spectrometry. *Biological Trace Element Research*, *5*(3), 149–163. https://doi.org/10.1007/BF02916619

Schnürer, A., & Nordberg, Å. (2008). Ammonia, a selective agent for methane production by syntrophic acetate oxidation at mesophilic temperature. *Water Science and Technology*, *57*(5), 735–740. https://doi.org/10.2166/wst.2008.097

Seravalli, J., Gu, W., Tam, A., Strauss, E., Begley, T. P., Cramer, S. P., & Ragsdale, S. W. (2003). Functional copper at the acetyl-CoA synthase active site. *Proceedings of the National Academy of Sciences*, *100*(7), 3689–3694. https://doi.org/10.1073/pnas.0436720100

Shima, S., Warkentin, E., Thauer, R. K., & Ermler, U. (2002). Structure and function of enzymes involved in the methanogenic pathway utilizing carbon dioxide and molecular hydrogen. *Journal of Bioscience and Bioengineering*, *93*(6), 519–530. https://doi.org/10.1016/S1389-1723(02)80232-8

Sieber, J. R., McInerney, M. J., & Gunsalus, R. P. (2012). Genomic Insights into Syntrophy: The Paradigm for Anaerobic Metabolic Cooperation. *Annual Review of Microbiology*, *66*(1), 429–452. https://doi.org/10.1146/annurev-micro-090110-102844

Sikora, L. J. (1998). Benefits and Drawbacks to Composting Organic By-Products. In S. Brown, J. S. Angle, & L. Jacobs (Eds.), *Beneficial Co-Utilization of Agricultural, Municipal and Industrial by-Products* (pp. 69–77). Springer Netherlands. https://doi.org/10.1007/978-94-011-5068-2_6

Sung, S., & Liu, T. (2003). Ammonia inhibition on thermophilic anaerobic digestion. *Chemosphere*, *53*(1), 43–52. https://doi.org/10.1016/S0045-6535(03)00434-X

Tanimu, M. I., Ghazi, T. I. M., Harun, R. M., & Idris, A. (2014). Effect of Carbon to Nitrogen Ratio of Food Waste on Biogas Methane Production in a Batch Mesophilic Anaerobic Digester. *International Journal of Innovation*, *5*(2), 5.

Thanh, P., Ketheesan, B., Yan, Z., & Stuckey, D. (2016). *Trace metal speciation and bioavailability in anaerobic digestion: A review*. *34*(2), 122–136. https://doi.org/10.1016/j.biotechadv.2015.12.006

US Census Bureau. (2012). *2012 Wholesale Trade (NAICS Sector 42)*. Census.Gov. https://www.census.gov/data/tables/2012/econ/census/wholesale-trade.html

US Census Bureau. (2021a, December). *2018-2020 Annual Survey of Manufactures (ASM): Tables*. Census.Gov. https://www.census.gov/data/tables/time-series/econ/asm/2018-2020-asm.html

US Census Bureau. (2021b, December 16). *County Business Patterns by Industry: 2019*. Census.Gov. https://www.census.gov/library/visualizations/interactive/county-business-patterns-by-industry-2019.html

U.S. Census Bureau. (2022). *Census.gov*. Census.Gov. https://www.census.gov/en.html

U.S. Census Bureau QuickFacts: Virginia. (n.d.). Retrieved March 22, 2022, from https://www.census.gov/quickfacts/VA

US EPA. (2020). *2018 Wasted Food Report* (p. 37). https://www.epa.gov/sites/production/files/2020-11/documents/2018_wasted_food_report.pdf

US EPA, O. (2015a, April 16). *Sustainable Management of Food* [Collections and Lists]. https://www.epa.gov/sustainable-management-food

US EPA, O. (2015b, April 16). *Sustainable Management of Food* [Collections and Lists]. https://www.epa.gov/sustainable-management-food

US EPA, O. (2015c, December 23). *Overview of Greenhouse Gases* [Overviews and Factsheets]. https://www.epa.gov/ghgemissions/overview-greenhouse-gases

US EPA, O. (2016, April 15). *Basic Information about Landfill Gas* [Overviews and Factsheets]. https://www.epa.gov/lmop/basic-information-about-landfill-gas

US EPA, O. (2017, September 12). *Food: Material-Specific Data* [Overviews and Factsheets]. https://www.epa.gov/facts-and-figures-about-materials-waste-and-recycling/food-material-specific-data

US EPA, O. (2018, December 6). *Renewable Natural Gas* [Overviews and Factsheets]. https://www.epa.gov/lmop/renewable-natural-gas

USDA. (n.d.). *Food Waste FAQs*. Retrieved September 16, 2021, from https://www.usda.gov/foodwaste/faqs

Velmurugan, S., Deepanraj, B., & Jayaraj, S. (2014). Biogas Generation through Anaerobic Digetsion Process – An Overview. *RESEARCH JOURNAL OF CHEMISTRY AND ENVIRONMENT*, *18*, 80–94.

Virginia Tech 2020-21 Sustainability Annual Report (p. 90). (n.d.). Virginia Tech.

Voelklein, M. A., O' Shea, R., Jacob, A., & Murphy, J. D. (2017). Role of trace elements in single and two-stage digestion of food waste at high organic loading rates. *Energy*, *121*, 185–192. https://doi.org/10.1016/j.energy.2017.01.009

Vuillemin, A., Kerrigan, Z., D'Hondt, S., & Orsi, W. D. (2020). Exploring the abundance, metabolic potential and gene expression of subseafloor Chloroflexi in million-year-old oxic and anoxic abyssal clay. *FEMS Microbiology Ecology*, *96*(12). https://doi.org/10.1093/femsec/fiaa223

Wang, H., Fotidis, I. A., & Angelidaki, I. (2015). Ammonia effect on hydrogenotrophic methanogens and syntrophic acetate-oxidizing bacteria. *FEMS Microbiology Ecology*, *91*(11). https://doi.org/10.1093/femsec/fiv130

Wang, K., Yin, J., Shen, D., & Li, N. (2014). Anaerobic digestion of food waste for volatile fatty acids (VFAs) production with different types of inoculum: Effect of pH. *Bioresource Technology*, *161*, 395–401. https://doi.org/10.1016/j.biortech.2014.03.088

Wang, P., Wang, H., Qiu, Y., Ren, L., & Jiang, B. (2018). Microbial characteristics in anaerobic digestion process of food waste for methane production–A review. *Bioresource Technology*, *248*, 29–36. https://doi.org/10.1016/j.biortech.2017.06.152

Wang, R., Lv, N., Li, C., Cai, G., Pan, X., Li, Y., & Zhu, G. (2021). Novel strategy for enhancing acetic and formic acids generation in acidogenesis of anaerobic digestion via targeted adjusting environmental niches. *Water Research*, *193*, 116896. https://doi.org/10.1016/j.watres.2021.116896

Ward, A. J., Hobbs, P. J., Holliman, P. J., & Jones, D. L. (2008). Optimisation of the anaerobic digestion of agricultural resources. *Bioresource Technology*, *99*(17), 7928–7940. https://doi.org/10.1016/j.biortech.2008.02.044

Westerholm, M., Moestedt, J., & Schnürer, A. (2016). Biogas production through syntrophic acetate oxidation and deliberate operating strategies for improved digester performance. *Applied Energy*, *179*, 124–135. https://doi.org/10.1016/j.apenergy.2016.06.061

Westerholm, M., Müller, B., Arthurson, V., & Schnürer, A. (2011). Changes in the Acetogenic Population in a Mesophilic Anaerobic Digester in Response to Increasing Ammonia Concentration. *Microbes and Environments*, *26*(4), 347–353. https://doi.org/10.1264/jsme2.ME11123

Wulansari, B., & Kristanto, G. A. (2015). Methane potential of food waste from Engineering Faculty Cafeteria in Universitas Indonesia. *2015 International Conference on Sustainable Energy Engineering and Application (ICSEEA)*, 30–34. https://doi.org/10.1109/ICSEEA.2015.7380741

Xu, F., Li, Y., Ge, X., Yang, L., & Li, Y. (2018). Anaerobic digestion of food waste – Challenges and opportunities. *Bioresource Technology*, *247*, 1047–1058. https://doi.org/10.1016/j.biortech.2017.09.020

Yang, P., Peng, Y., Tan, H., Liu, H., Wu, D., Wang, X., Li, L., & Peng, X. (2021). Foaming mechanisms and control strategies during the anaerobic digestion of organic waste: A critical review. *Science of The Total Environment*, *779*, 146531. https://doi.org/10.1016/j.scitotenv.2021.146531

Yazdanpanah, A., Ghasimi, D., Kim, M., Nakhla, G., Hafez, H., & Keleman, M. (2018). *Impact of trace element supplementation on mesophilic anaerobic digestion of food waste using Fe-rich inoculum*. *25*, 29240–29255. https://doi.org/10.1007/s11356-018-2832-2

Yenigün, O., & Demirel, B. (2013). Ammonia inhibition in anaerobic digestion: A review. *Process Biochemistry*, *48*(5), 901–911. https://doi.org/10.1016/j.procbio.2013.04.012

Yi, J., Dong, B., Jin, J., & Dai, X. (2014). Effect of Increasing Total Solids Contents on Anaerobic Digestion of Food Waste under Mesophilic Conditions: Performance and

Microbial Characteristics Analysis. *PLOS ONE*, *9*(7), e102548. https://doi.org/10.1371/journal.pone.0102548

Yirong, C., Heaven, S., & Banks, C. (2014). Effect of a Trace Element Addition Strategy on Volatile Fatty Acid Accumulation in Thermophilic Anaerobic Digestion of Food Waste. *Waste and Biomass Valorization*, *6*, 1–12. https://doi.org/10.1007/s12649-014-9327-2

Zamanzadeh, M., Hagen, L. H., Svensson, K., Linjordet, R., & Horn, S. J. (2016). Anaerobic digestion of food waste – Effect of recirculation and temperature on performance and microbiology. *Water Research*, *96*, 246–254. https://doi.org/10.1016/j.watres.2016.03.058

Zhang, B., Zhang, L.-L., Zhang, S.-C., Shi, H.-Z., & Cai, W.-M. (2005). The Influence of pH on Hydrolysis and Acidogenesis of Kitchen Wastes in Two-phase Anaerobic Digestion. *Environmental Technology*, *26*(3), 329–340. https://doi.org/10.1080/09593332608618563

Zhang, C., Su, H., Baeyens, J., & Tan, T. (2014). Reviewing the anaerobic digestion of food waste for biogas production. *Renewable and Sustainable Energy Reviews*, *38*, 383–392. https://doi.org/10.1016/j.rser.2014.05.038

Zhang, L., & Jahng, D. (2012). *Long-term anaerobic digestion of food waste stabilized by trace elements* (No. 8). *32*(8), 1509–1515. https://doi.org/10.1016/j.wasman.2012.03.015

Zhang, L., Lee, Y.-W., & Jahng, D. (2011). *Anaerobic co-digestion of food waste and piggery wastewater: Focusing on the role of trace elements* (No. 8). *102*(8), 5048–5059. https://doi.org/10.1016/j.biortech.2011.01.082

Zhang, L., Ouyang, W., & Lia, A. (2012). Essential Role of Trace Elements in Continuous Anaerobic Digestion of Food Waste. *Procedia Environmental Sciences*, *16*, 102–111. https://doi.org/10.1016/j.proenv.2012.10.014

Zhang, R., El-Mashad, H. M., Hartman, K., Wang, F., Liu, G., Choate, C., & Gamble, P. (2007). Characterization of food waste as feedstock for anaerobic digestion. *Bioresource Technology*, *98*(4), 929–935. https://doi.org/10.1016/j.biortech.2006.02.039

Zhang, W., Chen, B., Li, A., Zhang, L., Li, R., Yang, T., & Xing, W. (2019). Mechanism of process imbalance of long-term anaerobic digestion of food waste and role of trace elements in maintaining anaerobic process stability. *Bioresource Technology*, *275*, 172–182. https://doi.org/10.1016/j.biortech.2018.12.052

Zhang, W., Li, L., Wang, X., Xing, W., Li, R., Yang, T., & Lv, D. (2020). Role of trace elements in anaerobic digestion of food waste: Process stability, recovery from volatile fatty acid inhibition and microbial community dynamics. *Bioresource Technology*, *315*, 123796. https://doi.org/10.1016/j.biortech.2020.123796

Zhang, W., Wu, S., Guo, J., Zhou, J., & Dong, R. (2015). Performance and kinetic evaluation of semi-continuously fed anaerobic digesters treating food waste: Role of trace elements. *Bioresource Technology*, *178*, 297–305. https://doi.org/10.1016/j.biortech.2014.08.046

Zhou, M., Yan, B., Wong, J. W. C., & Zhang, Y. (2018). Enhanced volatile fatty acids production from anaerobic fermentation of food waste: A mini-review focusing on acidogenic metabolic pathways. *Bioresource Technology*, *248*, 68–78. https://doi.org/10.1016/j.biortech.2017.06.121

Appendix A – Large scale community digester sizing calculations

Volume of FW treated per day

$$\frac{20{,}651.7\ metric\ tons}{year} * \frac{1\ year}{365\ days} = 56.58\frac{t}{day} = 56{,}580\frac{kg}{day} = 56{,}580\frac{L}{day}$$

Volume of FW slurry (2 parts FW, 1 part water) per day

$$1\ part\ water\ to\ two\ parts\ FW = 3 * 56{,}580\frac{L}{day} = 169{,}740\frac{L}{day}$$

Volume of FW treated over one retention time (15 days)

$$\frac{169{,}740\frac{L}{day} * 15\ days}{1000\frac{L}{m^3}} = 2546\ \mathrm{m}^3$$

Feedstock quality – mass of volatile solids per volume of feedstock

$$56{,}580\frac{kg}{day} * 10.64\%\ TS * 95.10\%\ VS = 5725\frac{kg\ VS}{day}$$

$$\frac{5725\frac{kg\ VS}{day}}{169{,}740\frac{L}{day} * \frac{1\ m^3}{1000\ L}} = 33.7\frac{kg\ VS}{m^3}$$

Organic loading rate (OLR)

$$OLR = \frac{flow\ rate * concentration}{reactor\ volume} = \frac{56.58\frac{m^3}{day} * 33.7\frac{kg\ VS}{m^3}}{2546.1\ m^3} = 0.75\frac{kg\ VS}{m^3 * day}$$

Amount of methane produced per day

$$0.75\frac{kg\ VS}{m^3 * day} * 0.363\frac{m^3\ CH_4}{kg\ VS} * 2546\ m^3 = 693\frac{m^3\ CH_4}{day}$$

Total volume of anaerobic digester

$$2546\ m^3 + \left(\left(\frac{2546\ m^3}{0.75}\right) * 0.25\right) = 3395\ m^3 = 3{,}395{,}000\ L$$

Working volume of anaerobic digester
$2546\ m^3 = 2{,}546{,}000\ L$

Headspace volume of anaerobic digester
$\left(\frac{2546\ m^3}{0.75}\right) * 0.25 = 848.7\ m^3$